IEEE Standards

IEEE Std 836-2001
(Revision of
IEEE Std 836-1991)

IEEE Recommended Practice for Precision Centrifuge Testing of Linear Accelerometers

IEEE Aerospace and Electronic Systems Society

Sponsored by the
Gyro and Accelerometer Panel

IEEE

Published by
The Institute of Electrical and Electronics Engineers, Inc.
3 Park Avenue, New York, NY 10016-5997, USA

7 November 2001

Print: SH94948
PDF: SS94948

Recognized as an
American National Standard (ANSI)

IEEE Std 836-2001
(Revision of
IEEE Std 836-1991)

IEEE Recommended Practice for Precision Centrifuge Testing of Linear Accelerometers

Sponsor

Gyro and Accelerometer Panel
of the
IEEE Aerospace and Electronic Systems Society

Approved 14 June 2001

IEEE-SA Standards Board

Abstract: This recommended practice provides a guide to the conduct and analysis of precision centrifuge tests of linear accelerometers, covering each phase of the tests, beginning with the planning. Possible error sources and typical methods of data analysis are addressed. The intent is to provide those involved in centrifuge testing with a detailed understanding of the various factors affecting the accuracy of measurement, both those associated with the centrifuge and those in the data collection process. Model equations are discussed, both for the centrifuge and for a typical linear accelerometer, each with the complexity needed to accommodate the various identified characteristics and error sources in each. An iterative matrix equation solution is presented for deriving the various model equation coefficients for the accelerometer under test from the centrifuge test data.
Keywords: accelerometer, accelerometer test, centrifuge, linear accelerometer

---

The Institute of Electrical and Electronics Engineers, Inc.
3 Park Avenue, New York, NY 10016-5997, USA

Print: ISBN 0-7381-2942-9 SH94948
PDF: ISBN 0-7381-2943-7 SS94948

Introduction

(This introduction is not a part of IEEE Std 836-2001, IEEE Recommended Practice for Precision Centrifuge Testing of Linear Accelerometers.)

This recommended practice was prepared by the Gyro and Accelerometer Panel of the Aerospace and Electronic Systems Society of the Institute of Electrical and Electronics Engineers. It provides a guide to the conduct and analysis of precision centrifuge tests of linear accelerometers and includes discussions of possible error sources in those tests. It provides guidance for each phase of the tests, beginning with planning, and it ends with a discussion of typical methods of data analysis.

A discussion of model equations is provided, both for the centrifuge and for a typical linear accelerometer, each with the complexity needed to accommodate the various identified characteristics and error sources in each. This recommended practice also presents an iterative matrix equation solution for derivation of the various model equation coefficients for the accelerometer under test, from the centrifuge test data. The matrix solution provides a two-quadrant best-fit of the centrifuge data to the chosen model equation.

This recommended practice is intended to provide those involved in centrifuge testing with a detailed understanding of the various factors affecting accuracy of measurement, both those associated with the centrifuge and those in the data collection process. Numerical examples are provided so that each factor can be quantitatively evaluated and its contribution to system error compared with the user's required accuracy. This allows the user to identify and evaluate those factors that are critical to a specific planned test. The matrix equation method of data reduction also provides a means of determining data validity as well as model equation adequacy, and yields the confidence intervals for each of the model equation coefficients.

This recommended practice consists of a main text and eight annexes. The main text provides the recommended practice for precision centrifuge testing following a tutorial section that is intended to provide the user with the understanding of critical factors in centrifuge testing, as well as the best methods for taking and reducing data.

Annex A is a compilation of the characteristics of known precision centrifuges from data provided from both users and manufacturers. The listing is intended as a guide to available facilities at the time of publication of this standard. Data provided should be considered as merely informative and not as specifications for the listed machines.

Annex B provides a discussion of evaluation of centrifuges, with references provided to sections of the standard that pertain to the attribute discussed.

Annex C provides a more general discussion of fitting theory, with particular regard to the often unique character of centrifuge data and corresponding accelerometer performance requirements. It discusses the application of the method of least squares by which matrix solutions such as that in the main tests are generated. It also describes the ease of understanding and use. These approximate methods generally address some measure of composite error, rather than directly evaluating model equation coefficients. For example, a common specification limits allowable deviations from a straight line determined by two specified points, such as zero-*g* and some specific value of input *g*.

Annex D discusses the limitations of and alternatives to centrifuge testing. Problems produced by the *g*-gradient, the spin rates required, and the difficulty of producing short high-*g* input pulses are among those discussed. Alternatives such as use of dividing heads and earth's gravity are discussed, along with sled testing and vibration testing. Double turntable centrifuge testing is described.

Annex E describes the processing of dual-proof-mass vibrating beam accelerometer centrifuge data. Annex F discusses scale factor calibration for high-*g* applications on an ultra-centrifuge. Annex G discusses thermal control and data acquisition on the centrifuge arm. Annex H is a bibliography.

The terminology used conforms to IEEE 100, *The Authoritative Dictionary of IEEE Standards Terms*, Seventh Edition, and IEEE Std 528-2001, IEEE Standard for Inertial Sensor Terminology. The units used conform to IEEE Std 268-1992, American National Standard for Metric Practice. In this standard, the symbol *g* is used to denote a unit of acceleration equal in magnitude to the local value of gravity at the test site. This symbol is thus distinguished from g, which is the standard symbol for gram.

Participants

This publication represents a group effort on a large scale. The major contributors to the original version of this recommended practice, IEEE Std 836-1991, were as follows:

Rex B. Peters, *Chair*

D. R. Anderson	M. D. Hooser	P. W. Ott
C. H. Barker	B. Katz	S. C. Piccione
S. F. Becka	K. J. Klarman	L. W. Richardson
J. S. Beri	M. G. Koning	C. L. Seacord
C. E. Bosson	E. L. Landenheim	G. L. Shaw
H. T. Califano	K. Lantiz	P. B. Simpson
A. T. Campbell*	T. C. Lear	N. F. Sinnot
A. Champsi	J. Lewis	R. B. Smith
J. F. Conroy	D. D. Lynch	T. S. Stanley
J. W. Davies	D. F. Macy	C. O. Swanson*
H. B. Diamond	R. D. Marquess	R. R. Thede
G. W. Erickson	H. D. Morris	L. O. Thielman
J. Feldman	G. E. Morrison*	C. I. Thornburg
A. H. Ferraris	G. C. Murray	L. A . Trozpek
T. A. Fuhrman	G. H. Neugebauer	R. L. Van Alstine
K. N. Green	J. G. Neugroshchl	B. J. Wimber*
R. E. Hartzell	D. F. Nieman	B. R. Youmans

While the development of IEEE Std 836-1991 was a group effort, the contributions of one member were fundamental to its preparation, and he clearly deserves special recognition. George H. Neugebauer developed the iterative matrix data reduction technique outlined in 7.3.3, 7.3.4, and 7.3.5 of IEEE Std 836-1991 (subclauses 9.3.3, 9.3.4, and 9.3.5 of IEEE Std 836-2001). In addition, he was extremely active in the development and subsequent refinement of most of the rest of the document. In large measure, the technical quality of this recommended practice resulted from his efforts.

A total of 68 individuals attended 15 meetings of the Gyro and Accelerometer Panel during preparation of this revised IEEE Std 836-2001. The following persons on the Gyro and Accelerometer Panel contributed to this revision, IEEE Std 836-2001:

Sid Bennett, *Chair*

David R. Anderson	Thomas A. Fuhrman	Charles Pearce
Michael E. Ash	Kerry N. Green	Rex B. Peters*
Cleon H. Barker	Yoshiaki Hirobe	Arkadii Sinelnikov
Stephen Bongiovanni	Ken Homb	Clifford O. Swanson*
Pierre Bouniol	Jean-François Kieffer	Mohammed Tehrani
Herbert T. Califano	Dmitri Loukianov	Leroy O. Thielman
A. T. Campbell*	David Lynch	Angelo Truncale
Michael Cirello	Jean Martel	Dennis Whitehead
Joseph D'Angelo	Robert Moore	David J. Winkel
George W. Erickson	Harold D. Morris	Bruce R. Youmans
Yuri Filatov	Bart Morrow, Jr.	

*Past Chair

The following individuals of the balloting group voted on this recommended practice. Balloters may have voted for approval, disapproval, or abstention.

Michael E. Ash	Tommy Ichinose	Arkadii Sinelnikov
Cleon H. Barker	Jean-François Kieffer	Clifford O. Swanson
Sid Bennett	Dmitri Loukianov	Daniel Tazartes
Stephen Bongiovanni	Bryan Lovitt	Mohammad Tehrani
Herbert T. Califano	Jean Martel	Lee Thielman
A. T. Campbell	Robert Moore	Christopher Trainor
George W. Erickson	Bart Morrow, Jr.	Angelo Truncale
Yuri Filatov	Peter Palmer	Bruce R. Youmans
Thomas A. Fuhrman	Charles Pearce	
Yoshiaki Hirobe	Rex B. Peters	

When the IEEE-SA Standards Board approved this recommended practice on 14 June 2001, it had the following membership:

Donald N. Heirmann, *Chair*
James T. Carlo, *Vice Chair*
Judith Gorman, *Secretary*

Satish K. Aggarwal	James H. Gurney	James W. Moore
Mark D. Bowman	Richard J. Holleman	Robert F. Munzner
Gary R. Engmann	Lowell G. Johnson	Gerald H. Peterson
Harold E. Epstein	Robert J. Kennelly	Ronald C. Petersen
H. Landis Floyd	Joseph L. Koepfinger*	John B. Posey
Jay Forster*	Peter H. Lips	Gary S. Robinson
Howard M. Frazier	L. Bruce McClung	Akio Tojo
Ruben D. Garzon	Daleep C. Mohla	Donald W. Zipse

* Member Emeritus

Also included are the following nonvoting IEEE-SA Standards Board liaisons:

Alan Cookson, *NIST Representative*
Donald R. Volzka, *TAB Representative*

Savoula Amanatidis, *IEEE Standards Managing Editor*

Contents

IEEE Recommended Practice for Precision Centrifuge Testing of Linear Accelerometers

1. Overview

1.1 Scope

This recommended practice describes the conduct and analysis of precision tests that are to be performed on linear accelerometers using centrifuge techniques. The term "precision," in this context, refers to tests that are conducted to evaluate accelerometer parameters, as opposed to those conducted to establish environmental survivability only. Evaluation may take the form of determining the coefficients of the accelerometer's model equation, except for bias and scale factor, which are most accurately determined by static multiposition tests. Alternatively, evaluation may only establish that the accelerometer output complies with specific error limit criteria.

1.2 Purpose

The principal error sources encountered during precision centrifuge testing of linear accelerometers are described, along with those test practices and data reduction techniques that have been found most efficient in minimizing or compensating for them.

2. References

This recommended practice shall be used in conjunction with the following publications. In the event of any conflict, the recommended practices of this document shall have precedence over those in the listed documents.

When the following standards are superseded by an approved revision, the revision shall apply.

IEEE/ASTM SI 10-1997, Standard for Use of the International System of Units (SI): The Modern Metric System.[1]

[1]IEEE publications are available from the Institute of Electrical and Electronic Engineers, 445 Hoes Lane, P.O. Box 1331, Piscataway, NJ 08855-1331, USA (http://www.standards.ieee.org/).

IEEE Std 260.1-1993, American National Standard Letter Symbols for Units of Measurement (SI Units, Customary Inch-Pound Units, and Certain Other Units).

IEEE Std 315-1975, IEEE Graphic Symbols for Electrical and Electronics Diagrams.

IEEE Std 528-2001, IEEE Standard for Inertial Sensor Terminology.

IEEE Std 1293-1998, IEEE Standard Specification Format Guide and Test Procedure for Linear, Single-Axis, Non-Gyroscopic Accelerometers.

3. Definitions, symbols, and acronyms

For the purposes of this recommended practice, the following terms and definitions apply. IEEE 100, *The Authoritative Dictionary of IEEE Standards Terms*, Seventh Edition [B6][2] should be referenced for terms not defined in this clause.

3.1 Definitions relevant to centrifuge testing

3.1.1 arm stretch (ΔR_{AS}): Elongation, due to centrifugal loading, of the mechanical structure connecting an accelerometer to the centrifuge spin axis beyond the static value (R_0).

3.1.2 bucking: An unusually strong interaction between certain terms in a nonorthogonal series due to a similarity in the functions that they represent.

3.1.3 Central Limit Theorem: A theorem that states that under general conditions the probability distribution of the sum of n statistically independent random variables (or their average) approaches the Gaussian (or normal) distribution as n approaches infinity, no matter what the individual distribution functions might be. In-so-far as the total error in a measurement or in the average of a number of measurements is the sum of a number of small independent errors, total measurement error tends to be Gaussian, unless dominated by a single source of error such as quantization noise. *Syn:* **Normal Convergence Theorem.**

3.1.4 centrifuge: A device consisting of a motor- or engine-driven arm structure of sufficient dimensions and strength to allow the rigid mounting and subjecting of one or more inertial grade accelerometers to centripetal acceleration levels ranging from fractions of 1 g to over 200 g.

3.1.5 centrifuge arm axis: A line perpendicular to the axis of rotation of a centrifuge through the effective center of mass of the accelerometer under test.

3.1.6 coning: Precession of a centrifuge due to imbalance.

3.1.7 dynamic error: An error that is present when a centrifuge is rotating.

3.1.8 dynamic leveling error: Any angular deflection of the accelerometer mounting fixture from a horizontal line perpendicular to the centrifuge centripetal acceleration vector.

3.1.9 gravity (g_L). *See:* **plumb-bob gravity.**

3.1.10 Normal Convergence Theorem. *See:* **Central Limit Theorem.**

3.1.11 plumb-bob gravity: The force per unit mass acting on a mass at rest at a point on the earth, not including any reaction force from the suspension. The plumb-bob gravity includes the gravitational attraction of the Earth, the effect of the centripetal acceleration due to the earth rotation, and tidal

[2]The numbers in brackets correspond to those of the bibliography in Annex H.

effects. The direction of the plumb-bob gravity acceleration defines the local vertical down direction, and its magnitude defines the unit of acceleration g used in accelerometer scale factor calibration at a test site (with compensation for tidal effects if accuracy warrants).

3.1.12 radial stiffness: A direct measure of the resistance of the centrifuge axis to deflection due to a horizontal force at the center of rotation; it must take into account the effects of all compliances of the structure, including the bearings, connection to the floor, and the foundation upon which the machine is mounted.

3.1.13 static error: An error that is present when a centrifuge is not rotating; it may change with arm position.

3.1.14 static leveling error: An error in the acceleration seen by a test item due to misalignments of the accelerometer input axis to the centrifuge and gravity vector.

3.2 Symbols and acronyms

Symbol	*Name*	*Reference Clause*
$[\mathbf{A}]$	acceleration matrix	9.3.3, 9.3.4
$\vec{a}$	general acceleration vector	6.3.3
a_b	centripetal acceleration due to earth rotation	5.3
a_c	true average centripetal acceleration of the centrifuge	5.2, 6.1.4, 6.2.2, 6.2.3, 6.3.1, 6.3.2, 6.3.3, 7.2.6, 9.3.3
$\vec{a}_c$	vector quantity of a_c	5.2
$\hat{a}_c$	measured average acceleration	6.3.1, 6.3.2
a_{c+}	centripetal acceleration of the centrifuge along the +IA	6.1.7
a_{c-}	centripetal acceleration of the centrifuge along the −IA	6.1.7
a_g	component of gravitational acceleration along centrifuge a_c	7.2.4
a_h	horizontal component of Coriolis acceleration	6.3.3, 7.2.2, 9.3.2, 9.3.3
a_i	acceleration along sensor IA	5.1, 6.2.2, 6.2.3, 6.4.1, 7.1
a_{i+}	positive input acceleration	9.3.3
a_{i-}	negative input acceleration	9.3.3
a^*_{i+}	iterated estimate of a_{i+}	9.3.3
a^*_{i-}	iterated estimate of a_{i-}	9.3.3
a_{ik}	kth input acceleration	9.3.3
a_o	acceleration along sensor output axis	6.1.2, 6.1.5, 7.1, 7.2.1, 7.2.2, 7.2.6
a_p	acceleration along sensor pendulous axis	6.2.3, 7.1
a_r	average total radial acceleration	7.2.6
a_{ra}	radial acceleration in the sensor frame	7.2.6

a_s	indicated sensor output (g)	5.1, 6.2.3, 6.4.1, 7.1, 9.3.3
$\vec{a}_T$	vector quantity of total acceleration at ECM	5.2
a_{Ta}	tangential acceleration in the sensor frame	7.2.6
a_V	average total vertical acceleration	7.2.6
a_{Va}	vertical acceleration in the sensor frame	7.2.6
a_0	centripetal acceleration due to the static value of centrifuge radius (normalized to g units)	6.1.2, 6.1.5, 7.2.1, 7.2.5
$[\mathbf{B}]$	input matrix	9.3.3
C	rate of drift in angular velocity	6.3.2, 7.2.2
c_+	positive scale factor error	9.3.3
c_-	negative scale factor error	9.3.3
C_2	fitted quadratic coefficient	9.3.5
C_3	fitted cubic coefficient	9.3.5
C_{AS}	coefficient of arm stretch ($\Delta R/R/g$)	6.1.2, 6.6.3
C_d	deflection coefficient (angle/a_i)	6.2.2, 6.2.3
C_{dcr}	coefficient of dynamic center of rotation	6.1.5
$[\mathbf{D}]$	data matrix	9.3.3
d_{ii}	diagonal element of $[\mathbf{A}]^{-1}$	9.3.4
d_k	kth data point	9.3.3
E	sensor output (output units)	5.1, 7.1
ECM	effective center of mass	6.1.1, 6.1.7, 6.1.8, 7.2.1, 8.2.2, 9.3.3
E_r	average output when centrifuge is rotating	9.1.1
E_s	average output when centrifuge is static	9.1.1
$[\mathbf{F}]$	function matrix	9.3.3
f	number of degrees of freedom	9.3.4
f_w	frequency of periodic variation (wow or flutter)	6.3.1, 7.2.2, 7.2.6
G	gravitational constant ($6.672\,59 \times 10^{-11}$ m^3/(kg·s^2))	5.3
g	unit of acceleration	
g_L	local value of gravitational acceleration	5.3, 6.2.2, 7.2.4, 7.2.6
$\vec{g}_L$	vector quantity of g_L	5.2, 5.3
g_N	Newtonian gravitational force per unit mass	5.3
$[\mathbf{H}]$	coefficient matrix	9.3.3
h_j	constant coefficient	9.3.3

IA	sensor input axis	5.1, 6.2.1, 6.2.2, 8.2.2, 8.2.3, 9.1.1, 9.1.4, 9.2.2
k	stiffness	6.1.5
[**K**]	coefficient matrix	9.3.3
K_i	ith polynomial coefficient	9.3.4
K_{io}	cross-coupling coefficient	6.2.3, 7.1, 8.3.1, 9.3.3, 9.3.5
K_{ip}	cross-coupling coefficient	6.2.3, 7.1, 8.3.1, 9.3.3, 9.3.5
K_{oo}	second-order output axis coefficient	7.1, 8.3.1
K_{op}	cross-coupling coefficient	7.1, 8.3.1
K_{oq}	odd-quadratic coefficient	6.1.5, 7.1, 9.3.3, 9.3.4
K_{pp}	second-order pendulous axis coefficient	6.2.3, 7.1, 8.3.1, 9.3.5
K_{ooo}	third-order output axis coefficient	7.1, 8.3.1, 9.3.5
K_{ppp}	third-order pendulous axis coefficient	7.1, 8.3.1, 9.3.5
K_s	specific stiffness of centrifuge arm	6.1.2
K_0	bias (g)	5.1, 6.1.4, 9.5.3
K_{0+}	apparent bias for $a_i > 0$	7.1, 9.3.3
K_{0-}	apparent bias for $a_i < 0$	7.1, 9.3.3
K_1	sensor scale factor (output units/g)	5.1, 6.4.1, 7.1, 9.1.1, 9.3.3
K_{1+}	apparent scale factor for $a_i > 0$	7.1
K_{1-}	apparent scale factor for $a_i < 0$	7.1
K_{10}	scale factor at $t = 0$	6.4.1
K_2	second-order coefficient	6.1.5, 6.1.7, 6.2.1, 6.2.3, 6.4.3, 6.6.2, 7.1, 8.2.2, 8.3.1, 9.3.3, 9.3.4, 9.3.5
K_3	third-order coefficient	6.2.1, 6.4.3, 7.1, 8.3.1, 9.3.3, 9.3.5
k	stiffness	6.1.5
k_T	scale factor temperature coefficient	6.4.1
m_a	arm mass	6.1.5
M	test object mass	6.1.2
$\lvert M_i \rvert$	ith minor of A	9.3.4
N	number of test inputs	9.3.4
[**N**]	noise matrix	9.3.3
N_+	number of positive inputs	9.3.3, 9.3.4

N_-	number of negative inputs	9.3.3, 9.3.4
n_k	noise component	9.3.3
OA	output axis	7.1, 8.2.3, 8.3.1
PA	pendulous axis	7.1, 8.2.3, 8.3.1
r	residual	9.3.4
R	effective radius, distance from centrifuge rotation axis to sensor ECM	5.0, 5.2, 6.1.2, 6.1.6, 6.3.1, 6.3.2, 6.3.3, 6.6.2, 7.2.1, 9.3.3
$\vec{R}$	vector quantity of R	5.0, 5.2
R_{cm}	initial center of mass offset due to imbalance	6.1.5
R_e	equatorial radius of the earth	5.3
R_0	static value of arm radius	6.1, 6.1.5, 6.1.6, 7.2.1, 7.2.2, 7.2.6, 9.1.1, 9.3.3
R_+	radius for acceleration along +IA	6.1.7
R_-	radius for acceleration along −IA	6.1.7
ΔR	total deviation from nominal radius	7.2.1, 7.2.6, 9.3.3
ΔR_a	dynamic radius error proportional to a_c	7.2.1, 7.2.6
ΔR_{AS}	change in arm radius due to centrifugal loading beyond the static value	6.1.2
ΔR_d	nonlinear dynamic error in radius	7.2.1, 7.2.6
ΔR_{dcr}	shift in dynamic center of rotation	6.1.5
ΔR_+	radius deviation for +IA acceleration	7.2.1
ΔR_-	radius deviation for −IA acceleration	7.2.1
t	Student's t	9.3.4
t	time	6.3.1, 6.3.2, 6.4.1, 7.2.2, 7.2.3
t_1	period over which average centrifuge rate is measured	6.3.1, 6.3.2
$\vec{V}$	tangential velocity of the ECM with respect to the surface of the earth	6.3.3
α	coefficient of thermal expansion of the arm	6.1.6
δ	misalignment of rotation axis from vertical	7.2.4
δ_c	coning angle	6.2.2, 7.2.6
$\Delta\phi_{Ta}$	a_c proportional dynamic misalignment	7.2.5, 7.2.6
$\Delta\phi_{Td}$	nonlinear dynamic tangential misalignment	7.2.5, 7.2.6
$\Delta\phi_{Va}$	a_c proportional dynamic misalignment	7.2.5
$\Delta\phi_{Vd}$	nonlinear dynamic vertical misalignment	7.2.5

$\Delta\omega_d$	deviation from average centrifuge angular velocity	7.2.2, 7.2.6
δ_o	misalignment angle between IA and case reference IA about OA (rad)	7.1
δ_p	misalignment angle between IA and case reference IA about PA (rad)	6.2.3, 7.1, 9.3.3
δ_0	average arm misalignment from horizontal	7.2.4, 9.3.3
θ_g	projection of θ_{ri} on vertical plane containing IA	9.3.3
θ_{ri}	total misalignment angle between radius and IA	9.3.3
λ	latitude	5.3, 6.3.3
μ	normalized magnitude of largest residual	9.3.4
μ_c	confidence limit check value	9.3.4
ξ_+	random noise component	9.3.3
ξ_-	random noise component	9.3.3
ρ	density of centrifuge arm (mass per unit volume)	6.1.2
$\sigma(r)$	standard deviation of residuals	9.3.4
$\sigma(K_i)$	standard deviation of coefficient K_i	9.3.4
ϕ	phase of periodic variation at the start of the data sample	6.3.1, 7.2.6
ϕ_T	total sensor misalignment about a tangential axis including sensor and mount	6.2.2, 7.2.5, 7.2.6, 9.3.3
ϕ_{To}	initial mount displacement	6.2.2
ϕ_{T+}	static tangential misalignment of +IA	7.2.5
ϕ_{T-}	static tangential misalignment of −IA	7.2.5
ϕ_V	sensor misalignment about vertical axis	6.2.3, 7.2.5, 7.2.6, 9.3.3
ϕ_{Vo}	initial alignment angle about vertical axis	6.2.3
ϕ_{V+}	static vertical misalignment for +IA	7.2.5
ϕ_{V-}	static vertical misalignment for −IA	7.2.5
Ω	earth rotation rate, also known as earth rate	5.3, 7.2.6
$\vec{\Omega}$	vector quantity of earth rotation rate	6.3.3
Ω_V	local vertical component of earth rotation rate	6.3.3, 7.2.3, 7.3.6
ω	centrifuge rotational angular velocity	5.2, 6.1.5, 6.3.3, 6.6.2, 7.2.2
$\vec{\omega}$	vector quantity of ω	5.2
ω_p	amplitude of centrifuge periodic angular velocity variation	6.3.1, 7.2.2, 7.2.6
ω_s	centrifuge angular velocity at start of data sample	6.3.2, 7.2.2, 7.2.6
$\omega(t)$	instantaneous centrifuge angular velocity	6.3.1, 6.3.2

ω_0	average centrifuge angular velocity	6.3.1, 6.3.2, 7.2.2, 7.2.3, 7.2.6, 9.1.1
ω_n	natural resonant frequency of centrifuge structure	6.1.5

4. Summary

The term "centrifuge" is used in this document to mean a device consisting of a motor- or engine-driven arm structure with sufficient dimensions and strength to allow the rigid mounting and subjecting of one or more inertial-grade accelerometers to centripetal acceleration levels ranging from fractions of 1 *g* to over 200 *g*. The term "precision" suggests an exactness or advancement in the state-of-the-art over and above environmental survivability centrifuge testing. Precision centrifuge testing is used to calibrate accelerometer model parameters. The accuracy required for this calibration depends on the application of the accelerometer. Typical applications are shown in Table 1, which may be used as a general guideline.

Table 1 — Accelerometer performance

Maximum range		Super high	High	Medium	Low
m/s^2	(*g*)	performance (10 ppm CE or better)[a]	performance (100 ppm CE)	performance (1000 ppm CE)	performance (1% CE)
10–200	1–20	Inertial navigation	Guidance (ship/aircraft/cruise missile)	Attitude control	Attitude control Switch-stage separation Instrumentation
200–2000	20–200	Ballistic missile	Tactical missile	Ordnance	Instrumentation
1000–3000	100–300	Earth re-entry Planetary entry	Earth re-entry Planetary entry	Switch-fusing Missile re-entry	Car crash Instrumentation
$3000–1\times10^6$	$300–1\times10^5$		Jupiter entry	Artillery Rail gun	Car crash Instrumentation Fusing

[a] The acronym "ppm CE" means "parts per million composite error" (IEEE Std 528-2001).[3]

It is standard practice of both manufacturers and users to first characterize inertial accelerometers in a 1-*g* field through the use of an earth-bound dividing head or precision rotational device of some kind (IEEE Std 1293-1998). This allows "precise" graduations of 1-*g* acceleration to be applied to an accelerometer for the purpose of measuring its scale factor and error coefficients. Unfortunately, the 1-*g* maximum limit that can be reached using this method is usually far less than the acceleration level experienced in the application. A common test for force rebalance accelerometers is to insert a current into the accelerometer's torquer in an attempt to simulate the acceleration levels required in the application. This test, however, demonstrates only that the accelerometer electronics will handle currents associated with the higher *g* levels expected.

Linear vibrators and rocket sleds may also, in certain cases, be used to measure accelerometer performance characteristics. The fact remains, however, that centrifuge testing must generally be used to perform precision measurements.

The practice recommended in this document is intended to be useful to a broad spectrum of centrifuge users. Since the needs of a user interested in routine testing of a high-volume 1% accelerometer differ

[3]Information on references can be found in Clause 2.

substantially from those of a designer doing developmental testing on a highly specialized 10-ppm accelerometer, each clause contains information that pertains to the different levels of precision. Therefore, one may extract the information pertinent to any desired level without becoming deeply involved in considerations that are inappropriate.

In addition to the procedures and supporting theory, which are the heart of the document, there are eight annexes. Annex A describes the features of some typical centrifuge installations, including a look at hardware designed for different production rates and different levels of precision.

Annex B continues this analysis with a description of methods for evaluating a given centrifuge installation. Annex C provides further background for the data reduction clause by presenting a limited treatment of the theory of fitting model equations to noisy test data, including such variations as percentage weighted fits and "Min–Max" fitting.

Annex D describes the theoretical and practical limitations of centrifuge testing, and outlines some alternative test methods that might be used to evaluate certain aspects of accelerometer behavior at high *g* levels. Double turntable centrifuge and tilted-centrifuge testing are described.

Annex E describes the processing of dual-proof-mass vibrating beam accelerometer (VBA) centrifuge data. Annex F discusses scale factor calibration for high-*g* applications on an ultra-centrifuge. Annex G discusses thermal control and data acquisition on the centrifuge arm. Annex H is a bibliography.

Distributed through the document are treatments of special subjects, such as the use of supplemental tests and supplemental analyses to support centrifuge testing, dual accelerometer centrifuge testing as well as arm stretch and droop measurements to remove the effects of arm stretch and droop, and recommendations about the use of combined environments.

5. Model equations

Centrifuge testing, while capable of great precision, must be a carefully designed experiment to minimize the many possible error sources peculiar to this type of testing.

In order to develop centrifuge test techniques and understand error mechanisms, mathematical models showing input/output relationships for the centrifuge and accelerometer are developed in this and subsequent clauses. The accelerometer to be modeled is based on the pendulous torque-balance type instrument, but the principles are applicable to other types.

In centrifuge testing, the accelerometer is mounted on the centrifuge arm in a fixture that holds it in fixed alignment with respect to the acceleration vector. Assume a coordinate system X, Y, and Z with the origin at the intersection of the arm and the centrifuge spin axis with X along the arm and Z along the spin axis. The spin axis is aligned with local vertical and the directed distance from the spin axis to the effective center of mass (ECM) is defined as R, as shown in Figure 1.

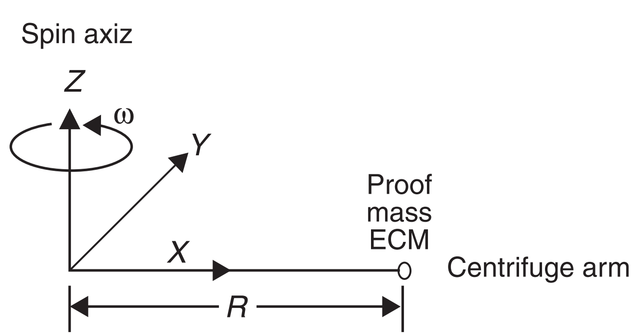

Figure 1—Accelerometer mounted on centrifuge

5.1 Simplified accelerometer model

Ideally, the acceleration indicated by the accelerometer is expressed as

$$a_s = \frac{E}{K_1} = K_0 + a_i \tag{1}$$

where

a_s is the indicated sensor output (g),

E is the sensor output (output units),

K_1 is the sensor scale factor (output units per g),

K_0 is the bias (g),

a_i is the acceleration along sensor input axis (IA) (g).

Although the SI unit of acceleration is the meter per second squared, accelerometer output is often expressed in terms of g, the magnitude of the local plumb-bob gravity (see 3.1.13).

This simplified model may be satisfactory for some applications, but for more precise applications a model equation including nonlinear and cross-axis terms may be required (see Clause 7).

5.2 Simplified centrifuge model

Ideally, the centripetal acceleration of the centrifuge (a_c) imposed on the instrument under test is expressed as

$$\vec{a}_c = \vec{\omega} \times \left(\vec{\omega} \times \vec{R}\right) \quad \text{(length per unit time squared)} \tag{2}$$

where

$\vec{\omega}$ is the centrifuge rotational angular velocity (rad/s),

$\vec{R}$ is the directed distance from rotation axis to the ECM.

and since $\vec{R}$ is perpendicular to $\vec{\omega}$

$$\vec{a}_c = -\omega^2 \vec{R} \tag{3}$$

with magnitude

$$a_c = \omega^2 R \tag{4}$$

The total test input ($\vec{a}_T$) applied at the ECM is centripetal acceleration plus local gravity ($\vec{g}_L$):

$$\vec{a}_T = \vec{a}_c + \vec{g}_L \tag{5}$$

The component of $\vec{a}_T$ along IA is a_i.

The primary unit of these quantities is usually normalized to local g units (see 5.3), whereby g_L becomes unity.

This simplified model may be satisfactory for some applications, but for more precise applications, a detailed model equation of the centrifuge, with higher-order terms resulting from temperature, mechanical interactions, and instrumentation errors, may be required.

These errors are different for every centrifuge and measurement system and must be individually evaluated for significance. An individual model equation containing only the significant error terms must be developed for each setup. In order to develop a custom model equation, typical error equations for each error source identified are listed in Clause 6 so that they can be evaluated and significant terms combined in cookbook fashion to provide a correct equation for each test.

5.3 Simplified gravity model

The term "local gravity" (g_L) as used in this recommended practice refers to "plumb-bob gravity," which is the force per unit mass exerted by the earth on a mass that is at rest relative to the earth. Its direction defines the local vertical and its magnitude is that of the vector sum of Newtonian gravitational force per unit mass and the centripetal force arising from the earth's rotation, divided by the mass.

According to Newton's law of gravity, there exists a mutual attractive force F between any two masses m_1 and m_2 at a distance d between their effective centers so that

$$F = \frac{G m_1 m_2}{d^2} \tag{6}$$

where G is the gravitational constant

$$G = 6.67259 \times 10^{-11}\ \mathrm{m^3/(kg \cdot s^2)} \tag{7}$$

In the case where one of the masses is the earth (5.975×10^{24} kg), a gravitational field may be defined at the surface such that the force on a test mass is

$$F = m g_N \tag{8}$$

where g_N is the Newtonian gravitation.

Since this has the same form as the inertial law

$$F = ma \tag{9}$$

and the theory of relativity states that, in principle, the effects of gravitation and acceleration are indistinguishable, g_N is defined as the gravitational acceleration and has the units of length per unit time squared.

The centripetal acceleration due to the earth's rotation in inertial space is perpendicular to the earth's rotation axis and is nominally

$$a_b = R_e \Omega^2 \cos\lambda \quad \text{in magnitude} \tag{10}$$

where

Ω is the earth rotation rate,

R_e is the earth equatorial radius,

λ is the latitude of the mass.

At the equator, this amounts to $0.03392\ \mathrm{m/s^2}$ and decreases to zero at the poles. The local acceleration due to gravity g_L is the vector difference of the gravitational attraction acceleration and the earth rotation centripetal acceleration.

The acceleration of gravity also varies because the earth is not spherical and because of density variations in the earth's crust. The acceleration of gravity is further affected by elevation. A typical equation for the variation of g_L with latitude λ and altitude h (in meters) is approximated by

$$g_L = 9.780356(1 + 0.0052885 \sin^2 \lambda - 0.0000059 \sin^2 2\lambda) - 3.086 \times 10^{-6} \quad \mathrm{m/s^2} \tag{11}$$

(See *International Critical Tables*, *Vol. 1*, [B7] and *CRC Handbook of Chemistry and Physics 1997–1998* [B2].) By international agreement, the standard value of gravity is defined to be $9.80665\,\mathrm{m/s^2}$.

This value corresponds closely to the formula value at 45° latitude and sea-level elevation.

The downward force of gravity acting on the proof mass and case of an accelerometer at rest on the earth is balanced by the upward restoring force of the support acting on the case of the accelerometer. For a torque or force servoed rebalanced accelerometer, since the upward force on the case requires an additional servoed restoring force of the same polarity on the proof mass to keep the proof mass at its null position, and the measure of accelerometer output is the restoring force or torque on the proof mass, the output of an accelerometer at rest on the earth therefore indicates an acceleration of g_L upward. A similar argument for an open-loop accelerometer against an elastic restraint or a vibrating beam accelerometer yields the same result.

In the calibration of an accelerometer scale factor, the local plumb-bob gravity acceleration g_L is frequently used as a reference.

For accelerometer testing, the local value of gravity g_L should be determined by an organization that specializes in performing such surveys. In the United States, gravity and site location surveys are carried out by the U.S. Coast and Geodetic Survey and the National Imagery and Mapping Agency (formerly Defense Mapping Agency). More information can be obtained from Internet Web sites.

6. Test error sources

This clause endeavors to identify many frequently encountered error sources, and to provide a means to evaluate their significance to the test planned. This clause is organized in the fashion of an expansion in partial derivatives or sensitivity coefficients. Each subclause examines one error source and evaluates its contribution to total error, as though it were the only error source acting. Subclause 6.6.2 considers those few cases where error sources interact sufficiently that their combined effects may need to be examined as a separate issue. To the extent possible, the forms of the errors are described as an aid to their identification in test data. Error effects are accordingly described in terms of their ability to masquerade as test unit errors when not properly identified and corrected. In particular, they are described in terms of errors in evaluation of the coefficients of a model equation, such as that described in Clause 7.

Measures must be taken to minimize or compensate for significant errors that would be based on the level of precision required in the particular application. These measures can take the form of instrumentation added to a basic centrifuge, or special test procedures (such as multiple-sensor testing to reject common mode errors), or both.

6.1 Radius uncertainty

A major problem of centrifuge testing is radius uncertainty. Factors contributing to this uncertainty are

a) uncertainty in the static radius;
b) dynamic changes in radius; and
c) changes in radius due to the environment.

Each contributor to radius uncertainty will be discussed and examples given to show the magnitude of the errors they may cause.

6.1.1 Uncertainty in static radius

To determine the static radius to the ECM of the test accelerometer, it is necessary to know the location of the center of the arm, the location of the ECM relative to the reference surfaces of the accelerometer, and the dimensions and interfaces of all the mechanical components between these points, including test fixtures. For high-precision applications, it may be necessary to know this stack-up of dimensions to an overall accuracy on the order of 1 μm. On a 1-m nominal radius machine, for example, 1 μm introduces an error in applied acceleration of 1 ppm.

Few, if any, centrifuges provide a direct means to measure static radius to useful accuracies, even assuming that the position of the ECM inside the accelerometer is accurately known. Therefore, the static radius must be estimated from the output of the instrument under test.

Many estimation techniques have been used to determine static radius, and the most popular of these are described in Clause 9 and Annex C. In 9.3.3, this document introduces an algorithm that puts this estimation on a statistically rigorous footing.

A necessary condition for these estimates to be accurate is that the radius must be fixed during the test, or that changes in radius during the test are compensated for in the input data.

6.1.2 Arm stretch

Arm stretch (ΔR_{AS}) is the elongation of the mechanical structure connecting the accelerometer to the centrifuge spin axis beyond the static value (R_0), and is due to centrifugal loading. If the radius change is due only to arm stretch, the equation for radius is

$$R = R_0 + \Delta R_{AS} \tag{12}$$

or

$$R = R_0\left(1 + \frac{\Delta R_{AS}}{R_0}\right) \tag{13}$$

Because the arm stretch is proportional to load (hence acceleration a), one can write

$$R = R_0\,(1 + C_{AS}\,a) \tag{14}$$

where C_{AS} is a constant whose dimension is the inverse of acceleration, or alternatively acceleration divided by acceleration squared. Then

$$a = R\omega^2 = R_0\,(1 + C_{AS}\,a)\,\omega^2 \tag{15}$$

This error increases the magnitude of the applied acceleration for either polarity and is therefore an odd-quadratic term (K_{oq}) in the accelerometer output data. In testing precision accelerometers, every effort should be made to estimate the effect of arm stretch and, if significant, to correct the input acceleration data.

The magnitude of this error can be estimated by calculating its value for the simple case of an arm with constant cross-section by integrating the elastic strain over its length. For the component due to loading of the arm by its own mass:

$$S(x) = \frac{1}{A}\int_0^x \omega^2(R - x')\rho A\,dx' = \rho\omega^2\left(R_{\mathrm{x}} - \frac{x^2}{2}\right) \tag{16}$$

where

$S(x)$	is the stress at x,
R	is the test radius (arm length),
x, x'	are distances inward from the stress-free end,
A	is the cross-sectional area,
ρ	is the density (mass per unit volume).

Then, strain $= S/Y$ (dimensionless) and

$$\frac{\Delta R}{R} = \frac{1}{R}\int_0^R \frac{S}{Y}\,dx = \frac{(\rho/y)\omega^2 R^2}{3} \tag{17}$$

where Y is Young's modulus.

It should be noted that the strain is independent of the constant cross-sectional area A. Furthermore, it is also nearly independent of the arm material for those materials commonly used in precision centrifuges, such as steel or aluminum, for which

$$\frac{\rho}{Y} \approx 3.8 \times 10^{-8}\ \mathrm{s}^2/\mathrm{m}^2 \tag{18}$$

Replacing $\omega^2 R^2$ with $R_0 a$ gives

$$\frac{\Delta R}{R} = \frac{R_0 a}{3}\frac{\rho}{Y} = C_{\mathrm{AS}}\,a \Rightarrow C_{\mathrm{AS}} = \frac{R_0}{3}\frac{\rho}{Y} \tag{19}$$

where C_{AS} is the nonlinearity coefficient caused by stretch of the bare arm. For a 1-m radius, its value is 1.27×10^{-8} $(\mathrm{m/s^2})^{-1} = 0.12\ \mu g/g^2$.

The arm stretch due to the test-object mass will add to that of the bare arm. The tensile load is the test-object mass M multiplied by the acceleration. The corresponding tensile stress is

$$S = \frac{Ma}{A} \tag{20}$$

giving

$$\frac{\Delta R}{R} = \frac{1}{R}\int_0^R \frac{S}{Y}\,dx = \frac{Ma}{AY} \tag{21}$$

In this case, both area and arm material are clearly significant. As an example, if the 1-m arm is of aluminum with a cross-sectional area of $0.01\ \mathrm{m}^2$, a 5-kg test object will produce an additional stretch equivalent to $C_{\mathrm{AS}} = 7.04 \times 10^{-9}$ $(\mathrm{m/s^2})^{-1} = 0.07\ \mu g/g^2$.

6.1.3 Accelerometer proof mass deflection

The effects of proof mass deflection under applied acceleration are indistinguishable from those of arm stretch, since both result in a change of radius to the ECM proportional to applied centripetal acceleration and both will produce an apparent odd quadratic term (K_{oq}) in the accelerometer output data. It differs only in that it is produced by an interaction between test-unit and test-bed characteristics and cannot be characterized in the same way that a fixed test-bed error might be. The magnitude of the deflection can vary from near-zero to as much as 2.5 μm/g, depending on sensor design. Accelerometer packages that contain internal isolators may experience large deflections. Since the deflection is internal to the accelerometer or sensor package, physical measurements of the effect cannot be made on the centrifuge. However, the deflection can be estimated and used to correct the input data if the static compliance of the constraint is known.

For example, if the accelerometer being tested has a proof mass compliance such that the natural frequency is 1000 Hz (equivalent to a translational mass-spring system with a deflection of 0.25 μm/g), then with a 1-m distance to the center of rotation, the increase in distance per g is 0.25 ppm. This results in an apparent 0.25 μg/g^2 odd-quadratic error due to gradient in acceleration applied by the centrifuge. Note that this error is comparable in magnitude to that in the arm stretch example of 6.1.2.

6.1.4 Arm bending

Since the arm of a centrifuge has a finite stiffness, it will tend to sag due to the effects of gravity. Centrifugal forces acting on imbalances of the arm may cause bending in the vertical and/or horizontal plane.

The output of an ideal accelerometer (see 5.1) consists of a bias term (K_0) and a linear term proportional to acceleration along the input axis ($K_1 a_i$). When testing an accelerometer on a centrifuge, the bias term will include a component of local gravity if the input axis is not perfectly horizontal. Arm bending may also cause this misalignment to change as a function of a_c.

A secondary effect of arm bending is the resulting radius change due to the change of end slope during the test. This has the same form of error as arm stretch and will appear as an acceleration-squared term. If a high degree of precision is required, it is important to locate the ECM of the accelerometer as close as possible to the neutral axis of the arm, thereby minimizing the effects of arm bending. For typical centrifuges, deflections are on the order of a fraction of a milliradian, and the resulting radius change due only to beam curvature is less than 1 ppm. However, for a 1-m radius centrifuge where the ECM of the test accelerometer is mounted 15 cm above the arm neutral axis, a beam deflection of 1 mrad will produce a radius error of 150 ppm.

6.1.5 Dynamic center of rotation

The centrifuge axis of rotation is defined by a set of bearings that may be ball, roller, hydrodynamic, or other. Good-quality bearings typically control the axis of rotation within 0.1 μm at slow speeds. If the arm is balanced along its axis and in the vertical plane, that accuracy will be maintained at the higher speeds required for accelerometer tests. If the centrifuge arm with the accelerometer and its mounting fixture is unbalanced in a vertical plane, the resulting torque will cause the axis of rotation to tilt. If the arm is balanced in the vertical plane but unbalanced radially, the axis of rotation will shift radially and may also tilt, depending on the location of the radial bearings and on their individual stiffnesses. Thus, in general, the axis of rotation will move in some orbital fashion that differs from that defined by the bearings at slow speed.

The simplest case to consider is that of a planar approximation in which the arm imbalance is static only—i.e., the arm is loaded symmetrically above and below its neutral axis, but one end is slightly heavier than the other so that the center of mass is shifted slightly along the arm axis by a distance

R_{cm}. Then, as the arm rotates, it will shift in the direction of the initial offset due to the centrifugal force on the arm. The offset is given approximately by

$$\Delta R_{dcr} = \frac{(R_{cm} + \Delta R_{dcr}) m_a \omega^2}{k} \tag{22}$$

where

ΔR_{dcr} is the shift in the dynamic center of rotation,

R_{cm} is the initial center of mass offset due to imbalance,

m_a is the arm mass,

ω is the centrifuge rotational angular velocity,

k is the radial stiffness.

The term "radial stiffness" is a direct measure of the resistance of the centrifuge axis to deflection due to a horizontal force at the center of rotation, and must include the effects of all compliances of the structure, including the bearings, connection to the floor, and the foundation on which the machine is mounted. Then

$$\Delta R_{dcr} = \frac{R_{cm}(m_a \omega^2 / k)}{1 - (m_a \omega^2 / k)} \approx R_{cm}\left(\frac{m_a \omega^2}{k}\right) \tag{23}$$

This approximation corresponds to assuming $m_a \omega^2 / k \ll 1$, or $(\omega/\omega_n)^2 \ll 1$, where $\omega_n{}^2 = k/m_a$; i.e., assuming that the rotational frequency is much smaller than the resonant frequency of the arm on its bearings and support structure. Since ω, the centrifuge rotational angular velocity, rarely exceeds 5 revolutions per second, the assumption is usually true.

In this case, ΔR_{dcr} is proportional to ω^2, and therefore is proportional to the nominal centripetal acceleration a_0. Substituting the proportionality constant C_{dcr},

$$R = R_0 + \Delta R_{dcr} = R_0 (1 + C_{dcr} |a_0|) \tag{24}$$

The centripetal acceleration is then

$$a_c = \omega^2 R_0 (1 + C_{dcr} |a_0|) = a_0 (1 + C_{dcr} |a_0|) \tag{25}$$

The effect of an imbalance in the centrifuge arm is to introduce a false second-order term. If C_{dcr} remains unchanged when IA is reversed, then only the odd-quadratic nonlinearity coefficient K_{oq} will be affected. If C_{dcr} changes sign but not magnitude when IA is reversed, then only the quadratic coefficient K_2 will be affected. In either of these cases, the magnitude of the coefficient error will be C_{dcr}.

In general, C_{dcr} will be different for the two polarities, so both K_2 and K_{oq} will be affected.

The significance of this term is most readily appreciated by an example. Assume

$\Delta R_{dcr} = 100\ \mu m$

$R_0 = 1\ m$

$a_0 = 30\ g$

Then

$$C_{dcr} = 3.3\,\mu g/g^2 \tag{26}$$

The 100-μm motion is unlikely to be noticed without sensitive instrumentation, whereas $3.3\,\mu g/g^2$ can be quite significant.

The assumptions used in this simple analysis are valid in a great many cases. Sometimes, the signature of imbalance may be more complicated. For example, it may not be true that $\omega \ll \omega_n$, in which case a significant fourth-order term appears and the structure may even pass through resonance where phase effects become significant. In addition, the bearing structure may not be isoelastic and its compliance will then vary cyclically with arm rotation.

6.1.6 Thermal expansion

Since the acceleration produced by the centrifuge is directly proportional to the arm length, any change of length caused by thermal expansion represents an error source. In its simplest form, where the entire centrifuge arm is operating at a temperature different from that where the arm length was measured, the arm length can be computed as

$$R = R_0(1 + \alpha\,\Delta T) \tag{27}$$

where

ΔT is the temperature rise above calibration temperature,

α is the coefficient of thermal expansion of the arm.

It should be noted that a number of difficult complications can arise in situations where this error source is significant, where the temperature of the arm is a function of time as a result of heating or cooling during the centrifuge run itself, or where there is a significant heat flow along the arm that causes a temperature gradient to exist. In these cases, the arm temperature must be monitored and the input acceleration data corrected for the changes in R_0.

As a quantitative example, when the arm is made of cast iron with $\alpha = 13$ ppm per degree Celsius, and the arm temperature changes 5° from the calibration temperature, a change in arm length of 65 ppm results.

6.1.7 Radial asymmetry with acceleration polarity

The radius errors described in 6.1.1 acquire a special importance when the test unit IA is reversed to test both the positive and negative parts of the input range. Since the location of the ECM is typically not known within 0.8 mm, there is almost always a significant change in radius when the input axis is reversed. If this change is not compensated for, the resulting output data will appear to have scale factor asymmetry, which can easily corrupt estimates of linearity coefficients.

Even-order coefficients are strongly affected by such asymmetry, and radius estimates based on approximations are frequently not accurate enough to avoid gross errors in these coefficients. The best-known way to minimize this effect is to use the algorithm of 9.3.3, with separate measurements of positive and negative scale factor where needed.

For example, if the ECM location is in error by 1 mm on a 1-m radius centrifuge, the error will be 1000 ppm. At the $50\,g$ level, this amounts to $50\,g \times 1000\,\text{ppm} = 50{,}000\,\mu g$, the same error produced by a K_2 of $20\,\mu g/g^2$ at $50\,g$.

6.1.8 Instrumentation methods and errors

The determination of centrifuge radius can be divided into two areas: the determination of the nominal or static radius and the determination of dynamic changes in radius. The static radius can be determined several ways, depending on the accuracy of the test to be performed. Measurements of the radius may be possible with a mechanical arrangement such as an Invar rod and a micrometer. However, the accuracy of measurements by this method is typically limited by endpoint determination to about 1000 ppm. For greater accuracy, it is usually preferred to let the test item measure the static radius. This is covered in depth in Clause 9, Data reduction.

Several devices and methods are available for measuring dynamic radius changes. Each device must not only measure the stretch of the centrifuge arm, but must also measure any changes in the dynamic center of rotation. If the device itself cannot do this, it must be supplemented with other devices.

A laser interferometer is an optical device that may be mounted either on- or off-board of the centrifuge arm. A major advantage of optical systems is that, assuming provisions for optical access have been made, the radius growth can be measured right at the test item. Another advantage is that the output of the device, analog or digital, is continuously available for monitoring. The major disadvantages of this system are its sensitivity to temperature and air density, typically producing errors of several parts per million under normal laboratory conditions. If more precise measurements are required, the optical path should be evacuated and the temperature controlled.

Proximity detectors (capacitive, inductive, or laser) are devices that are usually mounted off-board and measure the distance and droop between the wall and the centrifuge arm as it goes by. They do not use any centrifuge slip-rings and they are not exposed to forced convection heat transfer currents. They are reliable, easy to use, and inexpensive. However, they do have two major disadvantages. Their output is valid only as the arm or the test item swings by, so the data must be sampled by some kind of fast-sampling analog-to-digital converter, since it is valid for only a few milliseconds. Second, the proximity detectors cannot measure the stretch of the arm at the test package, but must instead look at the surrounding structure, which may not be indicative of that at the test package.

Radius measurement devices cannot be used to compensate for the uncertainty in the location of the ECM or for asymmetry with acceleration polarity. These problems are most readily handled during the data reduction and are discussed in Clause 9. Another technique for compensating for arm stretch effects is to use dual accelerometer testing (see 6.6.3).

6.2 Alignment uncertainty

In order to properly define the accelerations along the principal accelerometer axes, it is necessary to know the misalignments between those axes and the centrifuge arm, the axis of rotation, and the gravity vector. In some cases, dynamic terms that cause deflections or changes in the alignment due to centripetal loading or temperature changes must be considered. These error sources must be considered whenever appropriate to achieve the level of precision required.

6.2.1 Static leveling error

Static leveling error refers to errors in the acceleration seen by a test item due to misalignments of the accelerometer IA to the centrifuge and gravity vector. A static error is one that is present when the centrifuge is not rotating, and may change with arm position. Typical misalignments are between an accelerometer IA and its mounting surface, the mounting surface and the centrifuge rotation axis, and the rotation axis relative to gravity. As long as the misalignments are truly static (i.e., they do not change as a function of the centrifuge g level), they affect the apparent bias (zero-order term in the data) but have little or no effect on the higher-order coefficients (K_2 and K_3). For this reason, a centrifuge test cannot be used to accurately determine the accelerometer bias, but as long as the misalignments are less than about 1°, their effects on the K_2 and K_3 coefficients are negligible.

Tilting of the main centrifuge rotation axis is an error source that requires special consideration, in that the acceleration input has a component that varies sinusoidally with each revolution but is independent of centrifuge angular velocity. This error can be eliminated by averaging the accelerometer output over complete revolutions of the arm. At zero rate, a number of readings must be taken and averaged, with the arm stopped at equally spaced intervals through 360°.

6.2.2 Dynamic leveling error

For an accelerometer mounted with its IA nominally parallel to the centrifuge centripetal acceleration vector, any angular deflections of the mounting fixture about a horizontal line perpendicular to the acceleration vector result in a change in the component of gravitational acceleration along the accelerometer IA. A change in the component of centripetal acceleration along the IA also results. Considering this misalignment, the acceleration along the IA can be written as

$$a_i = a_c \cos \phi_T + g_L \sin \phi_T \tag{28}$$

where

a_i is the acceleration along sensor IA,

a_c is the centripetal acceleration of the centrifuge,

ϕ_T is the mount deflection angle,

g_L is the local value of gravitational acceleration unit.

For most applications, small angle approximations can be used for $\sin \phi_T$ and $\cos \phi_T$, giving

$$a_i = a_c + g_L \phi_T \tag{29}$$

If ϕ_T varies linearly with centripetal acceleration, it can be written as

$$\phi_T = \phi_{To} + C_d a_c \tag{30}$$

where

ϕ_{To} is the initial mount misalignment,

C_d is the deflection coefficient (angle/a_c).

The acceleration along the sensor IA becomes

$$a_i = a_c (1 + g_L C_d) + g_L \phi_{To} = \omega^2 [R (1 + g_L C_d)] + g_L \phi_{To} \tag{31}$$

The proportional term, $a_c g_L C_d$, produces additional acceleration in the test-unit input axis, which is indistinguishable from that which would be caused by a small change in the test radius, as shown in the second part of the equation. Since the true radius is never known exactly in a centrifuge test and must be estimated by means of the separately measured scale factor, this change produces no error in the indicated nonlinearity. A coefficient of 1 arc-second per g is equivalent to a radius change of only 5 ppm.

The constant term, $g_L \phi_{To}$, is similar to a change in accelerometer bias in that it produces a small change in indicated acceleration, which is added to all data points. For example, 1 arc-second is equivalent to 5 μg. Angles in excess of 0.5° are required to produce significant errors in indicated nonlinearity, even in precision testing.

However, when the sensor IA is not approximately parallel to the arm, small deflections can strongly affect recovery of the nonlinearity, coefficients. For example, when the IA is vertical, the acceleration along its IA is

$$a_i = a_c \sin \phi_T + g_L \cos \phi_T \tag{32}$$

or, using small angle approximations,

$$a_i = a_c \phi_T + g_L \tag{33}$$

If ϕ_T varies linearly with centripetal acceleration, this becomes

$$a_i = C_d a_c^{\ 2} + \phi_{To} a_c + g_L \tag{34}$$

If not compensated for, this results in errors in determining accelerometer cross-axis sensitivities to the square of acceleration. For example, a deflection of 1 arc-second results in a $5\,\mu g/g^2$ error in the determination of the coefficients K_{oo} or K_{pp}.

A common source of dynamic leveling error is the mode of motion called "coning." When a centrifuge turns very slowly, its axis of rotation defines a line that is fixed in the rotating structure. The line perpendicular to this rotating structure axis through the ECM of the accelerometer under test defines the centrifuge arm axis. As the centrifuge angular velocity is increased, forces due to imbalance can drive the elastic compliance of the bearings and their support structure to cause the structure axis to trace out a cone about the rotation axis, as shown in Figure 2. This motion is synchronous with the basic rotation rate, ω.

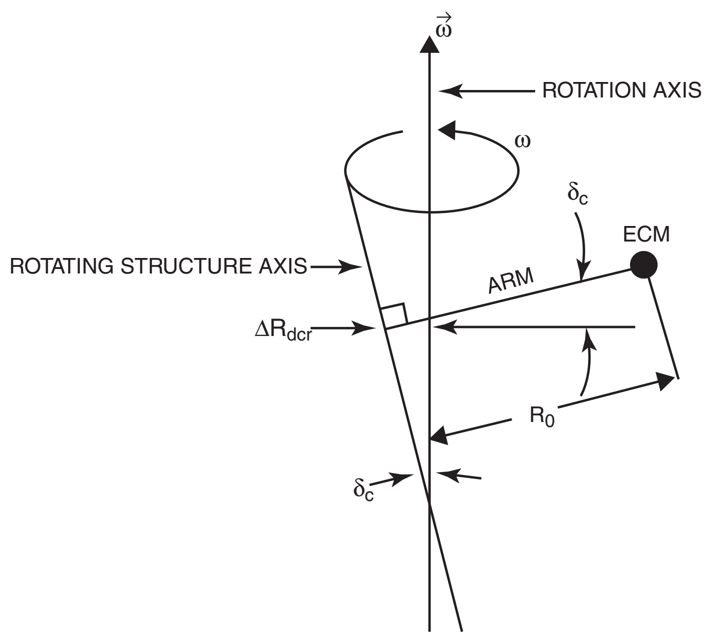

Figure 2—Centrifuge coning

The radius of the cone as measured at the level of the centrifuge arm is the radius change due to a shift in the dynamic center of rotation, R_{dcr}, which was introduced in 6.1.5. The cone angle δ_c is a contributor to dynamic leveling error. Coning is a prominent feature of many centrifuge analyses for two reasons. First, the displaced structure axis/arm coordinate system is the one to which test fixtures are typically related. Second, the geometry of the coning motion is one of the features commonly measured by auxiliary instrumentation, such as bearing support motion detectors.

6.2.3 Sensor misalignment about a vertical axis

Misalignments and changes of the IA about a vertical axis have no effect on the coupling of gravity, but they do affect the component of a_c that lies along the sensor IA. Static misalignment creates only a scaling error, which is indistinguishable from radius uncertainty. Changes in misalignment that are a function of applied acceleration, e.g., due to arm and fixture compliances, may produce linearity errors in the input acceleration that can masquerade as linearity errors in the sensor output. These linearity effects generally can be identified and compensated for by means of multiple-orientation testing.

Multiple-orientation testing may require specification of nominal angles with respect to the centripetal acceleration vector that are too large to be treated by small angle approximations. The format of the rotation angle ϕ_V, accordingly, is somewhat different than in the previous clause:

$$\phi_V = \phi_{Vo} + C_d a_c \tag{35}$$

$$a_i = a_c \cos \phi_V \tag{36}$$

where

ϕ_{Vo} is the initial alignment angle,

$C_d a_c$ is the variation in ϕ_V due to a_c.

Since $C_d a_c$ is assumed to be a small angle, trigonometric approximations may be used in the expansion of cos ϕ_V:

$$\cos \phi_V = \cos \phi_{Vo} \cos(C_d a_c) - \sin \phi_{Vo} \sin(C_d a_c) = \cos \phi_{Vo} - C_d a_c \sin \phi_{Vo} \tag{37}$$

$$a_i = a_c \cos \phi_{Vo} - C_d a_c \sin \phi_{Vo} \tag{38}$$

The first a_i term, which contains only static components of ϕ_V, shows only a small error in apparent radius due to uncertainties in ϕ_{Vo}, generally within the uncertainty band for radius. The second term adds a quadratic linearity error.

If the test sensor is assumed to have linearity errors of the form

$$a_s = a_i + K_2 a_i^{\,2} + K_{ip} a_i a_p + K_{pp} a_p^{\,2} + \text{terms containing } a_o, a_o a_i, \text{ or } a_o a_p \tag{39}$$

and a_o is small, then to second order in a_c

$$a_s = a_c \cos \phi_{Vo} + K_2\, a_c^{\,2} \cos^2 \phi_{Vo} + K_{ip}\, a_c^{\,2} \cos \phi_{Vo} \sin \phi_{Vo} + K_{pp}\, a_c^{\,2} \sin^2 \phi_{Vo} \tag{40}$$

More than one orientation will be required to separate all the input and output terms that contain a_c^2. When $\phi_{Vo} = 0^\circ$, there is no input error due to the effects of this clause, so K_2 can be determined unambiguously. When $\phi_{Vo} = 90^\circ$, the C_d input error can be confused with the K_{pp} output error. If the test is repeated with $\phi_{Vo} = -90^\circ$, however, and the fixture design is such that C_d does not change, the input error will change sign, allowing the two effects to be separated. Similarly, if $\phi_{Vo} = 45^\circ$, even after the K_2 and K_{pp} terms are accounted for, there remains a C_d term that can masquerade as K_{ip}. Once again, if the test is repeated at 225°, the input error will change sign while the output error remains unchanged.

The magnitude of the effect depends, of course, on the accuracy and compliance of the fixture. If the uncertainty in ϕ_{Vo} is 0.001 rad, and $C_d a_c = 0.001$ rad at $a_c = 20\,g$, then $C_d = 50\,\mu\text{rad}/g$. The apparent error varies from zero at $\phi_{Vo} = 0^\circ$ to 0.1% at $\phi_{Vo} = 90^\circ$. The K_{pp} error, if uncorrected, is $50\,\mu g/g^2$ and the K_{ip} error is $70\,\mu g/g^2$.

6.2.4 Misalignment about a radial axis

Misalignment of the test item about a radial centrifuge axis will have no effect on tests conducted with the accelerometer IA along the centrifuge arm. For orientations in which the accelerometer IA is perpendicular to the centrifuge arm, this misalignment will result in a component of gravitational acceleration being sensed by the accelerometer. This misalignment, if not compensated for, results in an apparent bias error but does not affect the determination of accelerometer nonlinearities, the primary purpose of most centrifuge tests.

6.2.5 Instrumentation methods and errors

The measurement of angular deflections of the test item about any of three orthogonal axes is best accomplished by some on-board device, as the nature of the rotating centrifuge environment makes the detection by some stationary off-board device nearly impossible. The most practical on-board devices are the same ones that are used for dynamic radius measurements (see 6.1.8). The same arguments as before apply for the optical and proximity detector devices, so the accuracy, readout resolution, slip-ring requirements, etc., for the device must be selected commensurate with the test requirements.

The reference with which these measurements are taken must be chosen with care. The measurement should be made with respect to some fixed reference (i.e., gravity). However, since the device is mounted on the centrifuge arm, it can move relative to the reference. Movements of the measurement device itself must either be minimized by careful placement on the centrifuge, or measured and compensated for.

6.3 Angular velocity uncertainty

Measurement of average angular velocity may not define the centrifuge acceleration with sufficient precision in the presence of a periodic variation of angular velocity. This subclause examines the effects of low-frequency variation (wow—typically once per revolution), higher-frequency variation (flutter—which may or may not be synchronous with rotational angular velocity), and frequency drift during the period of measurement. Earth rotation Coriolis effects are also defined.

6.3.1 Periodic angular velocity variation

The average centripetal acceleration on a centrifuge is given by

$$a_c = \frac{1}{t_1} \int_0^{t_1} \omega(t)^2 R\, dt \qquad (41)$$

where

t_1 is the period over which the average is taken,
$\omega(t)$ is the centrifuge angular velocity,
R is the centrifuge radius,
t is time.

If periodic variations (wow or flutter) occur, the centrifuge angular velocity can be given by

$$\omega(t) = \omega_0 + \omega_p \sin(2\pi f_w t + \phi) \qquad (42)$$

where

ω_0 is the average angular velocity,

ω_p is the amplitude of periodic variations,

f_w is the frequency of periodic variations,

ϕ is the phase angle of periodic variation at the start of the data sample.

Assuming the radius is constant, the average acceleration now becomes

$$a_c = \frac{R}{t_1}\int_0^{t_1}\left[\omega_0 + \omega_p \sin(2\pi f_w t + \phi)\right]^2 dt \tag{43}$$

The procedure commonly used to determine the average acceleration is to measure the average centrifuge rate over some time period t_1. The measured acceleration $\hat{a}_c$ is then given by

$$a_c = R\left\{\frac{1}{t_1}\int_0^{t_1}\left[\omega_0 + \omega_p \sin(2\pi f_w t + \phi)\right] dt\right\}^2 \tag{44}$$

The error caused by using the measured average rate is $\hat{a}_c - a_c$.

After multiplying out the squared terms and evaluating the integrals, this becomes

$$\hat{a}_c - a_c = -R{\omega_p}^2\left\{\frac{1}{2} + \frac{1}{8\pi f_w t_1}[\sin 2\phi - \sin 2(2\pi f_w t_1 + \phi)] - \frac{1}{(2\pi f_w t_1)^2}[\cos(2\pi f_w t_1 + \phi) - \cos\phi]^2\right\} \tag{45}$$

This consists of constant terms plus time-dependent terms. If the sample period consists of a whole number of cycles of periodic variations (f_w) or of sufficiently long averaging times (where $t_1 \gg 1/f_w$), this becomes

$$\hat{a}_c - a_c = -\frac{R\omega_p^2}{2} \tag{46}$$

or, if $\omega_P \ll \omega_0$,

$$\frac{\hat{a}_c - a_c}{a_c} = -\frac{1}{2}\left(\frac{\omega_p}{\omega_0}\right)^2 \tag{47}$$

A peak variation of 0.1% in angular velocity results in a -0.5 ppm error in the measured acceleration. When ω_p is a fixed percentage of ω_0, the estimated radius is in error, with negligible effect on derived nonlinearity coefficients. For variable ratios of ω_p/ω_0, odd coefficients such as K_{oq} and K_3 may be significantly affected. For example, some specially instrumented centrifuges have been observed to produce a variation in ω_p/ω_0 that is approximately proportional to $1/a_c$. In this case, the centrifuge-produced acceleration error is proportional to $1/a_c$, and odd order because it increases the magnitude of a_c for either polarity of input. This error in the centrifuge input will appear to be an error in the accelerometer output and will corrupt the values defined for such odd coefficients as K_{oq} and K_3.

6.3.2 Angular velocity drift

The average acceleration in the presence of drifts in angular velocity can be determined by expressing the angular velocity as

$$\omega(t) = \omega_s(1 + Ct) \tag{48}$$

where

C is the rate of drift in angular velocity (1/s),

ω_s is the centrifuge angular velocity at the start of the data sample (rad/s).

The average centripetal acceleration now becomes

$$a_c = \frac{R}{t_1}\int_0^{t_1} \omega_s{}^2(1+Ct)\,dt = R\,\omega_s{}^2\left(1+Ct_1+\frac{C^2t_1{}^2}{3}\right) \tag{49}$$

The measured average angular velocity is

$$\omega_0 = \frac{1}{t_1}\int_0^{t_1} \omega_s(1+Ct)\,dt = \omega_s\left(1+\frac{Ct_1}{2}\right) \tag{50}$$

The acceleration as determined from measured average angular velocity is

$$\hat{a}_c = R\,\omega_0{}^2 = R\,\omega_s{}^2\left(1+\frac{Ct_1}{2}\right)^2 \tag{51}$$

The error in determination of acceleration caused by drift in angular velocity can be shown to be

$$\hat{a}_c - a_c = -\frac{R\omega_s{}^2C^2t_1^2}{12} \tag{52}$$

or, if $\omega_P \ll \omega_0$,

$$\frac{\hat{a}_c - a_c}{a_c} = -\frac{C^2t_1{}^2}{12}\left(\frac{\omega_s}{\omega_0}\right)^2 = -\frac{C^2t_1{}^2}{12} \tag{53}$$

since $(\omega_s/\omega_0)^2 = 1$.

If the angular velocity drifts at a rate of 0.1% per minute, the error in the determination of acceleration is proportional to the square of the sample time at a rate of -0.08 ppm/min^2.

6.3.3 Earth rotation Coriolis effect

Whenever a body moves in a rotating reference frame, such as the earth's surface, it is subject to the Coriolis acceleration, which is expressed by the vector equation

$$\vec{a} = 2\vec{\Omega} \times \vec{V} \tag{54}$$

where, in the case of a centrifuge, $\vec{V}$ is the tangential velocity of the sensor ECM with respect to the surface of the earth, and $\vec{\Omega}$ is the earth rotation rate.

The horizontal component of this cross product is along the arm and is given by

$$a_h = 2\omega\,R\,\Omega_V \tag{55}$$

where Ω_V is the local vertical component of the earth rotation rate, closely approximated by

$$\Omega_V = |\vec{\Omega}|\sin\lambda \tag{56}$$

The Coriolis acceleration consequently has a value proportional to ω and either aids or opposes the centrifuge acceleration, depending on rotation sense and latitude λ.

Alternatively, the same algebraic result may be derived by assuming that the vertical component of the earth rotation rate simply adds to or subtracts from the centrifuge rate ω.

Since the centrifuge acceleration is

$$a_c = R\,\omega^2 \tag{57}$$

then

$$\frac{a_h}{a_c} = 2\frac{\Omega_v}{\omega} \tag{58}$$

As an example, the value of the Coriolis acceleration for a level centrifuge turning counterclockwise (CCW) at 1 revolution per second at 40° north latitude is 15 ppm and adds to the centripetal acceleration.

Since the magnitude varies linearly with ω, the Coriolis acceleration varies as the square root of centrifuge acceleration. Most centrifuge tests are made with the same rotation direction for both positive and negative accelerations; therefore, the Coriolis effect is that of an odd function in the data analysis. The effect can be calculated and compensated for by adding it vectorially to the estimated input data.

The vertical component of the cross product is along the rotation axis and is given by

$$a_v = 2\omega R\,\Omega_h \cos(\omega t) \tag{59}$$

where

Ω_h is $\left|\vec{\Omega}\right| \cos\lambda$, the horizontal component of the earth rotation rate,
ωt is the arm angle from north.

An accelerometer with its IA mounted vertically will sense this periodic error, which can be eliminated by averaging over complete arm revolutions.

6.3.4 Instrumentation methods and errors

Average centrifuge angular velocity can be determined by measuring the time required for the centrifuge to rotate through a known angle. This is most conveniently and accurately done by measuring the time required for a number of complete revolutions. The time is measured with a counter that has a precision time source as its input. The counter is triggered by an event marker that occurs once per centrifuge revolution. The accuracy of this measurement is limited only by the accuracy of the time source and the position repeatability of the event marker. A time source good to 1 μs will produce an angular velocity uncertainty of 1 ppm when measuring a time of 1 s. A 1-arc-second variation in the location of the event marker will produce an error of 0.8 ppm in angular velocity in a 1-revolution measurement. A greater concern in determining centrifuge angular velocity is insuring that the average angular velocity is determined over the same time period that the accelerometer output is measured. This is especially important if the centrifuge angular velocity is subject to large variations.

An alternate procedure for determining centrifuge angular velocity exists if the centrifuge is equipped with a continuous position readout, such as a resolver or encoder. The time for the centrifuge to rotate through a known angle as given by the position readout can be determined in the same manner as was described above using the once-per-revolution event marker. The error sources are the same as when using the marker; however, the accelerometer sample period is no longer required to be a whole number of centrifuge revolutions, but can be any time, provided the position readout can be read at the start and end of the data sample.

6.4 Sensor temperature effects

6.4.1 Sensor self-heating

This error source is found primarily in servo force or torque-balance accelerometers in which the power dissipated in the sensor varies as a function of input acceleration. Its precise form depends on the nature of the capture loop and on the geometry of the sensor, and on its mechanical interfaces. This error source displays both a transient and a steady-state mode of behavior. That is significant, because standard centrifuge tests are nearly steady-state in nature, whereas the high acceleration levels that produce significant self-heating tend to be transient in actual applications. The result is that the response measured may not be appropriate to the end-use conditions, even though the applied acceleration and the measurement of the response may be perfectly accurate. Sensor thermal time constants may be on the order of minutes, whereas the duration of high accelerations in actual use may be only seconds. As a result, normal measurement periods, which are typically several minutes, may be inappropriate. The general form of the self-heating equations starts with the following temperature equation:

$$\Delta T(t) = \rho \, P(a_s)(1 - e^{-t/\tau}) \tag{60}$$

where

$\Delta T(t)$	is the temperature rise at a critical location on the accelerometer at time t after the onset of acceleration (°C),
$P(a_s)$	is the power dissipation as a function of indicated acceleration,
ρ	is the thermal resistance to the heat sink (°C/W),
τ	is the thermal time constant (s),
t	is the time since onset of acceleration.

The self-heating effect is primarily due to electrical dissipation in a torquer coil, which ultimately heats the nearby magnet structure and changes the scale factor by changing the field strength of the magnet. The response thus takes the form

$$K_1 = K_{10}(1 + k_T \, \Delta T) \tag{61}$$

where

K_1	is the scale factor,
K_{10}	is the scale factor at $t = 0$,
k_T	is the scale factor temperature coefficient.

Thus, in the steady-state case, with very long centrifuge runs and assuming all other errors equal to zero, the indicated sensor output becomes

$$a_s = a_i(1 + k_T \, \Delta T) = a_i(1 + k_T \rho \, P(a_s)) \tag{62}$$

The form of the response thus depends on the form of $P(a_s)$. For the normal analog accelerometer, power varies as current squared and therefore as ${a_s}^2$, giving rise to an apparent cubic term in the indicated output. For a pulse-capture accelerometer in which the pulses are of equal current-time area and the pulse rate is proportional to acceleration, power is proportional to acceleration, and so there appears to be a quadratic term in the output. Note, however, that it carries the sign of the input and therefore affects K_{oq}.

These effects can be quite significant, since k_T is often of the order of 200 ppm/°C. A pulse-captured accelerometer that has a 1 °C temperature rise at 20 g might thus have an apparent K_2 (for single polarity) of 10 $\mu g/g^2$.

While short-duration tests simulating end use are very difficult and so very rare, it turns out that tests of sufficient duration to achieve full equilibrium are not very common either. Test durations based on achievement of centrifuge angular velocity stability and adequately averaged electrical measurements generally are not long enough to achieve steady-state thermally. The result is two-fold. First, the error due to sensor heating is diminished and may be somewhat variable from run to run. Second, and usually more noticeable, temperature rises associated with high acceleration may leave residuals that affect several subsequent points. For the common test sequence in which several points are taken in order of ascending *g* level and then the same points or a smaller subset are repeated in descending order, the result will appear to be hysteresis. The most typical symptom of this problem is that the hysteresis appears to be predominantly in scale factor—i.e., the apparent hysteresis is greater at intermediate points than it is at zero *g*. A test sequence in which data points are taken in random order of *g* level will show a scatter rather than a hysteresis, and when analyzed in comparison with the sequential test points may reveal an unsuspected thermal problem.

Load resistor self-heating also causes a scale factor error much the same as the heating of sensor magnets already discussed. The temperature rise of the load resistor modifies its resistance due to its temperature coefficient of resistance and changes its measurement voltage output. Load resistor self-heating tends to depend on whether the resistor is mounted on the arm with the sensor or in a stationary electronics rack. Also, if it is on the arm, it makes a difference whether it is mounted to the sensor or in a separate package where it heats only itself. These considerations are examined in more detail in 6.6.

6.4.2 Gradients due to self-heating and convection

Servoed sensors may also experience errors due to thermal gradients induced in the sensor by self-heating. The most common source of error is density gradients induced in the fluid of liquid-filled sensors, but errors can also occur in dry sensors due to temperature differences between elements added for temperature compensation or modeling and the principal contributors of the errors modeled.

In a minimum-fluid-volume liquid-filled sensor, small passages inhibit convection currents so that the principal error source is the difference in buoyancy at either end of the pendulum. This is typically on the order of a few hundred parts per million for a 1 °C gradient along the pendulum. If convection currents are significant, they tend to reduce the problem, but also cause it to be more complex—especially with regard to misalignment effects.

Gradients are typically proportional to temperature rise, so the forms of the equations that describe the steady state are essentially the same as those in 6.4.1. In the transient regime, however, the picture is more complex. The distribution of major masses will often induce thermal gradients that are proportional to heating rate, and so there can easily be two or more different effects, with markedly different time constants, that are dominant at different times during the transient period.

These error sources are difficult to estimate or measure and tend to be ignored as long as indicated hysteresis is small and results are repeatable with a standardized test. That may account for the observation that some sensors work better than others even though they have similar test results.

An added factor that can either diminish or add to the problems discussed above is that strong convection currents induced by high accelerations also tend to reduce thermal gradients. The error torques that are produced by these currents impinging on the pendulum can vary dramatically with acceleration level in some sensor designs.

6.4.3 Instrumentation methods and errors

The instrumentation of accelerometers to separate the effects of temperature variations (including self-heating) from other error sources must be carefully carried out since the most obvious effect, a drifting output signal, can easily be attributed to a number of other sources. Temperature sensors are best placed inside the accelerometer case, if possible. For torque-rebalance accelerometers, use of the resistance of the torquer itself as a direct measurement of the internal temperature of the accelerometer is recommended, since placement of an alternate temperature sensor in that critical location is difficult.

Since the most serious effects of self-heating occur at high *g* levels, as seen during centrifuge testing, the measurement of the effects of self-heating must be made through the slip-rings and yet retain integrity and accuracy. Thus, temperature measurements must be converted to high-level signals for data transmission and recording so that they will be unaffected by the circuitous path of the cabling. The temperature sensors on the outside of the accelerometer must be carefully bonded thermally to the critical locations, and the leads carefully chosen so that heat flow through the leads due to their thermal conductivity does not reduce the accuracy of the temperature measurement itself.

Since the temperature sensors are used for the purpose of measuring the thermal time constants as well as the magnitude of the errors due to self-heating and/or temperature gradients, the sensors themselves must be carefully chosen so that their own time constants will not influence the accuracy of the measurements. Some of the accelerometer time constants may well be much less than a minute. Although it may be possible to machine cavities for temperature sensors so that they will be tightly coupled to the desired area of the accelerometer, this capability is usually restricted to the manufacturer. A user must usually work externally and choose sensor locations for convenience as well as accuracy.

As noted above, the self-heating effects have both transient and steady-state components. Both may be important to the user. Most high-*g* input levels are likely to be transitory by nature and fall in the most difficult interval for measurement accuracy. This type of high-*g* transient may be difficult to simulate by use of a centrifuge so that accurate data can be taken to define the self-heating characteristics of the accelerometer under test.

The effects of self-heating can be magnified by either planned or accidental thermal isolation between the accelerometer and the mounting that usually comprises the heat sink. Stainless steel, which is a material commonly used by accelerometer designers because of its high mechanical stability, is a poor thermal conductor and may actually be used as a thermal isolator by other designers.

One of the least obvious effects of self-heating in accelerometers is that of modifying the nonlinearity coefficients derived from high-*g* centrifuge testing. This arises because most centrifuge testing is performed steady-state, and, unless the self-heating effects are monitored, will lead to the computation of values for K_2 and K_3 that are true only for steady-state high *g* levels. These coefficients are not valid for applications where the accelerometer is used to measure high-*g* transients that may last but a few seconds, such as are produced by fast-burning, high-*g* rocket engines.

6.5 Trend during test

If there was a change in the accelerometer output on the centrifuge arm from before to after a centrifuge test due to heating or other causes, it could be hypothesized that there was a trend in the accelerometer output during the test. This trend could be removed from the data before estimating model coefficients.

This technique is not valid if, for instance, there was a shift in accelerometer output caused by shock or other events during the test.

6.6 Accelerometer signal measurement

6.6.1 Sensor measurement effects

When monitoring signals, care must be exercised while routing the signal from the test unit on-board the centrifuge to the off-board device used to measure the signal. Analog signals must be protected against capacitively coupled noise by proper shielding techniques, and against voltages generated by a conductor moving in the earth's magnetic field by using twisted-pair conductors. Digital signals should be carried by twisted-pair conductors whose electrical properties will not degrade the quality of the signal.

The signal should also be protected against noise generated by slip rings. It is good practice to utilize parallel pairs of slip rings to carry critical signals so that intermittent failures of one pair of slip rings will not significantly degrade the quality of the signal.

If the signal is in the form of a current, a scaling resistor must be inserted in the output circuit, across which the output in the form of an analog voltage may be measured. Since the resistance of even the most precise resistors changes as a function of the current and temperature, this resistor must be characterized and the data correspondingly corrected. The resistance should be measured at several typical values of input current and characterized over a long period of time. Typical values of current should include the maximum, minimum, and several intermediate values expected during the centrifuge test. This test should be conducted over a period of time comparable to the actual centrifuge test. The resistor must also be characterized over the full range of temperatures expected during the test.

Off-board measurement of the accelerometer signal constitutes the heart of the data acquisition process and demands major consideration in several areas.

Accelerometer output signals in the form of analog voltages are most commonly measured with an integrating digital voltmeter (DVM). These DVMs come in a variety of accuracy levels and range from the three-digit, hand-held unit to the $7\frac{1}{2}$-digit, computer-compatible unit. Critical operating specifications must be matched to the accuracy level of the test.

The primary considerations are the resolution and accuracy of the DVM. Its resolution should ideally be one digit more than the smallest value of test-unit output to be measured, and the measurement accuracy likewise should be one order of magnitude better than the test accuracy required. For example, a test conducted at the 1% CE level on an accelerometer with a range of $10\,g$ and a scale factor of $1\ \mathrm{V}/g$ would require the output voltage to be measured to within 0.1 V dc.

Smallest value to be measured: $(0.01)(10\,g)(1\ \mathrm{V}/g) = 0.1\ \mathrm{V}$

Accuracy of DVM: $(0.1)/10 = 0.01\ \mathrm{V}$

Therefore, the DVM should have a measurement accuracy of at least 0.01 V. If the same accelerometer were tested at the 10 ppm CE level, the output should be measured to within 100 μV, and the accuracy of the DVM must be at least 10 μV.

Several other DVM operating specifications must be matched to the test accuracy level. They are as follows:

Nonlinearity. The total nonlinearity of the DVM over the full output range of the accelerometer should be one order of magnitude less than the voltage equivalent of the nonlinearity of the accelerometer to be tested.

Instability. The instability or drift of the DVM should be characterized over the period of time equal to that required to perform the centrifuge test.

Temperature sensitivity. The effect of temperature variations on the measurement accuracy of the DVM should be checked over the range of ambient temperatures expected throughout the duration of the test.

Effects of range change. Typical precision integrating voltmeters have several different input ranges. The most accurate meters typically have a resolution of 1 μV when the input range is less than 1 V. However, if the input is in the 1–10 V range, the resolution of the meter changes to 10 μV. Consequently, if the output of the test unit crosses the voltmeter range boundary during the test, the effect of decreased resolution must be taken into account when calculating the voltmeter measurement uncertainty. Also, if the voltmeter is to measure a large voltage followed immediately by a small voltage (i.e., a 28-V dc power supply followed by a millivolt accelerometer output voltage), some precision voltmeters allow the large voltage to bleed over and corrupt the small voltage measurement. Depending on the individual voltmeter, either a settling time should be provided between the measurements, or dual measurements should be taken and the first one ignored.

Analog integration time versus centrifuge position and period. Voltmeters cannot measure a voltage instantaneously. They must integrate or average the signal over some finite period of time. This time, known as the integrating time, varies greatly depending on the particular DVM and the resolution required of the measurement. Since the accelerometer output is averaged over some period of time, the average acceleration the test unit sees over this same time must be known. Therefore, one must know the centrifuge position and acceleration level during the sampling of the accelerometer output signal.

Since no centrifuge is perfect, it is difficult to predict the exact acceleration level the test unit is exposed to at any one particular point in time. However, centrifuge-induced errors are generally cyclic, repeating once per revolution of the arm. Since they are periodic, their effect on the test item can be reduced by sampling the test item output over a whole number of revolutions of the centrifuge. However, most DVMs do not have selectable integrating times (they average over a whole number of power line cycles), and the integration time will probably be fixed already by the resolution requirements of the measurement. There are at least two solutions to this dilemma. First, the period of the centrifuge can be varied so that it completes a whole number of revolutions during the DVM averaging time. Instead of testing the accelerometer at several discrete acceleration levels that are integral multiples of gravity, the unit is tested at acceleration levels that correspond to a whole number of revolutions of the arm while the test item is being sampled. Second, the test-item output can be averaged over a large number of centrifuge revolutions so the effect of centrifuge errors that were not averaged out will be greatly reduced. Both methods have advantages and disadvantages; hence, the technique must be chosen with regard to the particular accelerometer, centrifuge, and DVM used in the test.

Accelerometer output signals in the form of digital pulses must be measured with some sort of counter. The type of counter required is dictated by the output signal digitizing scheme. The schemes most often encountered utilize either unipolar or bipolar digitizing techniques. The unipolar method is characterized by a single pulse stream for both positive and negative values of input acceleration to the accelerometer. The digitizer is nominally biased to half of full-scale output. A pulse rate above the nominal value would indicate positive acceleration, whereas a pulse rate below the nominal value would indicate negative acceleration. A bipolar scheme consists of two pulse streams for a single test-unit output, one pulse stream for positive acceleration and one for negative. The two pulse streams must be combined to get the total indicated acceleration output of the test unit. The unipolar output can be measured with a single up-counter, whereas the bipolar output requires two up-counters or one up/down-counter.

The comments that follow apply to both up- and up/down-counters:

Clock. All digital counters require a timing clock. This clock frequency may be supplied from an external source to the counter or it may be internal. The counter's time measurement uncertainty is a function of this clock frequency and stability. The higher the clock frequency, the smaller the measurement resolution. The better the clock frequency stability, the more accurate the time measurement made by the counter. Typically, counter clock frequencies range from 100 kHz to 10 MHz. Accuracies range from several parts per million to about 0.0001 ppm for crystal oscillator time bases. When choosing a digital counter to measure the output frequency of an accelerometer, the clock frequency should be at least one order of magnitude higher than the highest accelerometer output frequency expected during the test. The accuracy should be at least an order of magnitude better than the expected measurement.

Accumulating pulses. Although it may appear simple, the task of measuring the output from an accelerometer requires detailed planning. If the test-item output is in the form of pulses, those pulses are accumulated over a period of time. The test-item output has units of pulses per second (pps) or hertz (Hz). There are two methods of accumulating pulses: first, measure the time to accumulate a specific number of pulses, and, second, count the number of pulses during a fixed interval of time. Whenever practical, the first method should be used, since it gives lower uncertainties in the pulse rate measurement as long as an average pulse rate per revolution can be adequately calculated. To implement this method, two counters are required—a preset counter and an interval counter. The preset counter accumulates accelerometer pulses to a preset number. Then it sends a pulse to the interval counter, resets to zero, and starts accumulating pulses again. The continuous interval counter counts time at the clock frequency. When it receives the pulse from the preset counter, it freezes that time, sends it to the computer, and continues counting clock pulses with no gaps. The computer uses the time interval required for the preset number of pulses to calculate the accelerometer frequency.

Digital integration time versus centrifuge position and period. Digital signals still require an averaging or accumulating time associated with the measurement of the test pulse rate. Consequently, the centrifuge position and acceleration level during the sampling period must be known.

As in the analog case, cyclic induced centrifuge errors must be given consideration when deciding how to take digital accelerometer data. The accumulating time can be adjusted to a fraction of the centrifuge revolution time, giving a whole number of samples per revolution. Data should be taken for a large number of revolutions; a typical example is 100 or more. Depending on how the data is combined for analysis, one can look at single- or multiple-revolution data. The cyclic errors are averaged out of the single-revolution data, and their effects are reduced in the multiple-revolution data because of the long sampling time.

Digital output accelerometers can be centrifuge-tested at any desired g level since the pulse accumulating time can be adjusted to give data samples over a whole number of revolutions.

6.6.2 Interactions

In nearly all precision centrifuge testing, the errors discussed in Clause 6, Test error sources, are sufficiently small compared with the linear quantities that they can be treated as though no interactions occur. They can be treated as linearly independent quantities that add algebraically by linear superposition. For example, if an error of $2.00\,\mu g/g^2$ is known to occur due to arm stretch and $5.00\,\mu g/g^2$ due to dynamic center of rotation (imbalance), then the net effect will be $7.00\,\mu g/g^2$. If the imbalance effect increases arm stretch 5 ppm/g, at 50 g the interaction term is equivalent to 250 ppm of $2\,\mu g/g^2$, or $0.0005\,\mu g/g^2$, and could certainly be ignored. Equivalently, if the error distribution is known to be approximately Gaussian with known statistics, then the statistics of the combined effect can be determined by root sum square (RSS).

There are a few situations where that is not a valid assumption, but they tend to be rather rare. For example, if applied g level is computed from $R\omega^2$, and R is in error by 0.1%, there will be a small error introduced into a determination of the K_2 coefficient. For the usual servoed accelerometer in which K_2 rarely exceeds $20\,\mu g/g^2$, the error will not exceed 0.2% of $20\,\mu g/g^2$, or $0.04\,\mu g/g^2$. In a precision test of a vibrating beam accelerometer that has a modelable nonlinearity of $5000\,\mu g/g^2$, a 0.1% error in radius could interact with the sensor nonlinearity to produce an error of $10\,\mu g/g^2$, which may be significant. Even in this case, though, when the test radius is estimated to greater precision by use of a separately measured scale factor (see 9.3.3), the error in K_2 will be reduced to a negligible level.

Noisy signals may also interact with even-order nonlinearities to produce rectification errors. It is rare for centrifuge vibration levels to be high enough to cause concern, but noisy sensor electronics may cause rectification errors in some voltmeters. For this reason, and because excess noise may imply a sensor fault or impending saturation, it is desirable to monitor analog signals with an oscilloscope or other real-time display system.

6.6.3 Test error elimination using multiple sensors

Multiple sensors are used in two principal ways to minimize or eliminate many centrifuge test-bed errors. The first and most common is a test technique that can be used on any centrifuge. It consists of testing pairs of similar accelerometers in a common test fixture that meets the following criteria: it holds the sensors as closely together as practical, it maintains a rigid relationship between their axes, and it makes provision for inverting the input axis of one sensor relative to the other so that the sensor pair may be tested both parallel and antiparallel. The second involves the addition of permanent instrumentation to the centrifuge in the form of one or more reference accelerometers, mounted with their input axes parallel to the arm axis, and usually at a smaller radius than the test sensors. A centrifuge arm that has been so modified is commonly called a ratio method centrifuge. Further details may be found in a paper by Peters [B14].

The sensor pair technique has greater ultimate accuracy than the ratio method when used in an appropriate way on a high-precision centrifuge. It is especially effective for separating test-bed errors that have different symmetry. In lieu of measuring arm stretch (see 6.1.8), dual accelerometer testing can be used to separate the effect of arm stretch, which appears as an odd quadratic (see 6.1.2), from normal square law accelerometer errors. This effect may be illustrated by a simplified example. Suppose two accelerometers are tested, the accelerometers having outputs E_1 and E_2, respectively (where the second numeric subscript identifies the accelerometer):

$$\frac{E_1}{K_{11}} = a_c + K_{21}a_c^{\,2} + C_{AS}|a_c|a_c \tag{63}$$

$$\frac{E_2}{K_{12}} = a_c + K_{22}\,a_c^{\,2} + C_{AS}|a_c|a_c \tag{64}$$

If the first accelerometer is inverted to produce output $E_1{}'$, then

$$\frac{E_1{}'}{K_{11}} = -a_c + K_{21}\,a_c^{\,2} - C_{AS}\,|a_c|a_c \tag{65}$$

Next, suppose that standard curve fitting techniques are applied, not to the raw accelerometer outputs, but to the combinations of outputs (where subscript "P" refers to parallel and subscript "A" refers to antiparallel) shown in Equation (66) and Equation (67):

$$\frac{E_1}{K_{11}} - \frac{E_2}{K_{12}} = (K_{21} - K_{22})a_c^{\,2} = K_P\,a_c^{\,2} \tag{66}$$

$$\frac{E_1{}'}{K_{11}} - \frac{E_2}{K_{12}} = (K_{21} + K_{22})a_c{}^2 = K_A a_c{}^2 \tag{67}$$

Then

$$(K_P + K_A) = 2K_{21} \tag{68}$$

$$-(K_P - K_A) = 2K_{22} \tag{69}$$

This example assumes perfect knowledge of scale factors and biases, and exactly matched test radii. It also assumes fixture symmetry such that C_{AS} does not change when accelerometer #1 is inverted. More detailed analyses show that K_2 or K_{ip}, for example, may be recovered with an accuracy of $0.01\ \mu g/g^2$ with assumptions about scale factor errors, bias errors, alignment errors, and ECM separations that are appropriate to a high-precision centrifuge. The details of such analyses vary with the test environment and the coefficients sought, but all are based on two assumptions: that ECM separation is constant for any given test run (parallel or antiparallel), and that angular deviations are common-mode. The technique may be applied to pairs of accelerometer triads as well as to single-axis accelerometers. It fails to return useful information in only a few cases. For example, the equations will return the difference between the K_3 coefficients of the two accelerometers, but not the coefficients themselves. In general, the method is an excellent way to gain added accuracy for developmental or qualification testing, where added test time is not a serious consideration.

The ratio method has seen production use in the form of a centrifuge with a single reference accelerometer mounted at one third of the radius of the nominal test station. The reference accelerometer is permanently installed in a temperature-controlled housing and is exposed to only one third the acceleration applied to the test sensors. A good-quality accelerometer will exhibit excellent stability in such an environment, and the indicated acceleration at the test radius will contain only one third the second-order nonlinearity and one ninth the third-order nonlinearity of a comparable sensor at the test radius. Measurements are taken by correcting sensor outputs for apparent bias and then recording the ratios of the test sensor outputs to the reference sensor outputs.

A single reference accelerometer automatically cancels any effects due to centrifuge angular velocity variations, as long as the test and reference samples are simultaneous. It also partially compensates for many other common centrifuge errors. However, a single reference remains sensitive to balancing error (see 6.1.5). Two or more reference accelerometers mounted at different locations on the arm and appropriately weighted can be used to cancel such sensitivity automatically and with no special action required of the operator. For example, with two sensors mounted at one third the nominal test radius on opposite sides of the arm, and the near-side reference accelerometer weighted twice as heavily as the far-side accelerometer, a 20:1 reduction of error due to imbalance is possible with the test specimen mounted within 10% of the nominal radius.

The use of a shorter radius to get the reference out of the way and improve its stability and linearity has two by-products, one good and one bad. The bad one is that the additional compliance introduced between the test and reference limits ultimate accuracy compared with the paired sensor test technique. The good one is that it makes possible a "round-robin" calibration scheme in which several accelerometers are tested at all test and reference positions, resulting in a set of test-bed coefficients that reflect the nonlinear coefficients of the reference accelerometers as well as those centrifuge errors that are relatively fixed and repeatable. This calibration may include errors that are not so well discriminated by the paired sensor technique. It can be repeated periodically, but in many cases may be needed only a few times in the life of the centrifuge. The ratio method provides a relatively inexpensive way to upgrade the performance of many older centrifuges, and is especially well suited to production testing.

7. Complete model equations

This clause provides an expansion of the simplified model equation presented in Clause 5 for the accelerometer under test. Included are terms that represent higher-order nonlinearities and cross-coupling effects, as well as terms that may represent sensor-related test errors from the centrifuge test itself.

This clause continues with a discussion of an expanded model equation for the centrifuge itself, incorporating the many test error sources discussed in Clause 6. It is recommended that the model equations for both the accelerometer and the centrifuge be carefully screened to eliminate those terms of minimal significance based on the desired level of test precision. Estimates of error magnitudes may be based either on experimental data from the centrifuge being used or on manufacturer's data.

7.1 Accelerometer model

For precision applications, a relatively complex model equation with high-order nonlinear and cross-axis terms is usually required. A normalized model equation of the instrument input/output function often used is as follows:

$$a_s = \frac{E}{K_1} = K_0 + a_i + K_2 a_i^{\,2} + K_3 a_i^{\,3} + K_{ip} a_i a_p + K_{io} a_i a_o + K_{op} a_o a_p + \delta_o a_p - \delta_p a_o + \cdots \tag{70}$$

where

E	is the sensor output (output units),
a_s	is the indicated sensor output (g),
K_0	is the bias (g),
K_1	is the scale factor (output units/g),
K_2	is the second-order coefficient (g/g^2),
K_3	is the third-order coefficient (g/g^3),
K_{ip}, K_{io}, K_{op}	are the cross-coupling coefficients [(g/g)/cross g],
a_i	is the acceleration along sensor IA (g),
a_p	is the acceleration along sensor pendulous axis (PA) (g),
a_o	is the acceleration along sensor output axis (OA) (g),
δ_o	is the misalignment angle between IA and case reference IA about OA (rad),
δ_p	is the misalignment angle between IA and case reference IA about PA (rad),
OA	is equal to IA $\times$ PA.

Since the a_i term is a function of the centrifuge, any deviation from the desired or ideal value will be expressed in the centrifuge model in 7.2.

For data reduction purposes, the model that is actually fitted to the test data may require additional terms to account for the effects seen in the accelerometer output as a result of sensor-related centrifuge test errors. In some cases, these may be nearly indistinguishable from actual sensor errors, while in others the form may be different enough from any effect that is physically reasonable for the sensor to permit separation by multiposition testing. Some specific errors to be considered are

a) Odd quadratic term ($K_{oq} a_i |a_i|$) (see 6.1.2, 6.1.5)
b) Apparent scale factor asymmetry (K_{1+}, K_{1-}) (see 6.1.7)

c) Apparent bias asymmetry (K_{0+}, K_{0-}) and pseudo-cross-coupling effects due to misalignment (see 6.2, 6.2.1, 6.2.2, 6.2.3)
d) Apparent scale factor hysteresis due to heating (see 6.1.6, 6.4)
e) Apparent bias hysteresis and cubic nonlinearity (see 6.4)
f) Interactions between the above error sources (see 6.6.2)

Each of these error sources should be evaluated separately and together to determine the additional significant terms that should be added to the accelerometer model equation.

Higher-order cross-axis terms may also be included in the model. These terms are normally small or negligible for most accelerometer mechanizations, but are often evaluated to prove this is so. Typical terms in this category are

$K_{pp}a_p^2$	Second-order pendulous axis coefficient
$K_{oo}a_o^2$	Second-order output axis coefficient
$K_{ppp}a_p^3$	Third-order pendulous axis coefficient
$K_{ooo}a_o^3$	Third-order output axis coefficient

7.2 Centrifuge model

A simplified model for the acceleration imposed on an instrument under test was given in 5.2. This model can be expanded to include the various perturbations that must be considered for an accurate determination of the acceleration applied to the instrument. These perturbations include radius errors (see 6.1), rate errors (see 6.3), alignment errors (see 6.2), and Coriolis acceleration (see 6.3.3).

7.2.1 Radius model

The total radius from the center of rotation of the centrifuge to the ECM of the accelerometer is

$$R = R_0\left(1 + \frac{\Delta R}{R_0}\right) \tag{71}$$

In this equation, R_0 is a static radius and ΔR is the total deviation from the static radius. ΔR will include static errors and dynamic errors that may be proportional to the centripetal acceleration. It may be expressed as follows:

$$\Delta R = \Delta R_+ + \Delta R_- + \Delta R_a\, a_0 + \Delta R_d \tag{72}$$

ΔR_+ is used ($\Delta R_- = 0$) when the input acceleration is positive, and ΔR_- is used ($\Delta R_+ = 0$) when the input acceleration is negative. Both terms together include all static errors—i.e., errors that are not affected by centripetal acceleration. These include uncertainties in the location of the center of rotation of the centrifuge and in the location of the ECM of the accelerometer. This static error also includes the difference in radius between the positive range of accelerations and the negative range. ΔR_a includes all dynamic errors that are proportional to centripetal acceleration. This includes errors caused by arm stretch resulting from centrifugal loading, changes in the location of the dynamic center of rotation and of the ECM, and by thermal expansion of the centrifuge arm. ΔR_d includes all dynamic errors that are not a linear function of centripetal acceleration. These errors may be caused by the same sources that caused ΔR_a but result in radius changes that are not linear with centripetal acceleration.

7.2.2 Centrifuge angular velocity model

The instantaneous angular velocity of the centrifuge can be given by

$$\omega = \omega_0\left(1 + \frac{\Delta\omega_d}{\omega_0}\right) \tag{73}$$

where

ω_0 is the average centrifuge angular velocity,

$\Delta\omega_d$ is the deviation from the average centrifuge angular velocity.

$\Delta\omega_d$ contains errors caused by sinusoidal variations in angular velocity of amplitude ω_p and at a frequency of f_w and drift in angular velocity at a rate of C. The total deviation in angular velocity at time t is therefore

$$\Delta\omega_d = \omega_p \sin(2\pi f \omega t + \phi) + \omega_s C t \tag{74}$$

7.2.3 Coriolis acceleration

The horizontal Coriolis acceleration along the centrifuge arm is given by

$$a_h = 2\omega_0 R_0 \Omega_V \tag{75}$$

where Ω_V is the local vertical component of the earth rotation rate. This will add to the centripetal acceleration if ω_0 is in the same direction as Ω_V, or subtract if in the opposite direction.

7.2.4 Gravitational acceleration

The component of gravitational acceleration that is directed along the centripetal acceleration vector is

$$a_g = g_L(\delta_0 + \delta \sin \omega_0 t) \tag{76}$$

where

δ_0 is the average misalignment of the centrifuge arm from horizontal

δ is the misalignment of the rotation axis from vertical

The effect of the sinusoidal term can be eliminated by taking data over an integer number of centrifuge revolutions.

7.2.5 Alignment model

The acceleration that is sensed by the accelerometer will be affected by alignment errors. These errors can occur about a radial axis, a tangential axis, and a vertical axis. Misalignments about a radial axis have very little effect on centrifuge testing and therefore will not be considered here. Misalignments about a tangential (ϕ_T) and vertical (ϕ_V) axis can be expressed as

$$\phi_T = \phi_{T+} + \phi_{T-} + \Delta\phi_{Ta} a_0 + \Delta\phi_{Td} \tag{77}$$

$$\phi_V = \phi_{V+} + \phi_{V-} + \Delta\phi_{Va} a_0 + \Delta\phi_{Vd} \tag{78}$$

In these equations, the ϕ_{T+} or the ϕ_{V+} term is used only when the acceleration is positive, and the ϕ_{T-} or the ϕ_{V-} term is used only when the acceleration is negative. These terms are static misalignments from the centripetal acceleration vector in the vertical plane and in the horizontal plane, respectively. They are caused by uncertainties in the location of the centripetal acceleration vector and by misalignments of the accelerometer IA. They will be different from the positive range of acceleration to the negative. The misalignments $\Delta\phi_{Ta}a_0$ and $\Delta\phi_{Va}a_0$ are proportional to the centripetal acceleration a_0 due to the static centrifuge radius (where the effect of variations in the radius can be ignored in the product). These alignment changes result from centrifugal loading and temperature effects. $\Delta\phi_{Td}$ and $\Delta\phi_{Vd}$ are other dynamic misalignments that change in other than a linear manner with centripetal acceleration.

7.2.6 Total acceleration

If the errors are small enough such that products of two or more small errors can be ignored, the total centripetal acceleration is

$$a_c = \omega_0{}^2 R_0\left(1 + 2\,\frac{\Delta\omega_d}{\omega_o} + \frac{R}{R_0}\right) \tag{79}$$

Its direction is toward the center of rotation of the centrifuge and perpendicular to the centrifuge angular velocity vector. The total acceleration in this direction also includes the earth rotation Coriolis acceleration, and the component of gravitational acceleration caused by misalignments of the centrifuge rotation vector from vertical and by coning of the centrifuge rotation axis. The total acceleration in the radial direction averaged over a whole number of revolutions is

$$a_r = \omega_0{}^2 R_0\left(1 + 2\frac{\Delta\omega_d}{\omega_0} + \frac{\Delta R}{R_0}\right) + 2\omega_0 R_0\Omega_V + g_L\,\delta_c \tag{80}$$

The acceleration in the vertical direction, perpendicular to the radial acceleration vector, is g_L plus a sinusoidally varying Coriolis acceleration that can be eliminated by taking data over complete revolutions. The vertical acceleration therefore can be written as

$$a_V = g_L \tag{81}$$

If centrifuge angular velocity variations are small enough such that angular accelerations can be ignored, the tangential acceleration is zero. In any case, the average tangential acceleration may usually be taken as zero.

These accelerations must now be transformed into the accelerometer coordinate frame. The misalignment angles are assumed to be small enough that small angle approximations can be used, and products of small angles or other small errors can be ignored. The resulting accelerations in the radial, vertical, and tangential directions of the accelerometer reference frame, respectively, are

$$\begin{aligned} a_{ra} &= \omega_0{}^2 R_0\left(1 + 2\frac{\Delta\omega_d}{\omega_0} + \frac{\Delta R}{R_0}\right) + 2\omega_0 R_0\Omega_V + g_L(\delta_c + \phi_T) \\ &= \omega_0{}^2 R_0\left(1 + 2\frac{\omega_p}{\omega_0}\sin 2\pi f_w t + 2\,\frac{\omega_s}{\omega_0}Ct + \frac{\Delta R_+ + \Delta R_-}{R_0} + \frac{\Delta R_a}{R_0}a_0 + \frac{\Delta R_d}{R_0}\right) \\ &\qquad + 2\omega_0 R_0\Omega_V + g_L(\delta_c + \phi_{T+} + \phi_{T-} + \Delta\phi_{Ta}a_0 + \phi_{Td}) \end{aligned} \tag{82}$$

$$a_{Va} = g_L + \omega_0{}^2 R_0(\phi_T + \delta_c) = g_L + \omega_0{}^2 R_0(\delta_c + \phi_{T+} + \phi_{T-} + \Delta\phi_{Ta}a_0 + \Delta\phi_{Td}) \tag{83}$$

$$a_{Ta} = \omega_0{}^2 R_0\phi_V = \omega_0{}^2 R_0(\phi_{v+} + \phi_{v-} + \Delta\phi_{va}a_0 + \Delta\phi_{vd}) \tag{84}$$

where

a_{ra} is the radial acceleration in the sensor frame,

a_{Va} is the vertical acceleration in the sensor frame,

a_{Ta} is the tangential acceleration in the sensor frame,

a_0 is the centripetal acceleration due to the static value of centrifuge radius,

ω_0 is the average centrifuge angular velocity,

$\Delta\omega_d$ is the deviation from average centrifuge angular velocity,

ω_p is the amplitude of centrifuge periodic angular velocity variation,

ω_s is the centrifuge angular velocity at the start of the data sample,

R_0 is the static value of arm radius,

ΔR is the total deviation from nominal radius,

ΔR_+ is the radius deviation for +IA acceleration,

ΔR_- is the radius deviation for –IA acceleration,

ΔR_a is the dynamic radius error proportional to a_c,

ΔR_d is the nonlinear dynamic error in radius,

Ω_V is the local vertical component of earth rotation rate,

g_L is the local value of gravitational acceleration,

δ_c is the coning angle,

ϕ_T is the total sensor misalignment about a tangential axis including sensor and mount,

ϕ_{T+} is the static tangential misalignment of +IA,

ϕ_{T-} is the static tangential misalignment of –IA,

$\Delta\phi_{Ta}$ is the a_c proportional dynamic misalignment,

$\Delta\phi_{Td}$ is the nonlinear dynamic tangential misalignment,

ϕ_V is the sensor misalignment about the vertical axis,

ϕ_{Vo} is the initial alignment angle about the vertical axis,

ϕ_{V+} is the static vertical misalignment for +IA,

ϕ_{V-} is the static vertical misalignment for –IA,

$\Delta\phi_{Va}$ is the a_c proportional dynamic misalignment,

$\Delta\phi_{Vd}$ is the nonlinear dynamic vertical misalignment.

These approximate equations provide a good description for the vast majority of cases of centrifuge testing. The few cases where the neglected terms may be significant are easily handled by the detailed treatments of Clause 6. For example, integer revolution averaging of centrifuge data that has a large wow component will provide a zero value for the cross-product term, $2\Delta\omega_d/\omega_0$, leaving only the neglected squared term, $(2\Delta\omega_d/\omega_0)^2$. If the wow is less than several hundred parts per million, the error is less than 0.1 ppm, and zero will generally be an acceptable answer. For larger wow values, the added details are easily appended.

These combined input models can be applied to the accelerometer model equations to provide a composite equation to be used for data reduction. Input terms that may affect the accelerometer coefficients and cannot be identified by a distinctive signature should be flagged for correction in the development of a detailed test procedure.

8 Test procedures

8.1 Test planning

Clause 8 discusses procedures to be considered when conducting centrifuge testing. It is divided into three subclauses: test planning, test preparation and calibration, and testing and data acquisition. The accelerometer should be subjected to a limited performance test appropriate to the precision required, both before and after the centrifuge tests.

8.1.1 Level of precision

The first step in planning any centrifuge test is to determine the level of precision that will be required. That determination affects every detail of the planning and execution that follows, from the choice of the centrifuge to be used, to the listing of measurements to be made and the methods by which they will be made and recorded, and finally to the way in which the measurements will be analyzed.

Level of precision assessments starts with the nature of the requirements to be met by the test units. Simple test envelopes with modest tolerances can be approached with tests of minimal complexity, while detailed model equations with tight tolerances on the coefficients require close attention to all phases of the tests. The precision of the requirements must then be compared with the error sources of the centrifuge to be used as described in Clause 6. This analysis will determine what measurements must be made and with what accuracy they must be made, as well as many other details of the test plan.

8.1.2 Measurements to be taken

A typical list for a typical centrifuge appears in 8.3. A maximum-effort list of measurements can be quite demanding in terms of time and equipment and should be used only when really required. The list to be prepared should be the minimum consistent with the requirements and the equipment available.

Slip-ring availability is an important aspect of equipment availability to be verified during the planning stage, especially where operational considerations dictate high current levels or the use of redundant signal paths for low noise.

Temperature must be given special attention, both as an error source and as a test requirement. Availability of controlled fixed- or variable-temperature chambers must be established and their accuracy must be suitable for the level of precision, taking account of the thermal coefficients of the instruments to be tested.

8.1.3 Method and format of data recording

The level of precision also affects the method of data collection. Besides the obvious requirements imposed on the instrumentation, level of precision will determine the format of the data recording, the number of measurements to be averaged for each data point, the averaging technique, the averaging time of each measurement, and the need for simultaneity of the averaging periods of related measurements. Simultaneity is especially important in relating centrifuge angular velocity to test sensor outputs of different test sensors when multiple-unit testing is undertaken for common mode error rejection.

Simultaneity considerations, as well as the accuracy of frequency measurements for digital-output test sensors, will often determine the quality of reference time standards in the data system.

8.1.4 Number and sequence of measurements

A rule of thumb for measurements containing random noise is that the minimum number should be that obtained by adding 2 to the number of coefficients to be fitted and then multiplying by 4. The number may also be determined by the number of positions required to evaluate the coefficients as outlined in 8.3. The determination of test positions early in the planning phase permits design and fabrication of appropriate test fixtures.

Thermal considerations, especially self-heating of the test sensor, may determine the sequence of data points, but generally each sequence will begin and end with two to four static measurements spaced in positions so as to average out axis tilt, with sufficient points in between to assure a good curve determination. Additional static measurements may be added during each run if there is reason to believe that sensor drift, especially thermal drift, may be significant during the runs.

Any special operational characteristics of a test sensor should be noted and taken into account in planning the test. For example, some vibrating beam accelerometers have two pendulums that may be at different radii when tested with IA radial, and this requires that sufficient measurements be taken to permit fitting as two separate sensors, followed by merging the models (see Annex E).

8.1.5 Data analysis

The method of data analysis must be determined during the planning phase to ensure that the required number and kind of measurements will be taken and that the way in which noise is averaged will be sufficient for the level of precision. The details of these considerations are discussed in 9.3 and in Annex C.

8.1.6 Data verification

Planning of centrifuge tests should always include provision for verification of data validity during the progress of the test so that problems can be detected and corrective action taken before the test setup has been torn down. The details will vary with the design of individual centrifuge installations, but will include such techniques as flagging excessive variation due to noise in multiple measurements at a set point, and verifying by the best means available that balance has been accomplished. Such means may come from bearing motion measurements or from settling indications from an auto-balance loop. Preliminary data reduction should be implemented to determine residuals for each data set to assure adequacy of the data before disturbing the test setup.

8.2 Test preparation and calibration

This subclause endeavors to identify the many elements of preparation for testing on a centrifuge to serve as a reminder list that will tend to minimize total test time while achieving the desired accuracy. Care taken before starting the test will also minimize the need to reschedule and rerun tests to add data or to correct procedural errors.

8.2.1 Centrifuge preparation

The centrifuge itself should be thoroughly checked for operational performance to determine that all of its systems are functional: that the angular velocity control system has the desired stability, the balancing mechanism is functional and can balance the rotor to the needed degree, and the slip rings have been cleaned to achieve low noise and low resistance.

Further, one should determine that the mounting fixtures have been drilled for the proper hole pattern to match the unit under test and have been mounted on the centrifuge arm with the proper facilities for radius determination and for heating and cooling as required. At this point, the fixtures should be aligned to the centrifuge axes and arranged for rotation through such angles as necessary to perform orthogonal or skewed axis tests.

8.2.2 Test setup

The necessary test instruments, all checked for calibration, should be gathered together and cabled into the desired configuration with the centrifuge, using double slip rings where necessary to minimize noise and/or data dropout. The entire setup should be checked out for operational performance before even mounting the unit under test, utilizing substitute signal sources of known value and signal shorts to demonstrate that the error contribution of the instrumentation system is zero, or at least known so that the data can be corrected during analysis. Special care must be taken if the slip rings themselves are included in any of the signal circuits so that signal uncertainty is minimized.

The effects of temperature on the measurements should be carefully considered before testing begins so that such errors can be minimized, either by thermal control or by monitoring and correcting the data. If temperature chambers are utilized, care must be taken to minimize any thermal electromotive forces (EMFs) in the data lines. During the testing, the temperature of the unit under test should be allowed to stabilize before taking the data at each acceleration level.

After mounting the accelerometer on the centrifuge table, the centrifuge should be spun up and balanced at rates up to the maximum to be used during the planned tests. For tests requiring high accuracy, balance should be near perfect, since the residual motion due to unbalance need not be great to produce serious errors in the computed value of the K_2 coefficient (see 6.1.5).

8.2.3 Accelerometer calibration

Since the data reduction techniques utilize the known constants of the accelerometer being tested, when accuracy requires, a static multipoint test on a precision horizontal-axis dividing head should be performed to obtain precise values of scale factor, bias, and misalignment on the unit under test. The test could include measurement of the temperature sensitivities by tumbling about one or two of the three major axes (IA, OA, and PA) to determine sensitivity of pertinent misalignments of the unit as well as scale factor and bias.

8.3 Testing and data acquisition

Most of the details of testing and data acquisition should be worked out during the test planning stage, but some of them are best determined interactively during the actual testing.

8.3.1 Number of centrifuge runs

The total number of runs is determined by the number of positions and the number of data sets taken at each position.

The number of positions tested depends generally on the coefficients to be evaluated. The most common testing positions are shown for reference in Figure 3 and Figure 4. They are normally used in pairs, and by far the most common pair is positions 1 and 2. The usual pairs and the corresponding coefficients are listed in Table 2. If analysis or tests indicate that the cross-axis coefficient K_{io} is less than K_{ip}, it might be as well to mount the accelerometer so that OA is horizontal and PA is vertical, particularly if the input range is greater than $\pm 10\,g$. This recommendation is based on the fact that the vertical component of the misalignment angle is easier to control than the horizontal component. Further details may be found in a report by Neugebauer [B11].

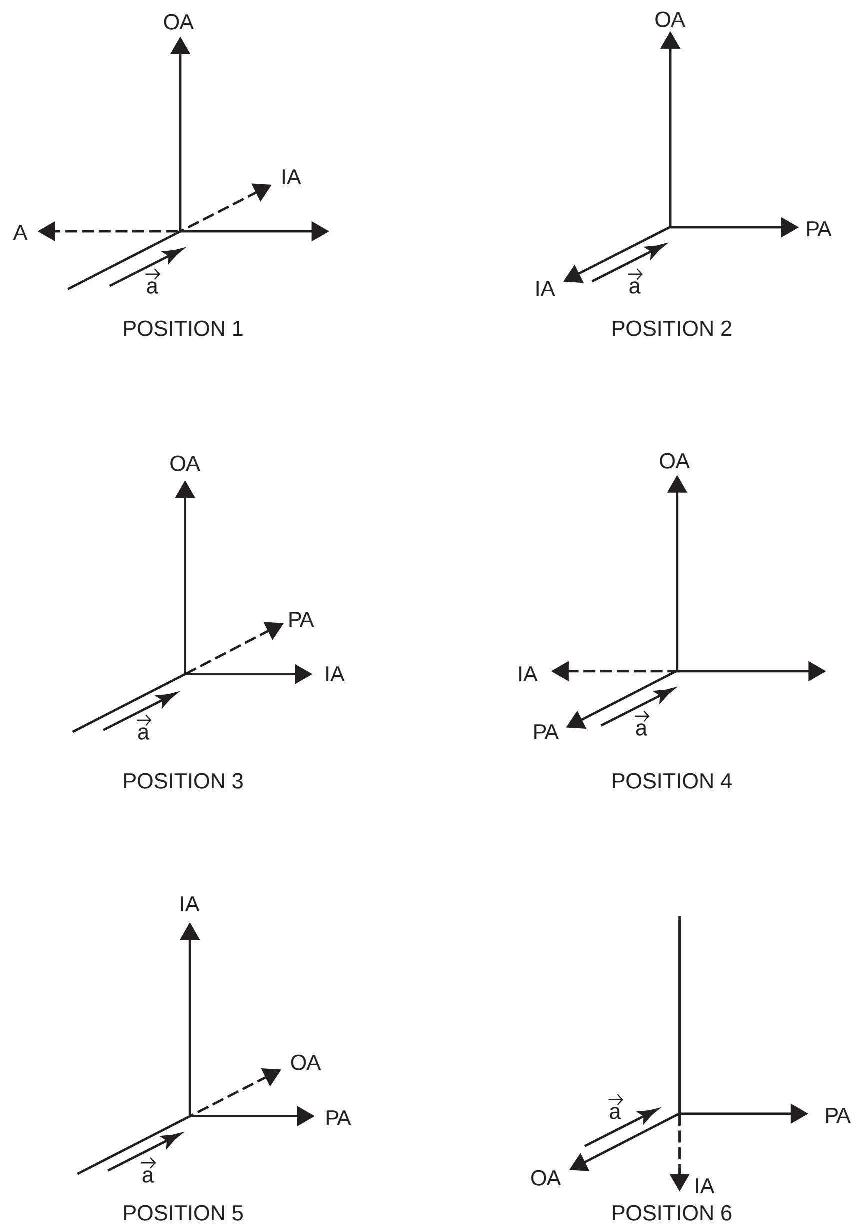

Figure 3—Accelerometer mounting positions

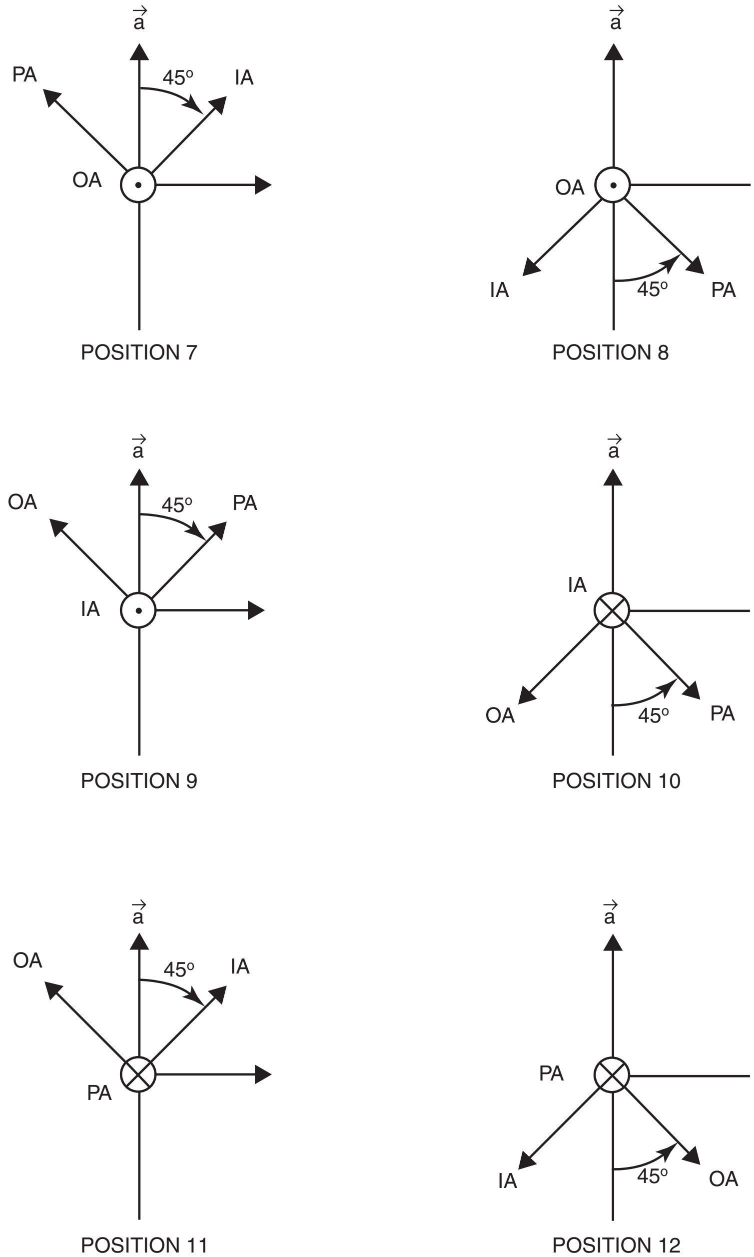

Figure 4—Accelerometer mounting positions (top views)

Table 2—Test position pairs

Position pair	Coefficients
1–2	K_{oq}, K_2, K_3
3–4	K_{pp}, K_{ppp}
5–6	K_{oo}, K_{ooo}
7–8	K_{ip}
9–10	K_{op}
11–12	K_{io}

The number of data sets required depends on the quality of data produced during the test (see 8.3.4). An estimate of the number of data sets required can be made from the accuracy margin of the test. The accuracy margin is the ratio of the standard error permitted by the specification or other test goal in the parameter to be tested to the estimated standard error of the measurement process for a single test of that parameter. For an accuracy margin of 10:1 or more, with no special problems encountered during the testing, a single set is generally sufficient. That is especially true in production testing where test and sensor characteristics are well established and actual test time is a major part of the cost. For research and development testing, or with an accuracy margin of 4:1 or less, at least two—but probably no more than four—sets of nominally identical measurements will normally be taken, to average random effects and to confirm repeatability. A special case exists where thermal effects may be significant, either from centrifuge heating or from sensor self-heating. In this case, two or more tests with different numbers or sequences of data points may be required.

The number and sequence of data points is generally an economic trade-off, assuming that the test sensors meet minimal short-term stability requirements. More data points are generally desirable to provide the best definition of the shape of the nonlinearity curve and the best averaging of random effects. As a rule of thumb, the minimum number of data points should be the number of coefficients to be determined increased by 2, then multiplied by 4.

Each centrifuge run should consist of a set of dynamic measurements preceded by and followed by a number of static measurements at different arm positions chosen to establish the sensor output at zero rate. These static data can be averaged to eliminate centrifuge misalignment errors. The minimum number is two measurements spaced 180° apart. The more common number is four measurements spaced 90° apart. For the dynamic set, most commonly, a number of equally spaced acceleration measurements are taken in ascending order up to the maximum test level, followed by an equal or smaller number of measurements in descending order back to stationary again. That is usually sufficient to determine linearity and to give an indication of repeatability and hysteresis.

When significant thermal effects are suspected or indicated, it may be advisable to run successive tests with a large number of data points followed by a small number in order to test over two substantially different time periods. A useful alternative is to apply the planned g levels in random order. This procedure will convert either hysteresis or thermal errors into random scatter and thus provide a convenient flag for unsuspected problems that may warrant additional testing (see 6.4.1).

Since scale factor as calibrated in 8.2.3 is usually more precise than the measurement of arm dimensions, the actual centrifuge radius may be estimated from acceleration data taken at a low level of acceleration (typically 1 g) for orientations 1 and 2 of Figure 3 (see 9.1.1), or by using the procedure of 9.3.3.

8.3.2 Resolution and noise

Rules for deciding when test plans and sensor or instrumentation characteristics provide adequate resolution for desired test accuracy are described in 6.6.1, but certain precautions must be observed during testing to ensure that test expectations are met.

In the case of analog sensors with analog-to-digital conversion on the output (specifically digital voltmeters), resolution and linearity may be significantly affected by the choice of meter ranges. Especially in the case of testing two or more sensors at once for common-mode rejection, it is important that both measurements be made on the same range. In some cases, slight adjustments of test levels may be required to produce that condition.

In the case of pulse rebalance sensors, the output pulse train should be checked during testing for evidence of moding, which could cause resolution to be significantly poorer than expected as well as indicating a sensor problem.

In all cases, noise should be monitored routinely for evidence of slip-ring dropouts, oscillations, wow and flutter, and excessive vibration. An oscilloscope or other real-time display system should routinely be provided to monitor analog signals. Digital signals can be automatically monitored by software that averages a number of points to establish each measurement and reject (and possibly flag) those measurements in which an appropriate statistical measure of scatter (e.g., standard deviation) exceeds a reasonable limit.

8.3.3 Data recording

Data-taking with pencil and paper is possible for limited aims under special conditions, but precision centrifuge testing may be assumed to use automated digital techniques under the direct control of a digital computer. The results are recorded on a suitable disk or magnetic tape.

The number of signals to be recorded will vary with the centrifuge selected and the tests to be conducted. A partial list might include the following (see 6.6.1):

— Output of test sensor(s) (analog/digital)
— Output of reference sensor(s)
— Sensor temperature
— Torquer resistance
— Voltage-to-frequency (V/F) converter temperature
— Fixture temperature
— Power supply input current
— Power supply line noise
— Scaling resistor temperature
— Centrifuge arm velocity and position
— Arm stretch sensor(s)
— Fixture rotation sensor(s)
— Imbalance sensor(s)

Standard laboratory practice will suffice for most centrifuge data recording, though high levels of precision may require special attention to such things as thermal EMFs in analog circuits. A special requirement of many centrifuge measurements is the need for simultaneity of certain measurements, and in particular the need for coincidence of integrating or averaging times. This need may require careful consideration, not only of software and analog hardware, but also of the internal functioning of such things as dual-slope integrating digital voltmeters. These considerations are discussed in more detail in 6.6.1.

8.3.4 Data verification

Since precision centrifuge tests tend to be time-consuming to set up and to conduct, it is important to monitor the data-taking process so as to have a reasonable assurance that the results are valid before the test setup has been torn down. Final verification may not be possible until completion of a full statistical evaluation of the data, but a number of useful checks can be accomplished in real time, or nearly so, during the course of testing.

If certain runs are repeated, especially after remounting of the test sensors, corresponding data should be spot-checked for the expected degree of repeatability. A special case of this test is the comparison of runs over different time periods when significant thermal effects are suspected.

If sensor temperature is recorded, it should be noted during the run to see if a thermal problem is indicated.

Some forms of data verification can be automated by adding tests to the software. An example already noted is the measurement of noise level during the common procedure of averaging several digital samples of each measurement. This step can provide a guard against data that may be invalid because of excessive wow and flutter or drift, due to excessive vibration, sensor noise under acceleration, or slip-ring dropouts or noise. Software flags can also be added to call attention to unreasonable or out-of-spec readings on such correction sensors as imbalance (run-out) monitors and arm stretch monitors.

Finally, a check should be made on the actual sensor data to ensure that it is reasonable. Provision can be made to fit a least-squares straight line to the data and print or plot the residuals from this line. Such a comparison can also be made in real time while the run is being conducted by fitting a mathematical straight line through initial zero-rate readings and a relatively low g point, such as 2 or 3 g. Differences between the actual data points and the values predicted by extrapolation of this line can then be printed or plotted nearly instantaneously as the measurements are made. This procedure may not constitute an analysis of the data, but it can provide sufficient suppression of the dominant linear term to make many sensor or setup problems readily apparent when they might otherwise go unnoticed.

9. Data reduction

This clause describes the data reduction techniques required to determine the accelerometer nonlinearity coefficients. The process consists of

a) Determination of the actual applied acceleration
b) Compensation of the accelerometer output data
c) Determination of a model equation to which the data may be fitted

Also provided in 9.3.1 and Annex C is a discussion of data reduction techniques for simpler requirements, which may not include evaluation of specific coefficients.

9.1 Determination of total acceleration input

9.1.1 Centripetal

The determination of centripetal acceleration requires knowledge of radius and the centrifuge angular velocity. The actual radius consists of the static radius plus any changes occurring during arm rotation. The static radius can be determined by physical measurements (see 6.1.8). The preferred method for precise applications when IA is along the arm is to use the scale factor measurements of 8.2.3 and the accelerometer data from low-level static acceleration data of 8.3.1. The radius is determined by first subtracting the average of the static outputs from the average accelerometer output when the arm is rotating. When divided by the scale factor, this gives the centripetal acceleration as

$$\frac{E_r - E_s}{K_1} = \omega_0^2 R_0 \tag{85}$$

where

E_r is the average output when the centrifuge is rotating,

E_s is the average output when the centrifuge is stationary.

Using the average centrifuge angular velocity (ω_0), the radius can be determined. The static radius may be different for positive and negative IA orientations and must be determined for each.

The change in radius measured as discussed in 6.1, or computed using some previously developed relationship between radius change and centrifuge rate, must be added to the static radius at each test level.

At each test level, the centrifuge angular velocity must also be determined as discussed in 6.3.4.

9.1.2 Coriolis

This is calculated as shown in 7.2.3, using values for centrifuge angular velocity and radius as shown in 9.1.1, and added to the centripetal acceleration if the centrifuge rotation is counterclockwise (CCW) in the Northern Hemisphere, or subtracted if it is clockwise (CW).

9.1.3 Gravitational

The component of gravitational acceleration that is directed along the IA of the accelerometer is determined as shown in 7.2.4. This may require the determination of misalignment at each test level. This measurement is described in 6.2.5. This acceleration is added to the centripetal and Coriolis accelerations to give the total.

9.1.4 Misalignment compensation for nonradial IA orientations

The significance of alignment-induced errors may be evaluated by reversal of the instrument IA. The reversal of the IA allows separation of the accelerometer coefficients from the effects of misalignment, as discussed in 6.2.3.

9.2 Compensations to accelerometer output

9.2.1 Bias and static alignment compensation

Data reduction of the accelerometer output begins with the conversion of all data into *g* units. This is done by dividing the output units by the scale factor in output units per *g* at the temperature of the test, correcting each data point individually if the unit temperature changed significantly during the test.

The next step in data reduction may be that of removing any bias or offset from the data by use of the output data when the centrifuge is not rotating, leaving only the output due to centripetal acceleration. This step is necessary only if percentage weighting of data will be used (see Annex C) and is otherwise optional.

As discussed in 6.2.1, any static misalignment about a horizontal axis will cause the accelerometer to sense a component of gravity, adding a constant value to the data that is indistinguishable from true sensor bias. Accordingly, the components must be treated together, and each direction of each run must be compensated for individually, since the misalignment term will most likely change when the accelerometer is rotated to reverse its sensing axis (see 5.1 and 6.2).

As an example, assume that the zero-rate data is taken with the arm positioned at the four points of the compass and averaged. This same process is performed for the starting and ending of each run, using the average of the values of the starting and ending bias, each corrected for temperature, for the compensation of the data for that run. That value is then subtracted algebraically from each of the data points taken during the run, making the implicit assumption that a zero-rate input produces a zero output signal.

This procedure automatically weights the zero-rate data more heavily in recognition of its greater reliability. This goal can also be achieved by direct application of the method of 9.3.3, provided that each of the several zero-rate points is entered independently and given a weight appropriate to its typically small variance.

9.2.2 Temperature compensation

If temperature effects are anticipated to be a significant cause of error, the output data from the centrifuge tests must be corrected using the monitored values of temperature of the accelerometer taken at each data point, along with the thermal sensitivity coefficients of scale factor, bias, and alignment as measured pretest (see 8.2.3).

The details of applying the compensations may depend on the specific accelerometer design. The following is appropriate for a typical torque-balance accelerometer.

Since the scale factor thermal coefficient modifies all the data, that correction should be made first by dividing the output at each point by the predicted value of scale factor for the temperature measured at that data point.

Next, the effects of thermal coefficients of bias and alignment can be compensated for. In the common case where IA is radial, their effects are indistinguishable from one another and their coefficients must be algebraically added to provide the correct net coefficient. This value is used to compute an accelerometer output offset correction for each data point, using the measured temperature at that data point. Applying this correction effectively modifies the data to read the value that would have been measured if the accelerometer had been held at the reference temperature. Similar corrections may be made for other orientations.

9.2.3 Other compensations

The data from the centrifuge run may be further processed to incorporate other compensations, which include

a) Effects of self-heating of sensor/load (see 6.4)
b) Temperature gradients (see 6.4)
c) Effects of measured arm stretch and droop (see 6.1.8)

The need for each of these compensations must be evaluated based on the design of the sensor being tested, using available technical information on the sensor as well as the centrifuge. The exact form of the compensation equations will change with the design of the accelerometer and must be derived for the exact test configuration (see 6.1 and 6.4).

9.3 Determination of accelerometer model coefficients

9.3.1 Simplified data reduction

Most applications of low-to-medium-precision accelerometers, and even some applications of high-precision accelerometers, require only that the total error due to nonlinearity remain within certain prescribed bounds. These bounds are typically described in terms of allowable departures from a reference straight line, and the task of reducing the data can be correspondingly simplified compared with the polynomial fits described in 9.3.3. When the total precision required is relatively low, the need for prefit data compensation may be greatly reduced as well.

Both the bounds and the reference straight line may take many forms, and may be subject to interpretation if not carefully described. In setting up to test such criteria, it is crucial that the test group and the user be fully agreed as to both the error bounds and the details of how they are to be applied to the measurements.

Rather than present the reader of this document with an arbitrarily chosen example out of the many cases possible, the editors refer those with interests in this area to Annex C, Fitting theory. This simplified treatment of the underlying theory provides insights into the complex fitting detailed in 9.3.3, along with sufficient guidance to design an efficient data reduction process for commonly encountered simplified cases.

9.3.2 Modeling methods

Although attention here is focused on determining the model equation coefficients for a single accelerometer mounted in positions 1 and 2 of Figure 3 in 8.3.1, the same general type of reasoning may be applied to other pairs of positions in Figure 3 and Figure 4 (see 9.3.5). For the analysis of dual accelerometer centrifuge test data, see 6.6.3.

If possible, the model equation should be obtained from a complete analysis of the mechanical structure and the electronics. If this is not feasible, dimensional analysis may be useful in determining the functional parameters for the model equation. When neither of the above alternatives is practical, an empirical equation, usually in the form of a power series in the input acceleration, may be adopted and tried. The power series may be modified to conform to some known characteristic of the accelerometer, or as found necessary from a study of the residuals (see 9.3.3). Regardless of how the model equation is chosen, it must be checked for adequacy as indicated in 9.3.4.

9.3.3 Determination of the coefficients

After the form of the model equation has been chosen, it is then necessary to determine the numeric values of the coefficients for each accelerometer. To illustrate the method of determining the coefficients from centrifuge data in positions 1 and 2 of Figure 3, the following model equation will be used:

$$a_s = E/K_1 = K_0 + a_i + K_2 a_i^2 + K_{oq}|a_i|a_i + K_3 a_i^{\;3} \tag{86}$$

where

- a_s is the indicated sensor output (g),
- a_i is the acceleration along IA (g),
- E is the sensor output (output units),
- K_0 is the bias (g),
- K_1 is the scale factor (output units/g),
- K_2 is the second-order coefficient (g/g^2),
- K_{oq} is the odd-quadratic coefficient (g/g^2),
- K_3 is the third-order coefficient (g/g^3).

The odd-quadratic coefficient above, which is added to the power series, may appear in some accelerometers due to thermal effects (see 6.4). It may also appear as an artifact of the data reduction procedure if the radial measurement errors in the two mounting positions differ. The iterative data reduction procedure described herein will remove the artifact component of the odd-quadratic coefficient.

9.3.3.1 Details of estimation procedure

In general, the sensor IA will not be precisely aligned with the radius through the ECM of the proof mass and will probably be different in the two mounting positions. Let θ_{ri} be the total misalignment angle between the radius through the ECM and IA. Let θ_g be the projection of θ_{ri} on a vertical plane containing IA. For small-angle approximations, $\theta_g = \phi_T$, and

$$\theta_{ri} = \sqrt{{\phi_T}^2 + {\phi_V}^2} \tag{87}$$

The sin θ_g is the component of local gravity acting along IA and is positive when the vector IA has an upward component. For reasons that will become evident, the angle θ_g must be kept small, say no more than 0.01 rad. This is easily accomplished by comparing the average static output of the accelerometer at two or more evenly spaced positions of the centrifuge arm, with the bias previously measured on a precision dividing head. The environment in the dividing head area should match the thermal environment in the centrifuge area closely enough that the bias is not affected by more than one or two thousandths of a g, or the scale factor by more than 0.1% when testing precision accelerometers.

The angles θ_{ri} and θ_g must be kept small enough that the components of θ_g and a_c along the cross axes have no significant effects. Thus, the limits on the allowable misalignments also depend on the magnitudes of the coefficients δ_p, δ_o, K_{ip}, and K_{io}.

It is good practice to check the bias and scale factor at the end of a centrifuge run, or even more often, to determine if there has been any drift in their values. If there has been drift, the accelerometer output should be corrected for the scale factor drift. If considered appropriate, the changes should be allocated on an elapsed time basis.

The measured radii to the ECM will also, in general, be in error and different in the two mounting positions. Let the true radius to the ECM be $R = R_0(1 + \Delta R/R_0)$, where R_0 is the measured radius and ΔR is the measurement error. Though the iterative procedure to be described presently does not require an accurate knowledge of the radii, it does require, as would any other data reduction procedure, that changes in radii be monitored as accurately as possible and the estimated input data be adjusted appropriately; i.e., multiply $(a_c + a_h)$ by $(1 + \Delta R/R_0)$ where ΔR is now the change in R from its original measurement.

If there are changes noted in misalignment angle θ_g during a test run, the input acceleration data should be adjusted appropriately. Since the misalignment angle θ_{ri} has only a cosine effect, slight changes can usually be neglected.

With the above misalignment and radial measurement errors, the true output of the accelerometer using the model equation is

$$\begin{aligned} a_s = {} & K_{0+} + K_{0-} + a'_{i+} + a'_{i-} + K_2[(a'_{i+})^2 + (a'_{i-})^2] + K_{oq}[(a'_{i+})^2 - (a'_{i-})^2] \\ & + K_3[(a'_{i+})^3 + (a'_{i-})^3] + \xi_+ + \xi_- \end{aligned} \tag{88}$$

where the terms with a subscript "+" apply only when $a_i > 0$ and terms with a subscript "–" apply only when $a_i < 0$. The true but unknown input accelerations are

$$a'_{i+} = \sin\theta_{g+} + a_{i+}\left(1 + \frac{\Delta R_+}{R_+}\cos\theta_{ri+}\right) \tag{89}$$

$$a'_{i-} = \sin\theta_{g-} + a_{i-}\left(1 + \frac{\Delta R}{R}\cos\theta_{ri-}\right) \tag{90}$$

where a_{i+} and a_{i-} are the best estimates of the input acceleration based on the measured radii plus Coriolis acceleration. The terms ξ_+ and ξ_- are the random noise components.

Equation (89) gives the true output, but there is no a priori knowledge of the true input accelerations a'_{i+} and a'_{i-} or of the noise. Therefore, the data will be fitted to the following approximate equation:

$$\begin{aligned} a_s = {} & K_{0+} + K_{0-} + (1 + c_+)a_{i+} + (1 + c_-)a_{i-} + K_2(a_{i+}^2 + a_{i-}^2) \\ & + K_{oq}(a_{i+}^2 - a_{i-}^2) + K_3(a_{i+}^3 + a_{i-}^3) \end{aligned} \tag{91}$$

where c_+a_{i+} and c_-a_{i-} are first approximations of the errors in the estimated input accelerations due to misalignment and radial measurement errors.

For greater computational accuracy, the above approximate equation can be rearranged into the following form:

$$\begin{aligned} a_s - a_i = {} & K_3[(a_{i+})^3 + (a_{i-})^3] + K_{oq}[(a_{i+})^2 - (a_{i-})^2] + K_2[(a_{i+})^2 + (a_{i-})^2] \\ & + c_-a_{i-} + c_+a_{i+} + K_{0-} + K_{0+} \end{aligned} \tag{92}$$

Matrix Equation (93) is obtained by applying the method of least squares to Equation (92). (For a more detailed discussion of this procedure see Neugebauer, 1987 [B12]).

$$\begin{bmatrix} \sum a_i^6 & (\sum a_{i+}^5 - \sum a_{i-}^5) & \sum a_i^5 & \sum a_{i-}^4 & \sum a_{i+}^4 & \sum a_{i-}^3 & \sum a_{i+}^3 \\ (\sum a_{i+}^5 - \sum a_{i-}^5) & \sum a_i^4 & (\sum a_{i+}^4 - \sum a_{i-}^4) & -\sum a_{i-}^3 & \sum a_{i+}^3 & -\sum a_{i-}^2 & \sum a_{i+}^2 \\ \sum a_i^5 & (\sum a_{i+}^4 - \sum a_{i-}^4) & \sum a_i^4 & \sum a_{i-}^3 & \sum a_{i+}^3 & \sum a_{i-}^2 & \sum a_{i+}^2 \\ \sum a_{i-}^4 & -\sum a_{i-}^3 & \sum a_{i-}^3 & \sum a_{i-}^2 & 0 & \sum a_{i-} & 0 \\ \sum a_{i+}^4 & \sum a_{i+}^3 & \sum a_{i+}^3 & 0 & \sum a_{i+}^2 & 0 & \sum a_{i+} \\ \sum a_{i-}^3 & -\sum a_{i-}^2 & \sum a_{i-}^2 & \sum a_{i-} & 0 & N_- & 0 \\ \sum a_{i+}^3 & \sum a_{i+}^2 & \sum a_{i+}^2 & 0 & \sum a_{i+} & 0 & N_+ \end{bmatrix} \times \begin{bmatrix} K_3 \\ K_{oq} \\ K_2 \\ c_- \\ c_+ \\ K_o \\ K_{o+} \end{bmatrix}$$

$$= \begin{bmatrix} \sum(a_s - a_i)a_i^3 \\ \sum(a_s - a_i)|a_i|a_i \\ \sum(a_s - a_i)a_i^2 \\ \sum(a_s - a_i)a_{i-} \\ \sum(a_s - a_{i+})a_{i+} \\ \sum(a_s - a_{i-}) \\ \sum(a_{s+} - a_{i+}) \end{bmatrix} \tag{93}$$

or

$$[\mathbf{A}]\,[\mathbf{K}] = [\mathbf{B}]$$

where

N_+ is the number of data points of a_{i+},

N_- is the number of data points of a_{i-}.

9.3.3.2 General formulation of estimation procedure

An alternative procedure may be used when computer software is available to do matrix arithmetic. It allows the computer to generate a matrix corresponding to the [**A**] matrix directly from the model equation and input data, thereby minimizing the possibility of algebraic or programming error. It is especially useful when the model equation differs from Equation (92) so that Equation (93) cannot be used directly.

First, consider that the model Equation (92) can be written more generally in the form

$$d_{\mathrm{k}} = \sum_{j=0}^{P} h_{\mathrm{j}} f_{\mathrm{j}}(a_{\mathrm{ik}}) + n_{\mathrm{k}} \tag{94}$$

where

- k is the kth data point,
- d_{k} is the $a_{\mathrm{sk}} - a_{\mathrm{ik}}$,
- h_{j} is the constant coefficient,
- n_{k} is the additive random noise,
- f_{j} is the function of input acceleration [e.g., if $h_3 = K_3$, $f_3(a_{\mathrm{i}}) = (a_{\mathrm{i+}})^3 + (a_{\mathrm{i-}})^3$]

For purposes of this subclause, the coefficient list must include c_+ and c_-.

If there are m data points to be fitted, Equation (94) becomes a matrix equation, with m rows:

$$\begin{bmatrix} d_1 \\ d_2 \\ \vdots \\ d_m \end{bmatrix} = \begin{bmatrix} f_0(a_{\mathrm{i1}}) & f_1(a_{\mathrm{i1}}) & \cdots & f_{\mathrm{p}}(a_{\mathrm{i1}}) \\ f_0(a_{\mathrm{i2}}) & f_1(a_{\mathrm{i2}}) & \cdots & f_{\mathrm{p}}(a_{\mathrm{i2}}) \\ \vdots & \vdots & \vdots & \vdots \\ f_0(a_{\mathrm{i}m}) & f_1(a_{\mathrm{i}m}) & \cdots & f_{\mathrm{p}}(a_{\mathrm{i}m}) \end{bmatrix} \times \begin{bmatrix} h_0 \\ h \\ \vdots \\ h_{\mathrm{p}} \end{bmatrix} + \begin{bmatrix} n_1 \\ n_2 \\ \vdots \\ n_{\mathrm{m}} \end{bmatrix} \tag{95}$$

Equation (95) cannot be solved directly since [**N**] is unknown and [**F**] is not, in general, a square matrix, but if Equation (95) is multiplied by the transpose of [**F**], two useful changes occur:

a) The product $[\mathbf{F}]^{\mathrm{T}}[\mathbf{F}]$ is seen to be a (p + 1) × (p + 1) square matrix
b) The least-squares criteria described in Annex C can be seen to be equivalent to $[\mathbf{F}]^{\mathrm{T}}[\mathbf{N}] = 0$.

Thus,

$$[\mathbf{F}]^{\mathrm{T}}[\mathbf{D}] = [[\mathbf{F}]^{\mathrm{T}}[\mathbf{F}]][\mathbf{H}] \tag{96}$$

Equation (96) is equivalent to Equation (93), and, in fact, will be found to be identical to it if the same model equation is used.

9.3.3.3 Solution of equations

Equation (93) or Equation (96) may be solved by any of the following standard methods:

a) Method of determinants
b) Gauss elimination method
c) Matrix inversion method

Method b) is generally the most accurate because it requires the fewest arithmetical operations. On the other hand, c) has the advantage that the elements on the principal diagonal of the inverted matrix may be used directly for determining the statistical uncertainty of the coefficients. The fact that matrix [**A**] is symmetrical permits a special matrix inversion method to be used that greatly reduces the number of computations, since it inverts only the upper triangle (including the principal diagonal).

From the solution of Equation (93), closer approximations to the input accelerations may be obtained. The revised input accelerations are

$$a^*_{\mathrm{i}+} = (1+c_+)a_{\mathrm{i}+} \tag{97}$$

$$a^*_{\mathrm{i}-} = (1+c_-)a_{\mathrm{i}-} \tag{98}$$

Equations (97) and (98) are not quite in the correct form since they do not properly include the effects of the gravity components $\sin\theta_{\mathrm{g}}$. However, if $\theta_{\mathrm{g}} < 0.01$ rad, the errors are acceptable.

With the improved approximations of Equations (97) and (98), the elements of Equation (93) are revised using the following formulas based on Equations (97) and (98):

$$\begin{aligned}
&\sum (a^*_{\mathrm{i}+})^k = (1+c_+)^k \sum a_{\mathrm{i}}+^k && k = 1, 2, \ldots, 6\\
&\sum (a^*_{\mathrm{i}-})^k = (1+c_-)^k \sum a_{\mathrm{i}-}^k && k = 1, 2, \ldots, 6\\
&\sum (a_{\mathrm{s}+} - a^*_{\mathrm{i}+})(a^*_{\mathrm{i}+})^{\mathrm{k}} = (1+c_+)^k \left[\sum (a_{\mathrm{s}+} - a_{\mathrm{i}+})a_{\mathrm{i}+}^k - c_+ \sum a_{\mathrm{i}+}^{k+1}\right] && k = 0, 1, 2, 3\\
&\sum (a_{\mathrm{s}-} - a^*_{\mathrm{i}-})(a^*_{\mathrm{i}-})^k = (1+c_-)k\left[\sum (a_{\mathrm{s}+} - a_{\mathrm{i}-})a_{\mathrm{i}-}^k - c_- \sum a_{\mathrm{i}-}^{k+1}\right] && k = 0, 1, 2, 3
\end{aligned} \tag{99}$$

With the revised elements in Equation (93), again solve for the model equation coefficients. The new linear coefficients c_+ and c_- may be used to further revise Equation (93). This iterative procedure converges very rapidly, so that only one or two revisions of the input data should reduce c_+ and c_- to less than 0.1 $\mu g/g$, which is usually sufficient.

In the model equation selected here for illustrative purposes, the powers of a_{i} are all integers, but Equations (99) apply equally well for noninteger values.

In order to accurately determine the nonlinear coefficients, it is necessary that the number of input/output data points substantially exceeds the total number of coefficients to be determined. The minimum number of data points required in any particular application cannot be answered categorically since it will depend on the form of the model equation, the required accuracy, the magnitude of the coefficients, the input acceleration range, and, very importantly, on the noise content of the data. The following may be useful.

a) $N_+ + N_- \geq 4(n+2)$, where n is the total number of coefficients to be determined. In the case of Equation (94), $n = 7$ and the total number of measurements is 36. There is a trade-off between increasing the number of measurements and not having the test extend over too long a period of time, which increases costs and accelerometer instabilities.
b) The reading should be taken over the maximum possible input range, both positive and negative. In no case should the range be less than the operational range. Care must be taken not to exceed the design limits that may cause permanent strains to develop. If the acceleration range is reduced by a factor of two, for example, the error in the cubic coefficient due to noise

would increase by a factor of eight and the error in the quadratic coefficient would increase by a factor of four. Since noise has a random distribution and may also be a function of the acceleration, the above relations are necessarily approximate.

c) The errors in the determination of all the coefficients vary directly as the standard deviation of the noise in the input/output data. Since noise has a random distribution, this relation is also necessarily approximate.
d) Increasing the number of input/output data points will reduce the effect of noise in the recovery of the coefficients. It is expected that increasing the number of data points by a factor of three would reduce the effect of noise by the square root of 3.
e) One of the most effective ways of reducing the effect of noise, while still having to handle only a reasonable amount of data, is to average the data over several revolutions of the centrifuge arm. If there are synchronous periodic variations in angular velocity (wow), the sample period should be over a whole number of revolutions (see 6.3.1). The longer the sample period, the less is the effect of noise and timing errors. On the other hand, the longer the sample period, the greater the effect of drift in bias and scale factor and of sensor self-heating (see 6.4). The choice of sample period is a matter of compromise of opposing effects and is a matter for engineering judgment.

A rough estimate of the noise at a given acceleration level may be obtained by noting the variations in output over each of a number of revolutions at a ‘‘steady’’ input acceleration.

9.3.4 Model adequacy

A model equation has been selected and the coefficients determined from centrifuge data taken over the full operational range of the accelerometer. The next step is to determine if the selected model equation adequately describes the input/output relationship. The true input/output relationship is of no concern here. That should have been considered when choosing the model equation. Extrapolation of a model equation, particularly an empirical one, beyond the limits of the test data should be done with caution, if at all.

The model equation should be checked by a subjective test for systematic errors and by objective statistical tests. To illustrate the procedure, Equation (86) will continue to be used as the model equation, but the same test may be applied to any other model equation. If the iterative data reduction procedure outlined above is used, then the final approximate equation whose coefficients were determined is

$$\begin{aligned} a_s = {} & K_{0+} + K_{0-} + a^*_{i+} + a^*_{i-} + K_2[(a^*_{i+})^2 + (a^*_{i-})^2] + K_{oq}[(a^*_{i+})^2 - (a^*_{i-})^2] \\ & + K_3[(a^*_{i+})^3 + (a^*_{i-})^3] \end{aligned} \tag{100}$$

where

$$a^*_{i+} = (1+c_{1+})(1+c_{2+})\ldots\ (1+c_{n+})a_{i+} \tag{101}$$

$$a^*_{i-} = (1+c_{1-})(1+c_{2-})\ldots(1+c_{n-})a_{i-} \tag{102}$$

are the revised values of the input accelerations, with $c_{1+}\ \ldots\ c_{n+}$ and $c_{1-}\ \ldots\ c_{n-}$ being successive values of c_+ and c_- to less than $0.1\ \mu g/g$, which may be neglected compared with unity. The accelerations a_{i+} and a_{i-} in Equations (101) and (102) are the original best estimates of the input accelerations with any corrections required because of bias changes or changes in radii.

If the iterative data reduction procedure is not used—say, for low-accuracy accelerometers—then replace Equation (100) by Equation (91) and ignore Equations (101) and (102), which would not apply.

The most important consideration in determining the adequacy of a model equation is the distribution of the residuals as a function of input acceleration. A residual is defined as the observed output less the calculated value from Equation (100) or Equation (91), as appropriate:

$$r = a_s - \{K_{0+} + K_{0-} + a^*{}_{i+} + a^*{}_{i-} + K_2[(a^*{}_{i+})^2 + (a^*{}_{i-})^2] + K_{oq}[(a^*{}_{i+})^2 - (a^*{}_{i-})^2] + K_3[(a^*{}_{i+})^3 + (a^*{}_{i-})^3]\} \quad (103)$$

As a check on the calculations, the sum of the residuals should be zero except for round-off errors.

Plot the residuals versus input acceleration and look for evidence of systematic errors. Although a computer can be programmed to apply statistical criteria, human judgment is usually needed to decide if there are any systematic errors. Sometimes, systematic errors are easier to recognize if averages at or near an acceleration level are plotted, rather than plotting each individual residual. However, this practice should not be carried too far, because if there are too few points, then even a purely random distribution of the residuals may appear to have a systematic component.

If there is a systematic error, the model equation should be changed or modified and the coefficients recalculated. Sometimes the required modification of the model equation is fairly obvious. For example, if the systematic error component is symmetrical about the zero acceleration ordinate and has three extremum values (maxima and minima), a fourth degree term should be added. Other systematic errors may require much ingenuity or intuition to decide what modifications should be made.

If there are no apparent systematic errors (systematic errors would invalidate the statistical criteria), then the next step is to determine the range of uncertainty of the coefficients at a given confidence level. First, the standard deviation $\sigma(r)$ of the residuals is needed:

$$\sigma(r) = \sqrt{\frac{\sum r^2}{f}} \quad (104)$$

where f is the number of degrees of freedom—i.e., the total number of data points used to determine the coefficients, less the number of coefficients. In the case of Equation (93),

$$f = N_+ + N_- - 7 \quad (105)$$

The standard deviation of the residuals should approximate the estimated errors of the input/output measurements.

Suppose that in a sample of 30 data points there is one for which the residual exceeds three times the standard deviation. Should that data point be included when determining the coefficients?

Since, on the average, less than 3 residuals in 1000 should exceed $3\sigma(r)$, it is evident that the computed standard deviation could be grossly in error, even if that residual is a true member of the population.

If there is such a data point, first check the records for any glitches in the power supply or other events that might have occurred at the time the data was taken. If an event did occur that would have affected the data, then that data point may be discarded, and the coefficients and residuals recalculated. Another fairly common source of error is the transposition of numbers in either the data-taking or the data-entry into the computer.

If there are no evident errors in the data, then a statistical test should be made to determine if the data point should be accepted or rejected. Unfortunately, there is no general agreement among statisticians on acceptance/rejection criteria. The following simple test gives results that are not substantially different from most proposed criteria:

$$\mu = \frac{|r|_m}{\sigma(r)} \qquad \text{where } |r|_m \text{ is the greatest absolute residual} \tag{106}$$

$$\mu_c = 1.25 + \ln\sqrt{\frac{N}{3}}, \qquad \text{for } N \geq 10 \tag{107}$$

If $\mu \geq \mu_c$, the probability is less than 5% that N readings from a normal population would include one reading so remote from the others. Therefore, the data point corresponding to $|r|_m$ should be discarded and new values of the coefficients should be calculated. If $\mu < \mu_c$, then the data point should be accepted.

The standard deviation of a coefficient K_i in the column matrix **[K]** of Equation (93) is

$$\sigma(K_i) = \sigma(r)\sqrt{d_{ii}} \tag{108}$$

where d_{ii} is the element on the principal diagonal of the inverted matrix $[\mathbf{A}]^{-1}$, which is in the same row as K_i.

If Equation (93) is solved by the method of determinants or by the Gauss elimination method, an alternative equation for the standard deviation of a coefficient is

$$\sigma(K_i) = \sigma(r)\sqrt{\frac{|M_i|}{|A|}} \tag{109}$$

where $|A|$ is the determinant of the matrix **[A]** and $|M_i|$ is the minor of determinant $|A|$ for the coefficient K_i. For example, the minor for the coefficient K_2 in Equation (93) is obtained by deleting the third row and the third column of **[A]**.

The confidence interval for the mean value of a coefficient K_i is

$$K_i = K_i \pm \frac{t\sigma(K_i)}{\sqrt{N_+ + N_-}} \tag{110}$$

where K_i is the calculated value obtained from the centrifuge data and t is the Student t statistic corresponding to a specified confidence level P and degrees of freedom f. The Student t statistic may be obtained from a statistics handbook for two-sided (two tails) test or by the approximate Equations (111), which are suitable for incorporation in a computer program. The errors in Equations (111) do not exceed 0.5% for $f \geq 4$ and must not be used for $f < 4$ because the errors increase very rapidly.

$$
\begin{aligned}
t &= 1.960 + \frac{2.392}{f - 1.082}, \qquad \text{for } P = 0.95 \\
t &= 1.645 + \frac{1.532}{f - 0.855}, \qquad \text{for } P = 0.90 \\
t &= 1.282 + \frac{0.840}{f - 0.622}, \qquad \text{for } P = 0.80
\end{aligned} \tag{111}
$$

For all practical purposes, if $f \geq 20$, then it is probably sufficiently accurate to use $t = 2$, 1.7, and 1.3 for $P = 0.95$, 0.90, and 0.80, respectively. For example, let $\sum r^2 = 2.487 \times 10^{-5}$, $N_+ + N_- = 34$, $f = 27$, $K_2 = 3.257 \times 10^{-6}$, and $d_{33} = 5.594 \times 10^{-8}$. Determine the 95% confidence interval for K_2 using Equation (112). Use $t = 2$.

$$\sigma(r) = \sqrt{\frac{\sum r^2}{f}} = \sqrt{\frac{2.487 \times 10^{-5}}{27}} = 9.599 \times 10^{-4}$$

$$\sigma(K_2) = \sigma(r)\sqrt{d_{33}} = 9.598 \times 10^{-4} = 2.270 \times 10^{-7}$$

$$K_2 = K_2 \pm \frac{t\sigma(K_i)}{\sqrt{N_+ + N_-}}$$

$$K_2 = 3.257 \times 10^{-6} \pm \frac{2 \times 2.270 \times 10^{-7}}{\sqrt{34}} \tag{112}$$

Therefore, there is a 95% probability that the mean value of K_2 lies in the interval $3.179 \times 10^{-6} \leq K_2 \leq 3.335 \times 10^{-6}$

If the confidence interval for a coefficient includes zero in its range, then it would be as well to check the confidence interval for $P = 0.50$, which gives what is usually called the probable error. If zero is still within the confidence interval, then the coefficient may be considered not significantly different from zero and dropped from the model equation.

9.3.5 Relationship of estimated coefficients to accelerometer performance model coefficients

Besides positions 1 and 2 in Figure 3 that are analyzed in 9.3.3, other pairs of positions in Figures 3 and 4 can be analyzed similarly. Instead of estimating model coefficients K_2 and K_3 as in 9.3.3, quadratic and cubic coefficients C_2 and C_3 are estimated.

The relationships between the estimated C_2 and C_3 coefficients and the model coefficients in Equation (70) for each pair of positions in Figures 3 and 4 are given in Table 3. Algebraic combinations of the results in Table 3 yield solutions for the K_{ip}, K_{op}, and K_{io} model coefficients.

Table 3—Coefficient relationships

Positions in Figures 3 and 4	C_2	C_3
1–2	K_{oq}, K_2	K_3
3–4	K_{pp}	K_{ppp}
5–6	K_{oo}	K_{ooo}
7–8	$0.5\ (K_2 + K_{pp} + K_{ip})$	$0.354\ (K_3 + K_{ppp})$
9–10	$0.5\ (K_{oo} + K_{pp} + K_{op})$	$0.354\ (K_{ooo} + K_{ppp})$
11–12	$0.5\ (K_2 + K_{oo} + K_{io})$	$0.354\ (K_3 + K_{ooo})$

Annex A

(informative)

Characteristics of known precision centrifuges

Table A.1 lists the characteristics of known precision centrifuges in the United States. Table A.2 lists the characteristics of the precision centrifuges at the Laboratoire de Recherches Balistiques et Aérodynamiques (LRBA) in Vernon, France, and at the D. I. Mendeleev Institute for Metrology in St. Petersburg, Russia.

Table A.1—Characteristics of known precision centrifuges in the United States

Centrifuge	**CIGTF**[a]	**CIGTF**[a]	**CIGTF**[a]	**Kearfott G & N**	**BEI**	**Martin Marietta**	**Micom**	**Draper Lab**	**Honeywell**	**Sandia**[a]	**Sandia Honey-well**	**Picatinny Arsenal**	**Hill AFB (from Kelly AFB)**
Location	**Holloman AFB, NM**	**Holloman AFB, NM**	**Holloman AFB, NM**	**Wayne NJ**	**Maumelle AK**	**Orlando FL**	**Hunts-ville AL**	**Hanscom AFB, MA**	**Redmond WA**	**Albu-quer-que, NM**	**Kansas City MO**	**NJ**	**Ogden UT**
Manufacturer Model	Genisco G460	Genisco	Contra-ves 444C[b]	SES, Inc.	Contraves 824HS-2[b]	Genisco 1024-1	Gyrex	Draper/ Carco[c]	Contraves 824HS-2[b]	Contra-ves 824S[b]	Contra-ves 444B[b]	AMT, Inc. 9.5-RP-1	AMT, Inc. 11.0-SP-1-SSAB
Acceleration													
Min (g)	0.5	0.25	0.5	0.1	0.001	1	0.002	0.2	0.002	0.1	0.01	0.4	0.3
Max (g)	30	100	50	200	100	300	100	35	100	200	150	200	150
Accuracy (ppm)	20	2	5	3	20	20	20	5–10	20	20	<1	20	10
Stability (ppm)	10	1	5	1–2	10	20	10		10	10	10	10	10
Rate													
Min (rpm)	13	6	12	4	1	32	1.5	4	1.5	11	4	20	15
Max (rpm)	103	116	121	535	343	550	343	55	343	500	500	600	383
Accuracy (ppm)	5–10	1	5	1	10	10	10	TBD	10	<1	<1	1	1
Stability (ppm)	5	0.5	5	0.5	10	5	10		10	<1	0.1	10	10
Phased-locked loop	yes	yes	yes	yes	yes	yes	yes	yes	yes	yes	yes	yes	yes
Encoder pulses/rev	640	720	720	23 040	720	600	720	720	720	3600	720/ 6000	6000	6000
Type[d]	TW	I	I	OP	I	TW	I	I	I	OE	I/OE	TW	TW
Arm radius (R)													
Nominal (m)	2.54	6.62	3.05	0.62	0.76	0.89	0.76	9.81	0.76	0.76	0.71	0.91	1.22
Elongation (ppm/*g*)	8	7		<0.02	0.2		0.27	0.5	0.27	0.9	<1	0.3	0.4
Static error (ppm)		<1		0.5	n/a		n/a	TBD	n/a		TBD		

Dynamic error (ppm)		<1		0.5	TBD		TBD	0.5	TBD		TBD		
Nominal tilt (s)	10	<1		0.5	11		11	TBD	11	L			
Measured means[e]	P	L		P, L			Q	P, L		L	L		
Specimen													
Volume (m^3)	0.027	0.75	0.091	0.0068	0.014	0.008	0.0042	0.0018	0.0042	0.013	0.0034	0.227	0.227
Dimensions (cm)	30 × 30 × 30	91 × 91 × 91	45 × 45 × 45	15 × 15 × 30	30 × 30 × 15	20 × 20 × 20	33 × 25 × 51	122 × 122 × 122	33 × 25 × 51	25 × 25 × 20	19 × 10 × 7.5	61 × 61 × 61	61 × 61 × 61
Mass (kg)	22.7	136.4	45.5	4.5	9.1	4.5	3.5	545	3.5	11.4	9.1	90.9	68.2
Balance[f]	D/A	D/A		D/A	M	M	M	M	M		D/A	M	D/A
Structural features													
Bearing type[f]	H/S	H/S	air	air	ball	H/S	ball	ball	ball	roller	air	ball	ball
CR platform	no	yes	yes	no	no	no	no	yes, 3 axis	no	no	no	no	no

[a] In storage.
[b] Contraves has been purchased by Carco.
[c] Draper centrifuge refurbished in 2000 by Carco (original Contraves hydraulic motor changed to electric motor).
[d] TW = toothed wheel; I = inductosyn; OE = optical encoder; OP = optical pickoff.
[e] P = proximity detectors; L = laser interferometer; Q = quartz rod.
[f] D/A = dynamic automatic; M = manual before run; H/S = hydrostatic.

Table A.2—Characteristics of known precision centrifuges outside the United States

Centrifuge	**LRBA—Laboratoire de Recherches Balistiques et Aérodynamiques**		**D. I. Mendeleev Institute for Metrology Metrological Systems, Inc.**				
Location	**Vernon, France**		**St. Petersburg, Russia**				
Manufacturer	Genisco	LRBA	Metrological Systems, Inc.				
Model	G460	80 g	CHP	DC-3 (double centrifuge)		TC-3 (tilted centrifuge)	
Modes	Constant Acceleration	Constant Acceleration	Constant Acceleration	Constant Acceleration	Variable Acceleration[a]	Variable Accel-eration[b]	Continuous Rotating Angle
Acceleration							
Min (g)	0.5	0.02	0.5	0.8	0.8	0.00001	1 μrad
Max (g)	28	80	75	50	25	1	2π rad
Accuracy (ppm)	100	5	2–5[c]	2–5[c]	3–10[c]	7–70 μg[c]	0.5 μrad[c]
Stability (ppm)	<100	1					
Rate							
Min (rpm)		6	23	13	30	3	48
Max (rpm)	105	224	280	294	1800	1800	600
Accuracy (ppm)	1	<1	<1[c]	<1[c]	<1[c]	<1[c]	<1[c]
Stability (ppm)	1	0.1					
Phased-locked loop	yes	yes	yes	yes	yes	yes	yes
Encoder pulses/rev	600	720	720	720	550	720	720
Type[d]	TW	OP	TW, OE, RLG	TW, OE, RLG	TW, OE, RLG	TW, OE, RLG	TW, OE, RLG
Arm radius (R)							
Nominal (m)	2.54	1.43	1	0.5	0.5	[e]	[f]
Elongation (ppm/g)		1	0.5	0.5	0.5		
Static error (ppm)		<1	0.2[c]	0.2[c]			
Dynamic error (ppm)							

Nominal tilt (s)		<1					
Measured means[g]			Q, L, P	Q, L, P	P	Q, L, P	Q, L, P
Specimen							
Volume (m^3)	0.16	0.07	0.018	0.002	0.002	0.002	0.002
Dimensions (cm)	80 × 40 × 50	35 × 38 × 50	30 × 30 × 20	15 × 15 × 10	15 × 15 × 10	15 × 15 × 10	15 × 15 × 10
Mass (kg)	80	25	20	10	2.7	2.7	2.7
Balance[h]	M/auto	M	M	M	M	M	M
Structural features							
Bearing type[h]	H/S	H/S	Air	Air	Air	Air	Air
CR platform	yes	no	yes	yes	yes	no	no

[a] 0.5–30 Hz variable acceleration.
[b] 0.05–30 Hz variable acceleration.
[c] Combined standard uncertainty (see ISO *Guide to the Expression of Uncertainty of Measurement*, 1993[B8]).
[d] TW = toothed wheel; I = inductosyn; OE = optical encoder; OP = optical pickoff; RLG = ring laser gyro.
[e] Center of mass of sensitive accelerometer element is located at the axis of rotation.
[f] Axis of rotation of angle transducer under test is directed along axis of rotation.
[g] P = proximity detectors; L = laser interferometer; Q = quartz rod.
[h] D/A = dynamic automatic; M = manual before run; H/S = hydrostatic.

Annex B

(informative)

Centrifuge evaluation

B.1 Introduction

This annex is a discussion of the methods one can use to evaluate the accuracy of a centrifuge. All the error sources listed here are discussed in detail in the main body of the document, so this annex is limited to a brief summary of considerations that affect centrifuge accuracy. Each error is clearly defined along with its effect on the test item and, where possible, the mechanism that gives rise to the error is explained. By examining the various clauses, one can decide which errors are likely to be present in a particular centrifuge, and if an effort to quantify them is justified.

B.2 Radius uncertainty

Subclause 6.1 provides a summary of the several errors that can contribute to test-item radius uncertainty, and 6.1.8 provides recommended instrumentation and methods of measuring the magnitude of each of the errors. These errors are present in all centrifuges and are significant in all but the most crude tests. Every effort should be made to quantify the effects and account for them.

B.3 Alignment uncertainty

Accelerometer input axis alignment to the centrifuge acceleration vector is discussed in 6.2, and 6.2.5 provides recommended instrumentation and methods of measuring the magnitude of the errors. The "common mode" method (see 6.6.3) of utilizing multiple test units to quantify and account for these errors should be given strong consideration, as it requires no special instrumentation and is easy to implement. It is especially appropriate here, as alternate methods of measuring small alignment errors have proved to be complex and not very successful.

The results of the centrifuge test are generally less sensitive to these alignment errors than they are to radius uncertainty errors. This is true as long as the test item is placed with its input axis parallel to the centrifuge acceleration vector. In tests where the input axis is placed perpendicular to the centrifuge arm, these errors are as significant as any other, and they require the same amount of attention.

B.4 Angular velocity uncertainty

Subclause 6.3 provides a discussion of the several angular-velocity-related errors introduced into centrifuge testing. Their causes and effects are explored, and in 6.3.4 the methods of measuring the magnitudes of the errors are outlined. Short-term angular velocity variations are usually not a problem as long as they do not cause errors in the measurement of average angular velocity. Average angular velocity uncertainties are significant in almost every centrifuge test since each 1 ppm variation in centrifuge rate gives a 2 ppm error in the centripetal acceleration. Fortunately, average rate stability is easy to measure as it depends on relatively mature technologies (time standards and position event markers).

B.5 Centrifuge operating environment

The overall centrifuge operating environment must be taken into account when performing a centrifuge evaluation. The centrifuge thermal environment can have a tremendous effect on test items, as well as on the centrifuge itself. These effects are discussed in 6.4 with the appropriate instrumentation methods outlined in 6.4.3. There are additional considerations that may affect the ability to conduct a quality test—availability and quality of slip rings. This and other considerations that may affect the ability to make a quality measurement of sensor output are discussed in 6.6. The significance of these errors can be tremendous, and therefore it demands careful attention.

Annex C

(informative)

Fitting theory

C.1 Introduction

This annex is a simplified discussion of the theory of curve fitting as it is most frequently applied to accelerometer data obtained by use of a centrifuge. It does not attempt to be rigorous or comprehensive. References for more serious study Cramer [B1], Crow [B3], Hoel [B4], Huff [B5], Kendall [B9], Meyer [B10], and Neugebauer [B11] are included in the bibliography in Annex H.

The curve fits considered are in many ways peculiar to the requirements and characteristics of centrifuge testing. They include a widely used deterministic fit, as well as the more conventional statistical ones. Statistical fits discussed are based on the least-squares criterion, which is straightforward to apply in diverse cases and which yields the most probable values for model equation coefficients when applied to data that is corrupted by normally distributed random measurement noise.

The implicit assumption that noise is normally distributed is widely accepted in statistical analyses because of the remarkable Central Limit or Normal Convergence Theorem. In simple terms, it states that the means of any measurement set will approach normal distribution if the individual noise contributors are random and the data set is sufficiently large. For lack of better information, it is almost universally applied to centrifuge data as well, even though there are often problems in doing so.

Centrifuge data points tend to be time-consuming to take, so centrifuge data sets tend to be sparse compared with most other statistical sets, and they tend to have nonrandom components such as thermal drifts as well. This character accounts for the survival of simple deterministic methods in many low-to-medium precision applications. It also reinforces the idea that centrifuge model equations must be chosen with special care to avoid combinations of terms that are so similar as to be difficult to separate, and that the results—even though they may be the best available—may require some judgment to interpret and apply.

The analysis of centrifuge data is an inherently nonlinear problem that introduces a degree of coupling between estimates of nonlinearity and estimates of accelerometer radius. There are many special techniques for resolving this problem, some of which are more accurate than others. The iterative technique described in 9.3.3 is the best currently known, and is recommended even for reduced order fits as simple as straight lines.

C.2 Two-point baseline

The simplest fit is a deterministic one that takes into account sensor scale factor or scale factors (if there is asymmetry) from a 1-g tumble test. The data required for the fit are the average accelerometer output when the centrifuge is not rotating, e_0, and the values of output and centrifuge rotational angular velocity at several approximate acceleration levels of interest, including at least one measurement at a value near a predefined reference acceleration that is typically in the range 1–3 g. The accelerometer output at this reference level is assumed to be that due to the linear output of the accelerometer, as shown in Equation (C.1):

$$a_{\mathrm{c}}(\mathrm{ref}) \triangleq \frac{e_{(\mathrm{ref})} - e_0}{K_1} \tag{C.1}$$

Subsequent acceleration inputs are then scaled from this value, as shown in Equation (C.2):

$$a_{\mathrm{c}} = a_{\mathrm{c(ref)}} \left(\frac{\omega}{\omega_{(\mathrm{ref})}} \right)^2 \tag{C.2}$$

Accelerometer errors then become, simply,

$$\varepsilon_{\mathrm{i}} = \frac{e_{\mathrm{i}} - e_0}{K_1} - a_{\mathrm{c(i)}} \tag{C.3}$$

These errors may then be fitted to accelerometer models or simply compared with an error envelope specification.

The advantages of this fit are its simplicity, especially when used with an envelope specification, and its ability to give real-time nonlinearity information during a run as a check on data validity.

The disadvantages are sensitivity to noise, especially at the single reference measurement, and sometimes a small systematic error due to ignoring the effect of nonlinearity at the reference level. Because of its static nature and averaged measurements, e_0 is usually the most reliable point taken, but e_{ref} errors produce an apparent scale factor error that has a multiplied effect on absolute error at high g. Nonlinearity at e_{ref} has a similar effect, but is limited by the magnitude of the nonlinear coefficients, and can usually be neglected for accelerations greater than about 10 times $a_{\mathrm{c(ref)}}$.

C.3 Statistical regression

Regression is the mathematical method of fitting an optimum model to a collection of experimental points. "Optimum" usually means that the model is fitted by the method of least squares; i.e., so that the sum of the squares of the fitting errors is minimized. The most common fit is simply the fitting of a straight line. The model fitted is of the form $y = ax + b$, where x is the input and y is the response, and a and b are constants, adjusted so that the quantity

$$\sum_{\mathrm{i}=1}^{n} (y_{\mathrm{i}} - ax_{\mathrm{i}} - b)^2 \tag{C.4}$$

is minimized. This minimization is accomplished by finding the minimum value of the summation with respect to both a and b:

$$\frac{\partial}{\partial a} \sum_{i=1}^{n} (y_{\mathrm{i}} - ax_{\mathrm{i}} - b)^2 = 0 \tag{C.5}$$

$$\frac{\partial}{\partial b} \sum_{i=1}^{n} (y_{\mathrm{i}} - ax_{\mathrm{i}} - b)^2 = 0 \tag{C.6}$$

To achieve this minimum value, a and b must simultaneously satisfy the equations:

$$\sum (y_{\mathrm{i}} - ax_{\mathrm{i}} - b)(-x_{\mathrm{i}}) = 0 \qquad \text{and} \qquad \sum (y_{\mathrm{i}} - ax_{\mathrm{i}} - b)(-1) = 0 \tag{C.7}$$

In matrix notation,

$$\begin{bmatrix} \sum x_i & \sum x_i^2 \\ n & \sum x_i \end{bmatrix} \begin{bmatrix} a \\ b \end{bmatrix} = \begin{bmatrix} \sum x_i y_i \\ \sum y_i \end{bmatrix} \tag{C.8}$$

leading to

$$a = \frac{\sum x_i \sum y_i - n \sum x_i y_i}{\left(\sum x_i\right)^2 - n \sum {x_i}^2} \tag{C.9}$$

$$b = \frac{\sum x_i \sum x_i y_i - \sum {x_i}^2 \sum y_i}{\left(\sum x_i\right)^2 - n \sum {x_i}^2} \tag{C.10}$$

Cases that involve a nonlinear function of the input may be treated in exactly analogous fashion, leading to similar but generally larger matrices, such as the one in 9.3.

The fit just described is unweighted, inasmuch as it contains no weighting factors to alter the importance of some measurements compared with others. The unweighted case occurs whenever all points are given the same weight. This condition is appropriate to the common case where the inputs (x_i) are treated as noise-free while the responses (y_i) contain noise, but all have the same variance. It is also appropriate when both x_i and y_i contain noise, but all x_i have the same variance and all y_i have the same variance.

Often, unequal weighting is used even when the above variance criteria are met, because the application places more importance on some parts of the g range than others. For example, when high-g excursions are relatively brief and infrequent, the specification may limit percent error rather than absolute error.

Weighted fits are computed in a manner closely analogous to unweighted fits, but with some important differences. Using the case of linear regression once again as an example, the quantity to be minimized takes the form

$$\sum \frac{(y_i a x_i - b)^2}{w_i} \qquad \text{(summation for } i = 1 \text{ to } n\text{)} \tag{C.11}$$

where w_i is now a weighting factor that can be used to emphasize certain data points and de-emphasize others. The corresponding solutions for a and b are similar in form and reduce to the equations already derived when all of the w_i are equal:

$$a = \frac{\sum \frac{1}{w_i} \sum \frac{x_i y_i}{w_i} - \sum \frac{x_i}{w_i} \sum \frac{y_i}{w_i}}{\sum \frac{1}{w_i} \sum \frac{{x_i}^2}{w_i} - \left[\sum \frac{x_i}{w_i}\right]^2} \tag{C.12}$$

$$b = \frac{\sum \frac{{x_i}^2}{w_i} \sum \frac{y_i}{w_i} - \sum \frac{x_i}{w_i} \sum \frac{x_i y_i}{w_i}}{\sum \frac{1}{w_i} \sum \frac{{x_i}^2}{w_i} - \left[\sum \frac{x_i}{w_i}\right]^2} \tag{C.13}$$

An important special case arises when one of the w_i terms is zero. This case occurs—e.g., during per unit weighting—where $w_i = x_i$ and the normal convention is that $w_1 = x_1 = 0$. The effect is that the first point becomes infinitely weighted. Actual division by zero creates computational difficulties, but the effect on the fit can be seen by formally taking the limit as w_1 goes to zero:

(all summations for $i = 2$ to n)

$$\lim_{w_1 \to 0} a = \frac{\sum \frac{x_i y_i}{w_i} + x_1 y_1 \sum \frac{1}{w_i} - x_1 \sum \frac{y_i}{w_i} - y_1 \sum \frac{x_i}{w_i}}{x_1^2 \sum \frac{1}{w_i} - 2x_1 \sum \frac{x_i}{w_i} + \sum \frac{x_i^2}{w_i}} \tag{C.14}$$

$$\lim_{w_1 \to 0} b = \frac{x_1^2 \sum \frac{y_i}{w_i} + y_1 \sum \frac{x_i^2}{w_i} - x_1 \sum \frac{x_i y_i}{w_i} - x_1 y_1 \sum \frac{x_i}{w_i}}{x_1^2 \sum \frac{1}{w_i} - 2x_1 \sum \frac{x_i}{w_i} + \sum \frac{x_i^2}{w_i}} \tag{C.15}$$

It is easily shown that these equations satisfy the requirement $ax_1 + b = y_1$, defining a line that passes identically through the point (x_1, y_1). In particular, if $x_1 = 0$, then $b = y_1$.

In the actual application of such a fit, the problem of dividing by zero is easily avoided by simply defining the infinitely weighted point a priori, and then fitting the remainder of the points with that coefficient no longer included as a variable. As a simple example, consider a case where the inputs are zero, $x_1, x_2, \ldots, x_n$, and the corresponding outputs are $y_0, y_1, \ldots, y_n$. A model of the form $y = ax^2 + bx + y_0$ may be per-unit weighted and fitted by making the transformation

$$\frac{y - y_0}{x} = ax + b \tag{C.16}$$

With the input data transformed as indicated, the fit can be made by standard linear regression software. In the case of a per-unit weighted straight line, the equation would be $y = ax + y_0$, which transforms to $(y - y_0)/x = a$.

The statistical fit for the slope, a, then becomes a simple algebraic average of the transformed inputs for the data samples

$$\frac{y_1 - y_0}{x_1}, \frac{y_2 - y_0}{x_2}, \ldots, \frac{y_n - y_0}{x_n} \tag{C.17}$$

When two-sided fits are needed, these weighting procedures can be used in a similarly straightforward manner with the iterative procedure of 9.3.3, with the matrix reduced to as little as 2×2.

In this procedure, bias removal is equivalent to infinite weighting of the point when the centrifuge is not rotating, provided that a bias coefficient is not included as one of the variables in the fit. Such removal is thus still appropriate if such weighting is used. Per-unit weighting is a relatively common case that requires it. The point when the centrifuge is not rotating represents the ideal reference data point for the remaining higher-g points, since it quantitatively represents the bias error in all the data due to both the accelerometer bias and its mounting misalignment. Note that the bias removed from the data is not the true accelerometer bias as measured by a precision tumble test and designated K_0 in the model equation of 7.1.

When the specification gives no special guidance, a common technique is to weight the residual of each point by the ratio $w_i = s_i/s_0$, where s_0 may be any arbitrary reference standard deviation, usually either the maximum or the minimum, and s_i is the standard deviation of the measurements taken at the given acceleration level.

Least-squares fits are often characterized by a correlation coefficient r, whose value is such that r^2 defines the fraction of variation in y that can be ascribed to a linear dependence on x. Correlation coefficients are of limited value in characterizing accelerometer linearity data for the following two reasons:

a) Linear fits often fail to characterize the accelerometer output to sufficient accuracy.
b) Inertial-grade accelerometers typically have such good linearity, even before modeling, that the difference between r^2 and 1 may get lost in the round-off errors of computation.

For example, in the limit of small modeling errors, it can be shown that

$$r^2 = 1 - 3\frac{\sigma^2}{F^2} \tag{C.18}$$

where

F is full scale,
σ^2 is mean square linearity error $= \frac{1}{n}\sum_{i=1}^{n}[y_{\mathrm{i}} - y(x_{\mathrm{i}})]^2$.

Consider a typical case where $F = 40\,g$ and $s = 100\,\mu g$ rms, so that

$$r^2 = 1 - 3\left(\frac{10^{-4}}{40}\right)^2 = 0.999\,999\,999\,98 \tag{C.19}$$

C.4 Model coefficients

For applications requiring high precision, accelerometer performance usually is specified in terms of the allowable magnitudes of coefficients in a specified model, or in terms of residual nonlinearity after linearization according to a specified model. A typical model is described in 7.1.

Many of the terms in such models form straightforward polynomials; i.e., power series in input acceleration. Individual terms in such series may or may not be associated with specific physical effects in the sensor. In the case where they are not, or the testing is not intended to evaluate such effects, the precise form of the series or the accuracy of individual coefficients is not a serious consideration as long as the overall residual errors are sufficiently small.

Other terms in typical accelerometer models are intimately connected with the physics of the sensor or have special effects on the end-use error budget. Many of these are rarely seen in statistical models of other kinds of instruments. Common examples include the cross-coupling terms such as K_{ip} and cross-axis linear terms such as K_{pp} or K_{oo}. When terms that have important individual effects are needed in the model, the accuracy of all individual coefficients is of great importance. Ensuring such accuracy requires, among other things, that the terms themselves be chosen with great care, and that only those terms that are physically defensible be included.

The need for such care arises from two characteristics of the series most commonly used. The first is that they lack the property of orthogonality. The second is that pairs of terms that represent functions having similar shapes or even similar symmetry may be subject to a phenomenon called "bucking" in the presence of sparse data containing random noise and especially non-Gaussian noise.

Orthogonal series, e.g., Fourier series, have the property that their terms are noninteracting. If a Fourier sine series having terms up to three times the frequency is fitted to periodic data, four coefficients (A_0, A_1, A_2, A_3) will be obtained plus, in general, a nonzero set of residuals. If those residuals contain a significant component at four times frequency, and a corresponding A_4 term is added to the fit, the new fit will return a nonzero value for A_4 and the root-mean-square (rms) value of the residuals will decrease, but the coefficients already fitted will not change. Unfortunately, the polynomial series that is appropriate for the modeling of centrifuge data lacks this property. When an additional term is added to these polynomial series, all coefficients may change value. For example, a simple power series of the form

$$A_0 + A_1 x + A_2 x^2 \tag{C.20}$$

which yields a particular set of coefficients when fitted to somewhat noisy data, will, in general, yield different values for A_0 through A_2 if a term $A_3 x^3$ is added to the series. If the cubic term is physically inappropriate, that may mean that the accuracy of the lower-power coefficients has been degraded, even though the quality of the fit, as indicated by the magnitude of the residuals, is improved.

The phenomenon of bucking is closely related to nonorthogonality. Bucking is simply an unusually strong interaction between certain terms in a nonorthogonal series due to a similarity in the functions that they represent. Such similarity allows opposing offsets in the coefficients largely to cancel the individual effects of the two terms. For example, in the above series, an added cubic term generally will have little effect on the A_0 and A_2 coefficients, which are of opposite symmetry, but may interact quite strongly with A_1. Other examples of terms from 7.1 that may buck each other strongly include K_3 and K_{oq} or K_2 and scale factor asymmetry, in two-sided fits, and any nonlinear terms whose magnitudes are comparable to the measurement noise in single-sided fits.

C.5 Envelope specifications

In medium- to low-precision application, and a few high-precision applications, the preferred form of specifications is an error envelope. The envelope may take several forms: specific allowable errors at specific *g* levels, a fixed envelope defined by two parallel lines (allowable error independent of *g* level), or what is often known as a "bow-tie" envelope. A bow-tie envelope is one that allows a fixed error (parallel limit line) at low *g* levels (e.g., between $+5g$ and $-5g$), but allows error to increase proportionally to input acceleration at higher *g* levels. Purely *g* proportional error envelopes are seldom seen, as they impose the impossible requirement of zero error at zero *g*.

Once an error envelope is defined, its interpretation is straightforward, since data points are either inside or outside the line. An important element of its definition, though, may not always appear explicitly. The envelope is intended to show the limits of departures from a straight line relationship between acceleration input and sensor output, but the method of defining the straight line may be subject to interpretation. The most common choices are

a) Two-point baseline
b) Best-fit straight line (BFSL)
c) Per-unit weighted BFSL
d) Miscellaneous unconventional fits, such as Min–Max.

Two-point baseline techniques are straightforward to implement and may be chosen because of their simplicity, but it should be noted that they work best with bow-tie envelopes or envelopes resembling the bow-tie. A major error source in this technique is the inaccuracy of measuring the reference-level data point, and errors in this point tend to produce errors proportional to *g* at higher acceleration levels.

Deviations from a best-fit straight line are based on a well-defined technique, except for two details. The first is the question of whether the zero-*g* output should be one of the coefficients in the fit. Including this coefficient may increase the number of sensors that pass this test, but the generally higher accuracy of the zero-*g* point suggests that this coefficient should be based on a heavily weighted point or even defined to be equal to the zero-*g* point to obtain the most meaningful end result.

The second is the question of whether there should be one BFSL for both polarities, or separate linear fits for each side. Totally separate fits for positive inputs and negative inputs, including separately fitted apparent bias and apparent scale factor terms, are quite widely used, even though envelope specifications normally assume a single straight line that applies to both polarities. The use of different coefficients for positive and negative inputs results in smaller residuals, and may allow marginal accelerometers to pass rather than fail the test criterion. This result depends on reference lines that differ from each other and from the single scale factor and bias reported on the data sheet, and is thus based on an optimistic indication of the true nonlinearity of the accelerometer.

Use of the iterative technique of 9.3.3 is a straightforward way to merge the positive and negative data with an appropriate common linear term. For this application, the 7×7 matrix shown as an example in that clause must be reduced to a 4×4 matrix by deleting the first three rows and the first three columns.

The considerations for a per-unit weighted best-fit straight line are similar, except that the question of weighting or suppression of the zero point is answered automatically. Per-unit weighted fits generally provide an optimum match to bow-tie type envelopes, since the weighting of errors at different g levels is directly compatible with the allowable error. At the same time, this fit may be defended as appropriate, provided that the application is indeed able to tolerate larger errors at higher g levels.

Min–Max fits are based on algorithms that iteratively adjust the reference linear model until the maximum error has been minimized—i.e., until the largest single residual is made as small as possible. Since the residuals may be weighted to suit the shape of any arbitrary error envelope before such fitting, this process can obviously be used to maximize the probability that any given test on any given accelerometer will be successfully passed. Apart from that, it has little to recommend it. Least-squares fits, weighted or unweighted, produce a far more significant indication of the behavior of an accelerometer in its end use.

Annex D

(informative)

Limitations of and alternatives to centrifuge testing

D.1 Limitations

Centrifuge testing, although extremely convenient for the test of many characteristics of accelerometers, has a number of limitations that may indicate the need to utilize some other kind of acceleration input. The following is a list of the major limitations, each of which must be evaluated in the context of the type of instrument being tested:

a) The centrifuge acceleration has a radial gradient (see 6.1.1).
b) Spin sensitivity of the unit under test may corrupt the acceleration measurement.
c) The ability of the centrifuge testing to provide absolute input acceleration is limited by the knowledge of the exact radius.
d) Short-duration dynamic inputs that require high onset rates are difficult to produce with high accuracy.
e) The ability to test accelerometers under combined environments such as acceleration/ temperature or acceleration/vibration is very limited.
f) The tests tend to be relatively costly and may require expensive equipment to achieve desired accuracy.
g) The number of facilities with precision centrifuge installations is limited.
h) Centrifuge tests require considerable setup time.

The gradient problem of a) in the preceding list is particularly important for accelerometers that contain two proof masses, such as some vibrating beam accelerometers. In tests of these, the centrifuge applies different input accelerations to the two masses, where linear motion acceleration would apply identical accelerations to the two masses.

The problem of d) is important in testing high-g accelerometers where the self-heating of the torque motor due to long durations at the high-g levels can cause marked shifts in the performance characteristics measured.

The problem of e) is of interest to those wishing to quantify the effects of an environment superimposed on various static g levels of input, the most common being vibration superimposed on high levels of acceleration, as would be experienced during a rocket launch.

D.2 Alternatives to centrifuge testing

D.2.1 Multipoint tumble testing under earth's gravity

The most common alternative to centrifuge testing is that of multipoint tumble testing, utilizing a precision dividing head. This type of equipment is more commonly available than precision centrifuge equipment.

The accuracy of the test system is limited by the dividing head and the small magnitude of nonlinear errors at 1 g or less. Since a 1 arc-second tilt angle at angles near horizontal represents an input error of nominally 4.85 μg, and dividing heads are easily available with accuracies in the range of

1–5 arc-seconds, the resultant test errors can be evaluated. Further benefits from multipoint testing are evaluation of parameters of the accelerometer from the same test: scale factor, scale factor asymmetry, bias, nonlinearity, hysteresis, and misalignment, along with change of parameters with temperature.

Of these parameters, only nonlinearity and hysteresis are easily measured on the centrifuge.

D.2.2 Sled testing

One of the most dynamic alternatives to centrifuge testing is use of a rocket sled. Using test tracks up to 20 km long, rocket-powered sleds provide input acceleration and deceleration profiles. These sled tests can provide input accelerations with high levels (up to 100 *g*) and short durations, though typical peak accelerations are in the range 5–20 *g* for 2–10 s, depending on the velocity capability of the vehicle and engine used.

After the period of acceleration and the reaching of peak velocity, typically achieved at engine burn-out, the sled begins slowing due to air drag, and is then decelerated to a stop using "water brakes," which function by scooping volumes of water from a trough during the stop. This technology has been developed to more closely simulate the combined environments of acceleration, vibration, and linear displacement usually encountered in actual field use. Although usually needed only to test complete inertial systems, sled testing can be used as an alternative to centrifuge testing for accelerometers.

The following is a list of limitations and problems associated with the use of sled testing:

a) Accelerations must be inferred from measurements of the timing of the sled motion down the track, from the measurement of the time required for the sled to move sequentially from the starting point to surveyed reference points at spaced intervals down the track.
b) The acceleration profiles are limited by available sleds, engines, and tracks, and are far more difficult to control than with a centrifuge. Variations of deceleration profiles are possible by presetting the depths of water in the water brake troughs, though with little precision.
c) The sleds provide limited values of high-*g* inputs and short time intervals at high *g*.
d) Lead time and setup time are both long for sled testing.
e) Availability of equipment is poor, and cost of single-sled runs is high.

Accuracy of sled testing for accelerometer performance is limited, since the precision measurements are distance- and time-based. From these data, the second integral of the measured acceleration can be determined, but is contaminated by variations in the leveling of the sensor during the sled run. Use of sled testing is normally restricted to testing of complete inertial measurement systems.

D.2.3 Vibration testing

For calibrating accelerometer nonlinear model coefficients on an electrodynamic or hydraulic vibrator, see IEEE Std 1293-1998, Annex L.

D.2.4 AC current injection testing

In many torque-balance accelerometers, the dominant contribution to nonlinearity is the square law effect of torquer current. Such accelerometers permit evaluation of this coefficient by means of a current injection test that uses simpler test equipment and test techniques than testing with a centrifuge. The validity of using this procedure as an alternative to centrifuge testing should be established by comparison with centrifuge data.

Nonlinearity in the accelerometer torquer scale factor generates errors at the accelerometer output that are proportional to higher powers of the torquer current. The predominant term in the power series expression for the torque is that associated with the square of the current. This coefficient is primarily a result of asymmetry of the torquer coil within its case-fixed soft iron magnetic circuit. This soft iron is required as a return path for the magnetic flux from the permanent magnet.

In general, the coil can be attracted to the soft iron independent of the direction of the current in the coil. Consequently, a constant force on the coil may occur for an ac current input to the coil. If the coil is centered in the magnetic circuit, then the net force is zero, but for a small asymmetry in the coil position relative to the magnetic circuit, there will be a constant net force on the coil. This rectification effect suggests an accurate and convenient technique for evaluating the K_2 coefficient. Thus, K_2 can be determined by observing the bias shift in the accelerometer as a function of rms values of ac current applied to the torquer coil. In many cases, measurements using this test are consistent with centrifuge data determinations of K_2 and are quite repeatable over time.

The nonlinearity coefficient K_2 produced by torquer nonlinearity is determined as follows. Steady-state dc torque current is recorded. Then, an ac sine wave current is added to the torquer coil and the steady-state dc current is again recorded. The torquer nonlinearity is calculated by

$$K_2 = \frac{I_2 - I_1}{K}\left(\frac{I_3}{K}\right)^2 \times 10^6\ \mu g/g^2 \tag{D.1}$$

where

- K_2 is the second-order coefficient ($\mu g/g^2$),
- I_1 is the accelerometer dc output current with no ac excitation (mA),
- I_2 is the accelerometer dc output current with ac applied (mA),
- I_3 is the ac excitation applied to torquer (mA rms),
- K is the torquer current scale factor (mA/g).

The choice of frequency and amplitude of the injected ac current (I_3) is dependent on test requirements, instrumentation characteristics, and input axis orientation. To avoid nonrepresentative pendulum motions, the frequency should be high enough, typically 5–10 times the servo bandwidth, while avoiding mechanical resonances. The amplitude should be large enough to provide an easily measured bias shift. At high amplitudes, self-heating must be considered, and orientation is then a trade-off between test fixture stability and the accelerometer temperature sensitivity.

D.3 Double turntable centrifuge

A turntable rotating at angular velocity ω_2 can be at the end of a centrifuge arm rotating at angular velocity ω_1, with the accelerometer effective center of mass (ECM) being on the turntable rotation axis (see Figure D.1). The centrifuge and turntable rotation axes are vertical and the accelerometer IA is horizontal. The centrifuge angular velocity ω_1 serves to apply centripetal acceleration to the accelerometer under test, and the turntable angular velocity ω_2 rotates the accelerometer IA into and away from the centripetal acceleration vector.

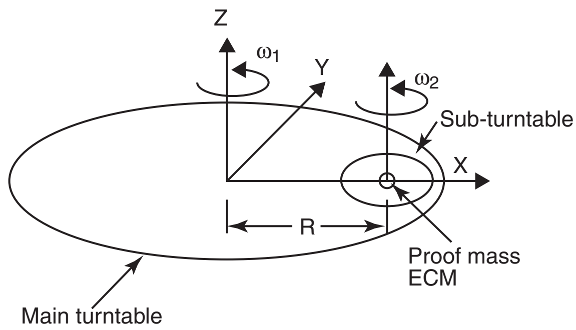

Figure D.1—Accelerometer mounted on double turntable centrifuge

Centripetal acceleration reproduced by a double turntable centrifuge is

$$a = \omega_1^2 R \cos \omega_2 t \tag{D.2}$$

An advantage of the double turntable centrifuge as compared with a vibrator is the independence of acceleration amplitude from frequency ω_2, so that it is possible to reproduce large accelerations within the range of low frequencies, e.g., for transfer function determination. See Smith et al 1962 [B15].

D.4 Centrifuge with tilted axis of rotation

A turntable rotating with an angular velocity ω is tilted at angle ϕ to the vertical axis Z. The accelerometer IA is directed along axis X, which is situated in the plane of the turntable (see Figure D.2). The acceleration reproduced by the centrifuge with a tilted axis of rotation when the mass center of the accelerometer sensitive element is over the centrifuge rotation axis is

$$a = g \sin \phi \sin \omega t \tag{D.3}$$

where g is the acceleration due to gravity.

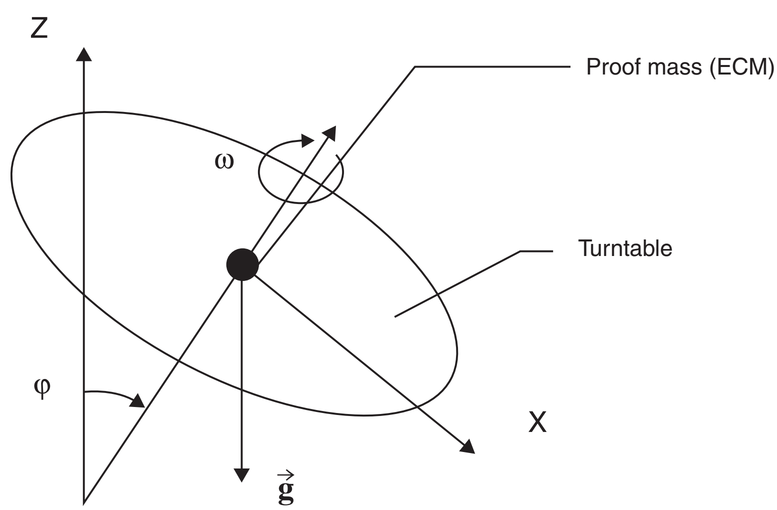

Figure D.2—Accelerometer mounted on a centrifuge with tilted axis of rotation

The centrifuge with a tilted axis of rotation reproduces variable acceleration with an amplitude that is independent of frequency, like the double turntable centrifuge. Both centrifuges used together may reproduce variable acceleration values in the amplitude range from 10^{-4}–10^{-5} g to a few tens of g. The accuracy of the centrifuge with a tilted axis of rotation in the amplitude range up to 1 g is better than that of the double turntable centrifuge.

Annex E

(informative)

Precision centrifuge tests on dual-proof-mass VBAs

E1. General equations

The vibrating beam accelerometer (VBA) uses two resonators in differential mode, so that under acceleration one resonator increases in frequency and the other resonator decreases in frequency. The measure of acceleration is the difference frequency, thereby common-mode rejecting a number of errors. It is thus desirable to use the difference frequency output of the VBA rather than the individual resonator frequencies in analyzing centrifuge data, and sometimes that is the only output that is available. See IEEE Std 1293–1998 for a detailed description of the VBA.

The two resonators are attached to one or two proof masses. In centrifuge testing, consideration must be given to the fact that the dual proof masses may be at different radii.

As shown in Figure E.1, a dual-proof-mass VBA can be divided into three frames R1, R, and R2, each corresponding to one effective center of mass, G1, G, G2, respectively:

R1	(G1, I1, O1, P1)	Frame R1 of the first half accelerometer at G1
R	(G, I, O, P)	Frame R of the accelerometer at G
R2	(G2, I2, O2, P2)	Frame R2 of the second half accelerometer at G2

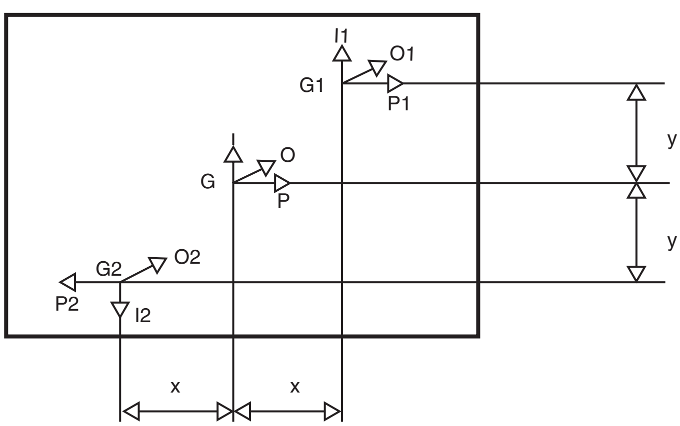

Figure E.1—Drawing of a dual-proof-mass VBA

The fundamental laws of dynamics in a solid body give the following relations between accelerations $\Gamma(G_i)$ at the different effective centers of mass G_i in terms of the angular velocity $\vec{\Omega}$:

$$\begin{aligned} \vec{\Gamma}(G_1) &= \vec{\Gamma}(G) + \frac{d\vec{\Omega}}{dt} \times GG_1 + \vec{\Omega} \times (\vec{\Omega} \times GG_1) = \vec{\Gamma}(\mathrm{G}) + \vec{\Omega} \times (\vec{\Omega} \times GG_1) \\ \vec{\Gamma}(G_2) &= \vec{\Gamma}(G) + \frac{d\vec{\Omega}}{dt} \times GG_2 + \vec{\Omega} \times (\vec{\Omega} \times GG_2) = \vec{\Gamma}(G) + \vec{\Omega} \times (\vec{\Omega} \times GG_2) \end{aligned} \tag{E.1}$$

Assuming that $||GG_1|| = ||GG_2||$, and $d\vec{\Omega}/dt = 0$, one can write

$$\begin{aligned} \vec{\Gamma}(G_1) &= \vec{\Gamma}(G) + \vec{\Gamma} \\ \vec{\Gamma}(G_2) &= \vec{\Gamma}(G) - \vec{\Gamma} \end{aligned} \tag{E.2}$$

with the following expression for Γ:

$$\Gamma = \begin{pmatrix} x\Omega_\mathrm{I}\Omega_\mathrm{p} - y(\Omega_\mathrm{O}^2 + \Omega_\mathrm{P}^2) \\ y\Omega_\mathrm{I}\Omega_\mathrm{O} + x\Omega_\mathrm{O}\Omega_\mathrm{P} \\ -y\Omega_\mathrm{I}\Omega_\mathrm{P} - x(\Omega_\mathrm{I}^2 + \Omega_\mathrm{O}^2) \end{pmatrix} = \begin{pmatrix} \gamma_1 \\ \gamma_2 \\ \gamma_3 \end{pmatrix} \tag{E.3}$$

Let the acceleration Γ(G) have components (a_I, a_O, a_P) in the frame R.

In the frame R, hence in the frame R1,

$$\vec{\Gamma}(G_1)_{R1} = \begin{pmatrix} a_\mathrm{I} + \gamma_1 \\ a_\mathrm{O} + \gamma_2 \\ a_\mathrm{P} + \gamma_3 \end{pmatrix}$$

$$\vec{\Gamma}(G_2)_{R1} = \begin{pmatrix} a_\mathrm{I} - \gamma_1 \\ a_\mathrm{O} - \gamma_2 \\ a_\mathrm{P} - \gamma_3 \end{pmatrix}$$

To transfer the components of a vector from R1 to R2, the sign of the first and third component has to be changed:

$$\vec{\Gamma}(G_2)_{R2} = \begin{pmatrix} -a_\mathrm{I} + \gamma_1 \\ a_\mathrm{O} - \gamma_2 \\ -a_\mathrm{P} + \gamma_3 \end{pmatrix} \tag{E.4}$$

If S_1 and S_2 are the two accelerometer outputs generated by $\vec{\Gamma}(G_1)_\mathrm{R1}$ and $\vec{\Gamma}(G_2)_\mathrm{R2}$, respectively, then

$$\begin{aligned} \frac{S_1(\Gamma(G_1)_\mathrm{R1})}{K_{11}} &= K_{01} + (a_\mathrm{I} + \gamma_1) + K_{21}(a_\mathrm{I} + \gamma_1)^2 + K_{31}(a_\mathrm{I} + \gamma_1)^3 \\ &\quad + K_\mathrm{O1}(a_\mathrm{O} + \gamma_2) + K_\mathrm{P1}(a_\mathrm{P} + \gamma_3) \end{aligned} \tag{E.5}$$

$$\begin{aligned} \frac{S_2(\Gamma(G_2)_\mathrm{R2})}{K_{12}} &= K_{02} + (-a_\mathrm{I} + \gamma_1) + K_{22}(-a_\mathrm{I} + \gamma_1)^2 + K_{32}(-a_\mathrm{I} + \gamma_1)^3 \\ &\quad + K_\mathrm{O2}(a_\mathrm{O} - \gamma_2) + K_\mathrm{P2}(-a_\mathrm{P} + \gamma_3) \end{aligned} \tag{E.6}$$

Developing these two expressions

$$\begin{aligned} \frac{S_1(\Gamma(G_1)_\mathrm{R1})}{K_{11}} &= K_{01} + a_\mathrm{I} + K_{21}a_\mathrm{I}^2 + K_{31}a_\mathrm{I}^3 + K_\mathrm{O1}a_\mathrm{O} + K_\mathrm{P1}a_\mathrm{P} \\ &\quad + \gamma_1 + (2K_{21}a_\mathrm{I}\gamma_1 + K_{21}\gamma_1^2) + (K_{31}\gamma_1^3 + 3K_{31}a_\mathrm{I}^2\gamma_1 + 3K_{31}a_\mathrm{I}\gamma_1^2) \\ &\quad + K_\mathrm{O1}\gamma_2 + K_\mathrm{P1}\gamma_3 \end{aligned} \tag{E.7}$$

$$\begin{aligned} \frac{S_2(\Gamma(G_2)_\mathrm{R2})}{K_{12}} &= K_{02} - a_\mathrm{I} + K_{22}a_\mathrm{I}^2 - K_{32}a_\mathrm{I}^3 + K_\mathrm{O2}a_\mathrm{O} - K_\mathrm{P2}a_\mathrm{P} + \gamma_1 + (-2K_{22}a_\mathrm{I}\gamma_1 + K_{22}\gamma_1^2) \\ &\quad + (K_{31}\gamma_1^3 + 3K_{32}a_\mathrm{I}^2\gamma_1 - 3K_{32}a_\mathrm{I}\gamma_1^2) - K_\mathrm{O2}\gamma_2 + K_\mathrm{P2}\gamma_3 \end{aligned} \tag{E.8}$$

It can be useful to measure the difference of the two outputs:

$$\frac{S(\vec{\Gamma}(G)_{\mathrm{R}})}{K_{11}+K_{12}} = \frac{K_{11}S_1(\vec{\Gamma}(G_1)_{\mathrm{R1}}) - K_{12}S_2(\vec{\Gamma}(G_2)_{\mathrm{R2}})}{K_{11}+K_{12}} \tag{E.9}$$

with

$$\begin{aligned} &K_1 = K_{11}+K_{12}; && K_0 = \frac{K_{11}K_{01}-K_{12}K_{02}}{K_1} \\ &K_2 = \frac{K_{11}K_{21}-K_{12}K_{22}}{K_1}; && K_3 = \frac{K_{11}K_{31}+K_{12}K_{32}}{K_1} \\ &K_{\mathrm{O}} = \frac{K_{11}K_{\mathrm{O1}}-K_{12}K_{\mathrm{O2}}}{K_1}; && K_{\mathrm{P}} = \frac{K_{11}K_{\mathrm{P1}}+K_{12}K_{\mathrm{P2}}}{K_1} \end{aligned} \tag{E.10}$$

and

$$\begin{aligned} &\Delta k_1 = K_{11}-K_{12} && \\ &\sum k_2 = K_{11}K_{21}+K_{12}K_{22}; && \Delta k_2 = K_{11}K_{21}-K_{12}K_{22} \\ &\sum k_3 = K_{11}K_{31}+K_{12}K_{32}; && \Delta k_3 = K_{11}K_{31}-K_{12}K_{32} \\ &\sum k_{\mathrm{O}} = K_{11}K_{\mathrm{O1}}-K_{12}K_{\mathrm{O2}}; && \Delta k_{\mathrm{P}} = K_{11}K_{\mathrm{P1}}-K_{12}K_{\mathrm{P2}} \end{aligned} \tag{E.11}$$

One can write:

$$\begin{aligned} \frac{S\left(\vec{\Gamma}(G)_{\mathrm{R}}\right)}{K_1} &= K_0 + a_{\mathrm{S}} + K_2 a_{\mathrm{S}}^2 + K_3 a_{\mathrm{S}}^3 + K_{\mathrm{O}}\, a_{\mathrm{O}} + K_{\mathrm{P}}\, a_{\mathrm{P}} \\ &\quad + \frac{1}{K_1}\begin{bmatrix} \Delta k_1\, \gamma_1 \\ +2\sum k_2\, a_{\mathrm{S}}\gamma_1 + \Delta k_2\, {\gamma_1}^2 \\ +\Delta k_3({\gamma_1}^3 + 3{a_{\mathrm{S}}}^2\gamma_1) + 3\sum k_3 \mathrm{a}_S {\gamma_1}^2 \\ +\sum k_{\mathrm{O}}\, \gamma_2 + \Delta k_{\mathrm{P}}\gamma_3 \end{bmatrix} \end{aligned} \tag{E.12}$$

E.2 Precision centrifuge model

Centrifuge tests are performed with the following configuration for the frame:

— The output axis is always vertical, pointing upward ($a_{\mathrm{O}} = 1\,g$, so that $K_{\mathrm{O}}a_{\mathrm{O}} = K_{\mathrm{O}}$ in consistent units).

— The input and pendulous axes are horizontal ($a_{\mathrm{P}} = 0$).

Assuming that we are able to compensate for the Coriolis effect, Equation (E.13) shows the only component of the centrifuge rate is on the output axis (I = P = 0):

$$\begin{pmatrix} \gamma_1 \\ \gamma_2 \\ \gamma_3 \end{pmatrix} = \begin{pmatrix} -a\Omega_{\mathrm{C}}^2 \\ 0 \\ -b\Omega_{\mathrm{C}}^2 \end{pmatrix} = \begin{pmatrix} -\dfrac{a}{R}|a_{\mathrm{S}}| \\ 0 \\ -\dfrac{b}{R}|a_{\mathrm{S}}| \end{pmatrix} = \begin{pmatrix} -\delta_1|a_{\mathrm{S}}| \\ 0 \\ -\delta_2|a_{\mathrm{S}}| \end{pmatrix} \tag{E.13}$$

The expression of the differential output becomes

$$\frac{S(\vec{\Gamma}(G)_{\mathrm{R}})}{K_1} = K_0 + a_{\mathrm{I}} + K_2 a_{\mathrm{I}}^2 + K_3 a_{\mathrm{I}}^3 + K_{\mathrm{O}} + \frac{1}{K_1}\begin{bmatrix} -\Delta k_1\,\delta_1 |a_{\mathrm{I}}| \\ -2\sum k_2\delta_1\, a_{\mathrm{I}}|a_{\mathrm{I}}| + \Delta k_2 \delta_1{}^2\,|a_{\mathrm{I}}|^2 \\ -\Delta k_3(\delta_1{}^3|a_{\mathrm{I}}|^3 + 3\delta_1|a_{\mathrm{I}}|^3) + 3\sum k_3\delta_1{}^2 \mathrm{a_I}{}^3 \\ -\Delta k_{\mathrm{P}}\,\delta_2|a_{\mathrm{I}}| \end{bmatrix} \tag{E.14}$$

Therefore, several additional terms appear:

$$\begin{aligned}\frac{S(\vec{\Gamma}(G)_{\mathrm{R}})}{K_1} &= K_0 + K_{\mathrm{O}} \\ &+ a_{\mathrm{I}} + \left(-\frac{\Delta k_1}{K_1}\delta_1 - \frac{\Delta k_{\mathrm{P}}}{K_1}\delta_2\right)|a_{\mathrm{I}}| \\ &+ K_2(1+\delta_1{}^2)a_{\mathrm{I}}{}^2 + \left(-2\frac{\sum k_2}{K_1}\delta_1{}^2\right) a_{\mathrm{I}}|a_{\mathrm{I}}| \\ &+ K_3(1+3\delta_1{}^2)a_{\mathrm{I}}{}^3 + \frac{\Delta k_3}{K_1}(\delta_1{}^3 + 3\delta_1)\left|a_{\mathrm{I}}{}^3\right|\end{aligned} \tag{E.15}$$

The differential accelerometer output is expressed by

$$\frac{S(\vec{\Gamma}(G)_{\mathrm{R}})}{K_1} = K_0 + K_{\mathrm{O}} + a_{\mathrm{I}} + A|a_{\mathrm{I}}| + K_2\left(1+\frac{a^2}{R^2}\right)a_{\mathrm{I}}{}^2 + B\,a_{\mathrm{I}}|a_{\mathrm{I}}| + K_3\left(1+\frac{3a^2}{R^2}\right)a_{\mathrm{I}}{}^3 + C\left|a_{\mathrm{I}}{}^3\right| \tag{E.16}$$

Some new terms have appeared in the centrifuge test model of such accelerometers:

- A depends on the mismatch of the two scale factors
- B Odd-quadratic term
- C Even-cubic term

The values calculated for K_2 and K_3 are not the actual ones. However, the error in K_2 and K_3 does not exceed some 10^{-4} of the coefficient, which is adequate for most calibrations.

Since the VBA resonator input axes in a dual-proof-mass VBA cannot be aligned IA parallel as well as antiparallel, two such VBAs have to be simultaneously tested to separate centrifuge arm stretch and tilt errors from VBA nonlinearities (see 6.6.3).

Annex F

(informative)

Scale factor calibration with a centrifuge

F.1 High-speed centrifuge

For applications with moderate levels of acceleration (up to 20 g or even over 100 g), scale factor and bias are calibrated in a 1-g tumble test. Nonlinear acceleration sensitive model coefficients are calibrated in centrifuge tests as explained in this document, or in a vibration test (see IEEE Std 1293-1998).

For the very high-g applications, scale factor would have to be calibrated in a centrifuge test. As an example, consider an open-loop capacitive pickoff micromechanical accelerometer on a silicon chip that has to measure accelerations over 10,000 g. The silicon chip accelerometer and its readout electronics are mounted in a special fixture that is attached to the centrifuge arm, with IA along the centrifuge arm.

A centrifuge that has been employed for calibrating the accelerometer scale factor has an arm radius of 12 cm, for which a centrifuge rate of 8631 revolutions per minute (rpm) provides 10,000 g of acceleration. An attainable 17,262 rpm provides 40,000 g of acceleration on the test article. Ultra-centrifuges used to separate components from biological specimens attain over 100,000 g of acceleration, although the structural stiffness of such a centrifuge's arm is not required to be as great as that used for measuring an accelerometer's scale factor.

Such high-speed centrifuges are not in the precision centrifuge class discussed in this recommended practice, but are adequate for the accuracy of the accelerometer under consideration. A high-speed centrifuge requires an armored containment vessel for safety.

The accuracy of the scale factor calibration is determined by how well the arm radius from the centrifuge rotation axis to the accelerometer's effective proof mass center is measured, since the centrifuge rotation rate can be accurately measured. For the class of accelerometer considered, variations in arm length do not necessarily have to be accounted for, if the micromechanical accelerometer fixture is well attached to the centrifuge arm. Alternatively, the variation in arm length at different rotation rates could be monitored and compensated for in estimating accelerometer parameters.

F.2 Scale factor calibration

Data is collected at different centrifuge rotation rates to provide, e.g., the following sequence of acceleration levels:

500 g
1,000 g
2,000 g
4,000 g
6,000 g
8,000 g
10,000 g

A quadratic polynomial is least-squares fit to the data to determine scale factor in volts per g, bias, and the K_2 nonlinearity term. The bias estimate can be compared with the zero-g bias measured with the accelerometer stationary with IA horizontal.

Results can be compared for the accelerometer IA toward and away from the center of rotation. The difference in scale factor measured in the two orientations can only be taken as a measure of the scale factor asymmetry to within the error in measuring the arm radii in the two orientations.

Annex G

(informative)

Data acquisition and thermal control in centrifuge testing

G.1 Thermal control on centrifuge arm

To calibrate accelerometer model coefficients as functions of temperature or to demonstrate performance over the temperature range of an application, a thermal chamber would have to be placed on the centrifuge or double centrifuge arm. For example, non-temperature-controlled operation over the range –65°C to +85°C might be required for automotive or military applications, with or without thermal compensation.

To reach the lower temperatures, the thermal chamber might require liquid nitrogen (or carbon dioxide) cooling, either from a liquid nitrogen dewar on the centrifuge arm or from liquid nitrogen piped onto the centrifuge arm through a rotary couple. The weight of the thermal chamber combined with the weight of the test article could reduce the acceleration that a centrifuge could impart to the test article, owing to loading of the centrifuge or double centrifuge bearings.

Testing of a small test article, such as a silicon chip micromechanical accelerometer, allows thermal control with a small thermoelectric heater–cooler rather than a thermal chamber, with resulting decrease in the load on the centrifuge or double centrifuge bearings. Only electric power has to be brought through slip rings for the thermoelectric heater–cooler and the article under test. The temperature of the test article could be monitored by a thermistor, with a thermal controller maintaining the temperature at each desired set point within the operating temperature range.

Thermoelectric heater–coolers are commercially available, such that current flowing in one direction cools a surface attached to the test article (perhaps covered with insulation) and discharges heat through another surface into a heat sink. Electric current flowing in the other direction heats the test article and cools the heat sink. In order to reach the lower temperatures on the test article, the heat sink might have to be provided with, e.g., a pellet of solid carbon dioxide.

In order to do testing at lower temperatures without water condensation or frost buildup, the article under test, the thermoelectric heater–cooler, and the heat sink could be in a hermetically sealed chamber bathed in dry nitrogen on the centrifuge arm, or the whole centrifuge or double centrifuge could be bathed in dry nitrogen.

G.2 Data acquisition on centrifuge arm

The output signals from an accelerometer under test could pass through slip rings on the centrifuge or double centrifuge, to be acquired by a data acquisition computer. The acquisition of analog signals requires the use of a voltmeter or A/D (analog-to-digital) converter. Proper conditioning and grounding of analog signals through slip rings to allow accurate data acquisition can be a difficult problem.

One solution to this problem is to have a microprocessor on the centrifuge or double centrifuge adjacent to the accelerometer under test, along with a frequency reference to provide the trigger for acquiring data. The A/D conversions of the accelerometer data are carried out without any slip-ring degradation, other data are acquired (such as second-turntable angle readout and temperature readings), and then sent by the microprocessor through the slip rings as a digital data stream to the data acquisition computer.

Another solution is to avoid the slip rings altogether for signal transmission, and to send the data from the microprocessor on the centrifuge or double centrifuge arm to the data acquisition computer using a radio link. The slip rings are used only to bring electric power and grounding to the equipment on the centrifuge or double centrifuge arm.

There are commercially available modules to accomplish this. The radiotransmitter and its antenna on the centrifuge arm interface to the microprocessor. At a radio frequency of about 2 GHz, a 100 kbit/s digital data stream is sent to the receiving antenna. The radio receiver interfaces to a board in the PC data acquisition computer.

The sending and receiving antennas are each single omnidirectional rods. The receiving antenna could be right over the rotation axis of the centrifuge, and the sending antenna on the rotation axis, so there is no Doppler shift between the sending and receiving antennas.

On a double centrifuge, the receiving antenna would again be over the main centrifuge rotation axis. The sending antenna is on the turntable rotation axis at the end of the centrifuge arm. Again, there is no Doppler shift between the sending and receiving antennas, because the line of sight velocity between the sending and receiving antennas is zero.

The data acquisition computer acquires the digital data stream from the radio link, and also acquires other data such as the centrifuge rotation angle and rate. The data can be filtered or averaged before being saved to disk at a lower rate. It is generally good test philosophy to oversample and acquire data at a high rate, and then filter and decimate to the lower rate required for analysis.

Annex H

(informative)

Bibliography

[B1] Cramer, H. *The Elements of Probability Theory*, Wiley, New York, 1955.

[B2] *CRC Handbook of Chemistry and Physics 1997–1998*. Boca Raton, FL: CRC Press, 1997–1998.

[B3] Crow, E.L., Davis, F.A., and Warfield, M.W., Statistics Manual, Dover, New York, 1960.

[B4] Hoel, P.G. *Introduction to Mathematical Statistics*, Wiley, New York, 1947.

[B5] Huff, D. *How to Lie with Statistics*, Norton, New York, 1954.

[B6] IEEE 100, *The Authoritative Dictionary of IEEE Standards Terms*, Seventh Edition.

[B7] *International Critical Tables of Numerical Data, Physics, Chemistry and Technology*. New York: McGraw-Hill, 1926–1930.

[B8] *ISO Guide to the Expression of Uncertainty of Measurement*, Geneva, Switzerland: Organization for Standardization, 1993.

[B9] Kendall, M.G. *The Advanced Theory of Statistics* (three vols), Charles Griffen and Co., London, 1967–1969.

[B10] Meyer, S.L. *Data Analysis for Scientists and Engineers*, Wiley, New York, 1975.

[B11] Neugebauer, G. H., ''Precision Centrifuge Testing of an Accelerometer,'' The Aerospace Corporation, San Bernardino Operations, Report No. APP-72 (S2970-11)-1, 16 May 1972. Published in the *Proceedings of the Sixth Guidance Test Symposium*, Holloman Air Force Base, New Mexico, October, 1972.

[B12] Neugebauer, G. H., ''An Improved Data Reduction Procedure for Accelerometer Centrifuge Data,'' *Proceedings of the Thirteenth Guidance Test Symposium*, Holloman Air Force Base, New Mexico, October, 1987.

[B13] Neugebauer, G. H., ''Effect of Noise in Precision Centrifuge Testing of Accelerometers,'' *Proceedings of the Sixteenth Guidance Test Symposium*, Holloman Air Force Base, New Mexico, October, 1993.

[B14] Peters, R. B., ''Use of Multiple Acceleration References to Obtain High Precision Centrifuge Data at Low Cost,'' *Proceedings of the First International Symposium on Inertial Components*, Institute of Mechanical Engineers, Newcastle upon Tyne, 1987.

[B15] Smith, R. O., Willis, E. A., and Hilten, J. S., ''A Dual Centrifuge for Generating Low Frequency Sinusoidal Accelerations,'' *Journal of Research of the National Bureau of Standards*, 1962, N4, pp. 357–362.

[B16] Wilks, S.S. *Mathematical Statistics*, Wiley, New York, 1955.

